

Generalized Linear Latent and Mixed Model:

method, bayesian estimation, advantages, and
applications to educational data.

Jose Manuel Rivera Espejo

Supervisor: Prof. Geert Molenbegrhs
Leuven Biostatistics and Statistical
Bioinformatics Centre (L-BioStat)

Co-supervisor: Prof. Wim Van den
Noortgate
Faculty of Psychology and Educational
Sciences

Thesis presented in fulfillment of
the requirements for the degree of
Master of Science in Statistics and Data Science
for Social, Behavioral and Educational Sciences

Academic year 2020-2021

Dedication

To Manuel, for being my friend and father.
To Margarita, Karina, Susan, and Marysu, for their relentless encouragement.
To Ana, for showing me the value of family, here in this moorland.
To both of you, as you are always in my mind.
And to all that knowingly or not, help me to get here.
I am lucky due to all of you.
I hope I make you all proud.

A Manuel, por ser mi amigo y mi padre.
A Margarita, Karina, Susan y Marysu, por su incansable aliento.
A Ana, por mostrarme el valor de la familia, aquí en este páramo.
A ustedes dos, que siempre las tengo en mente.
Y a todos los que sabiendolo o no, me ayudaron a llegar aquí.
Soy un suertudo gracias todos ustedes.
Espero llenarlos de orgullo.

Acknowledgment

To the friends that managed to keep me motivated through this rewarding endeavor. Thank you for all the great discussions, and your cool friendship. Thank you Qian "Erika", Luc, Jonathan, Youhee, Sarah, Nura, Jingpu, and Jasper. You were sent from heaven, if something like that exists.

Abstract

(work in progress)

Keywords:

Contents

1	Introduction	1
1.1	Preliminar considerations	1
1.2	Objectives	3
1.3	Organization	4
2	The GLLAMM for dichotomous outcomes	5
2.1	Model motivation	5
2.2	Model definition	6
2.2.1	Response model	6
2.2.2	Latent structure	9
2.3	Model assumptions	10
3	Bayesian estimation	11
3.1	Benefits and shortcomings	11
3.1.1	Why Bayesian?	11
3.1.2	Are you sure there's nothing wrong?	12
3.2	Bayesian GLLAMM for dichotomous outcomes	13
3.2.1	Posterior distribution	13
3.2.2	Prior distributions	14
3.2.3	Likelihood	14
3.2.4	Model identification	15
3.3	Computational implementation	15
3.3.1	Hamiltonian Monte Carlo	15
3.3.2	Where can I find this magical software?	17
3.3.3	What about burn-in and thinning?	17
3.3.4	Initial starts	17
3.3.5	Prior elicitation	17
3.4	To center or not to center	20
3.4.1	Wasn't HMC the solution to this?	20
3.4.2	So, how can we solve this?	22
4	Simulation Study	28
4.1	Conditions	28
4.2	Algorithm	29
4.3	Parameter estimation	31
4.3.1	Models and identification	31
4.3.2	Prior predictive investigation	33

4.4	Evaluation criteria	35
4.5	Results	37
4.5.1	Chain performance	37
4.5.2	Recovery capacity	41
4.5.3	Retrodictive accuracy	41
4.5.4	Time	41
5	Application	42
5.1	Instruments	42
5.2	Data	42
5.2.1	Collection	42
5.2.2	Sample scheme	42
5.3	Results	42
6	Conclusion and Discussion	43
6.1	Discussion	43
6.2	Conclusions	43
6.3	Future development	43
A	Additional plots and tables	44
A.1	Chapter 3: Bayesian estimation	44
A.1.1	To center or not to center	44
A.2	Chapter 4: Simulation study	47
A.2.1	Prior elicitation	47
A.2.2	Chain performance	48
B	Code	73
B.1	Chapter 3: Bayesian estimation	73
B.1.1	To center or not to center	73
B.2	Chapter 4: Simulation study	74
B.2.1	Algorithm	74
B.2.2	Results	79

List of Figures

2.1	Path diagram of the dimensional structure for a hierarchical cross-classified IRT model.	6
3.1	Prior predictive simulation. Examples of uninformative and mildly informative priors.	18
3.2	The Devil's funnel. Centered Parametrization. Stan.	21
3.3	Posterior sampling geometry. Centered Parametrization.	22
3.4	Posterior sampling geometry. Centered Parametrization with mildly informative priors.	23
3.5	The Devil's funnel. Centered Parametrization with prior information.	24
3.6	Posterior sampling geometry. Non-Centered Parametrization.	25
3.7	The Devil's funnel. Non-centered Parametrization.	26
4.1	Directed Acyclic Graph (DAG). First Order Latent Variables model (FOLV).	29
4.2	Directed Acyclic Graph (DAG). Second Order Latent Variables model (SOLV).	30
4.3	First-Order latent variable model (FOLV). Item Characteristic Curve (ICC) and Item Information Function (IIF).	34
4.4	First-Order latent variable model (FOLV). Hit rate per dimensions of interest.	35
4.5	First-Order latent variable model (FOLV). Hit rate per simulated covariate.	36
4.6	First-Order latent variable model (FOLV). Sample size 100, replica number 2. Centered parametrization. Mean difficulty per text. Trace, trank and auto-correlation plots.	38
4.7	First-Order latent variable model (FOLV). Sample size 100, replica number 2. Non-centered parametrization. Mean difficulty per text. Trace, trank and auto-correlation plots.	39
4.8	First-order latent variable model (FOLV). Sample size 100, all replicas. CP and NCP comparison plot.	40
A.1	The Devil's funnel. Centered Parametrization. JAGS	44
A.2	The Devil's funnel. Centered Parametrization with mildly informative priors. JAGS	45
A.3	The Devil's funnel. Non-Centered Parametrization. JAGS	46
A.4	Second-Order latent variable model (SOLV). Item Characteristic Curve (ICC) and Item Information Function (IIF).	47
A.5	Second-Order latent variable model (SOLV). Hit rate per dimensions of interest.	47
A.6	Second-Order latent variable model (SOLV). Hit rate per simulated covariate.	48

A.7	First-Order latent variable model (FOLV). Sample size 100, replica number 3. Centered parametrization. Difficulty deviation per text. Trace, trunk and auto-correlation plots.	49
A.8	First-Order latent variable model (FOLV). Sample size 100, replica number 3. Non-centered parametrization. Difficulty deviation per text. Trace, trunk and auto-correlation plots.	50
A.9	First-Order latent variable model (FOLV). Sample size 100, replica number 1. Centered parametrization. Difficulty per item. Trace, trunk and auto-correlation plots.	51
A.10	First-Order latent variable model (FOLV). Sample size 100, replica number 1. Non-centered parametrization. Difficulty per item. Trace, trunk and auto-correlation plots.	52
A.11	First-Order latent variable model (FOLV). Sample size 100, replica number 6. Centered parametrization. Individual's first sub-dimension. Trace, trunk and auto-correlation plots.	53
A.12	First-Order latent variable model (FOLV). Sample size 100, replica number 6. Non-centered parametrization. Individual's first sub-dimension. Trace, trunk and auto-correlation plots.	54
A.13	First-Order latent variable model (FOLV). Sample size 100, replica number 7. Centered parametrization. Individual's second sub-dimension. Trace, trunk and auto-correlation plots.	55
A.14	First-Order latent variable model (FOLV). Sample size 100, replica number 7. Non-centered parametrization. Individual's second sub-dimension. Trace, trunk and auto-correlation plots.	56
A.15	First-Order latent variable model (FOLV). Sample size 100, replica number 8. Centered parametrization. Individual's third sub-dimension. Trace, trunk and auto-correlation plots.	57
A.16	First-Order latent variable model (FOLV). Sample size 100, replica number 8. Non-centered parametrization. Individual's third sub-dimension. Trace, trunk and auto-correlation plots.	58
A.17	First-Order latent variable model (FOLV). Sample size 100, replica number 4. Centered parametrization. Regression parameters. Trace, trunk and auto-correlation plots.	59
A.18	First-Order latent variable model (FOLV). Sample size 100, replica number 4. Non-centered parametrization. Regression parameters. Trace, trunk and auto-correlation plots.	60
A.19	First-Order latent variable model (FOLV). Sample size 100, replica number 5. Centered parametrization. Correlation of sub-dimensions. Trace, trunk and auto-correlation plots.	61
A.20	First-Order latent variable model (FOLV). Sample size 100, replica number 5. Non-centered parametrization. Correlation of sub-dimensions. Trace, trunk and auto-correlation plots.	62
A.21	Second-Order latent variable model (SOLV). Sample size 100, replica number 9. Centered parametrization. Loadings. Trace, trunk and auto-correlation plots.	63

A.22 Second-Order latent variable model (SOLV). Sample size 100, replica number 9. Non-centered parametrization. Loadings. Trace, trank and auto-correlation plots.	64
A.23 Second-Order latent variable model (SOLV). Sample size 100, replica number 1. Centered parametrization. Correlation of sub-dimensions. Trace, trank and auto-correlation plots.	65
A.24 Second-Order latent variable model (SOLV). Sample size 100, replica number 1. Non-centered parametrization. Correlation of sub-dimensions. Trace, trank and auto-correlation plots.	66
A.25 Second-Order latent variable model (SOLV). Sample size 100, replica number 10. Centered parametrization. Highest-order dimension. Trace, trank and auto-correlation plots.	67
A.26 Second-Order latent variable model (SOLV). Sample size 100, replica number 10. Non-centered parametrization. Highest-order dimension. Trace, trank and auto-correlation plots.	68
A.27 First-order latent variable model (FOLV). Sample size 100, all replicas. CP and NCP comparison plot.	69
A.28 First-order latent variable model (FOLV). Sample size 100, all replicas. CP and NCP comparison plot.	70
A.29 Second-order latent variable model (SOLV). Sample size 100, all replicas. CP and NCP comparison plot.	71
A.30 Second-order latent variable model (SOLV). Sample size 100, all replicas. CP and NCP comparison plot.	72
A.31 Second-order latent variable model (SOLV). Sample size 100, all replicas. CP and NCP comparison plot.	72

List of Tables

4.1	FOLV running time statistics.	41
4.2	SOLV running time statistics.	41

Abbreviations

ACF	Auto-correlation function.
BUGS	Bayesian Inference Using Gibbs Sampling.
CFA	Confirmatory Factor Analysis.
CLT	Central Limit Theorem.
CP	Centered Parametrization.
DAG	Directed Acyclic Graph.
DDM	Dual Dependence Models.
EFA	Exploratory Factor Analysis.
FOLV	First-order Latent Variable.
GLLAMM	Generalized Linear Latent and Mixed Model.
GLM	Generalized Linear Model.
GLMM	Generalized Linear Mixed Model.
HMC	Hamiltonian Monte Carlo.
ICC	Item Characteristic Curve.
IIF	Item Information Function.
iHMC	Interleaved Hamiltonian Monte Carlo.
JAGS	Just Another Gibbs Sampler.
IRT	Item Response Theory.
MCMC	Markov Chain Monte Carlo.
ML	Maximum Likelihood.
MSEM	Multilevel Structural Equation Model.
NCP	Non-centered Parametrization.
RMSE	Root Mean Squared Error.
SEM	Structural Equation Model.
SOLV	Second-order Latent Variable.
UVI	Unit Variance Identification.
VI	Variational Inference.

Chapter 1

Introduction

1.1 Preliminär considerations

Local independence is one of the key assumptions of Item Response Theory (IRT) models, and it is comprised of two parts: (i) local item independence and (ii) local individual independence [3, 27]. In the former case, the assumption entails that the individual's response to an item does not affect the probability of endorsing another item, after conditioning on the individual's ability. While in the case of the latter, the assumption considers that an individual's response to an item, is independent of another person's response to that same item [64].

The literature has shown that IRT models are not robust to the violation of local independence. The transgression of the assumption affects model parameter estimates, inflates measurement reliabilities and test information, and underestimates standard errors (see Yen [76], Chen and Thissen [10], and Jiao et al. [32]).

However, item response data arising from educational assessments often display several types of dependencies, violating the local item and/or individual independence, e.g. testlets, where items are constructed around a common stimulus [74]; the measurement of multiple latent traits within individuals [64]; cluster effects, where correlation among individuals results from the sampling and measurement mechanism used to gather the data [63]; among others. A good motivating example, that will permeate this research, is the reading comprehension sub-test, from the Peruvian public teaching career national assessment. The test is designed to measure three hierarchically nested sub-dimensions of reading comprehension: literal, inferential, and reflective abilities. Furthermore, the items are bundled together in testlets related to a common text or passage. Finally, multiple cluster effects are present, e.g. at the region, and district level, just to mention a few.

Recent studies have proposed IRT Dual Dependency Models (DDM) to deal with the testlets and individual clustering dependencies observed in the data [17, 16, 15, 32, 13, 14, 64, 8]. The majority of these representations have been developed under the Bayesian framework, and they are similar in parametrization to multilevel models. On the other hand, an almost independent line of research, the Generalized Linear Latent and Mixed Models (GLLAMM) [57, 59, 69, 60], have extended the capabilities of hierarchical models on the estimation of multiple latent traits at different hierarchical levels. These developments have been motivated mostly under the frequentist framework, and they are similar in parametrization to a Multilevel Structural Equation Model (MSEM).

While the initial sense is that both developments are independent of each other, follow-

ing their literature, one can easily notice that they share more than a resemblance. Both follow a multilevel/hierarchical multidimensional approach to account for the clustering of persons within samples and/or items within bundles (DDM), or the latent structures within the individuals (GLLAMM). However, it is important to point out that in some cases the model parametrization between the two developments differs in a way, that some of them appear to be useful only under their specific contexts. Fortunately, their integration under the Bayesian framework is not only trivial, but it can be motivated under either type of model.

The benefits of the integration revolve around two facts: (i) educational data often presents all of the aforementioned dependencies and more, as in the motivating example; and (ii) as it was hinted in the second paragraph, to reach appropriate conclusions from the parameter estimates, IRT models need to account for all of these dependencies. The latter is particularly important as, more often than not, a researcher is interested in producing inferences at the structural level of the model, i.e. how a different set of manifest variables explain the variability in the latent variables, or how the latent variables explain other manifest or latent variables, at different levels. As an example, one might be interested in finding evidence if the latent “abilities” of the teachers are explained by their initial educational conditions, i.e. if they were educated in an institute, university, or both. The main purpose of this would be to identify the type of teacher that might benefit more from the in-service training¹, offered by the national educational authorities, making the intervention cost-effective.

From the previous description, one can infer that the proposed IRT representation would be complex and highly dimensional. Moreover, as educational assessments are usually scored in a binary way (the individual either endorse or not the item), and because not all individuals are assessed by all items, the model will be estimated with sparse data. From the modeling perspective, neither of the previous points presents a challenge for the bayesian framework. However, it has long been recognized that complex parametrizations, that allow this powerful modeling schemes, introduce pathologies that make Markov Chain Monte Carlo methods (MCMC) face performance challenges [18, 19, 50, 51, 6], e.g. not achieving stationarity and/or not making a proper exploration of the posterior sampling space. This is highly relevant because, in order to make inferences about the posterior distribution of the parameters, the chains need to achieve a requirement highly related to the performance of the method: ergodicity [45], i.e. stationarity, convergence, and good mixing [44].

Throughout the bayesian IRT literature, one often finds that four solutions are offered to ensure the fulfillment of the previous requirements, and they can be classified into two broad groups: (i) solutions that involve changing the settings of the MCMC method, and (ii) solutions that involve readjusting the Bayesian model.

In the first category, we find two proposals: (a) increasing the number of iterations per chain, with large burn-in and thinning processes, and (b) designing model-specific MCMC algorithms. The easiest to implement and more prevalent in the literature is the former, e.g. Fujimoto [16] used chains with 60,000 iterations, where 15,000 were discarded and the remaining were thinned in jumps of 3; while Fujimoto [15] used 225,000 iterations, with burn-in of 30,000 and thinning with jumps of 15. Among the drawbacks of this solution are the large computational times; the user involvement in deciding the specific

¹Intervention designed with the purpose of potentiating specific abilities in teachers that are currently part of the public teaching career.

setting for the process, which could be different for different parameters in the same model; and finally, the lack of confidence that larger chain iterations actually produce a proper posterior investigation. On the other hand, several authors have developed high-tech MCMC algorithms that aim to optimize their performance within a particular class of models [51]. In these cases, the developers re-evaluate not only the use of the programming language, with the purpose of speeding and improving performance (e.g. Fujimoto [16]); but also the inclusion of ad-hoc model assumptions, like prior conjugacy² for specific parameters or highly regularizing priors (see next paragraph), to mention a few. Examples of this solutions are in staple software developments like Mplus [47] or Stata [58]. It is clear from the previous that this solution is not accessible to all researchers, either because of the lack of programming skills, or the restrictive cost of access involved in acquiring the software. But more importantly, these solutions are not always applicable to a wider framework of similar models [51].

In the second category, we also find two proposed solutions: (a) re-write the model in an alternative parametrization, and (b) encode prior information through the prior distributions, i.e. use regularizing priors. On both solutions, the purpose is to ensure the identification of the parameters within the model, which helps to stabilize the MCMC procedure [22]. An example of the former is Fujimoto [16], who decomposed the items' discriminatory parameters into overall and specific item discriminations. For the latter, Fujimoto [17] used informative priors also for the items' discrimination parameters.

More often than not, researchers use two or more of the aforementioned solutions to reach an acceptable performance in the chains. However, as point out by Betancourt and Girolami [6], even the most simple hierarchical models present formidable pathologies, that no simple correction can be performed to visit the posterior distribution properly. This is true no matter the rotation/rescaling of the parameter, or the amount of data. In this context, several authors [18, 19, 50, 51, 6] showed that prior information can be included in the model, not only through the prior distributions, but also by encoding it in the model itself, changing the posterior sampling geometries, i.e. removing the dependence of the parameters on other sampled parameters, therefore favoring the performance of MCMC chains.

Given all of the above, the present research will focus on showing how easy it is to account for all of the dependencies that educational data often display, under the GLLAMM framework. Furthermore, given that only the literature related to gaussian hierarchical models have shown the benefits of changing the posterior sampling geometries, through the use of the non-centered parameterization [18, 19, 50, 51, 6], it seems sensible to provide a similar assessment for nonlinear hierarchical models, and in particular, the ones with latent stochastic processes like IRT [51]. Finally, the research will apply the newfound knowledge to data coming from a large Teacher's standardized educational assessments from Peru.

1.2 Objectives

As mentioned in the previous section, the present research has a three-fold purpose:

1. Motivate the Bayesian GLLAMM for binary outcomes [57, 59, 69, 60]. The rep-

²when the prior and posterior distribution belong to the same parametric family.

resentation will emphasize the modeling of multiple hierarchical latent structures and testlets. This, in turn, will effectively blur the division between the GLLAMM framework and IRT models.

2. Empirically evaluate the benefits of changing the posterior sampling geometry, in the context of the Bayesian GLLAMM for binary outcomes. The emphasis here will be on comparing the centered and non-centered parametrizations [18, 19] in terms of performance of the chains, the parameter's recovery capacity, the retrodictive accuracy, and the ability of the model to produce appropriate inferences.
3. Apply the model and its parametrization to a real data setting. Here the emphasis will be to assess the conclusions arrived from the application of the model, and what they could imply for the educational authorities.

Given the aforementioned goals, the researcher believes the master's thesis contributes to the literature in two aspects:

1. In a theoretical and methodological sense, as the research is focused on describing a model that effectively controls for the multiple dependencies usually observed in educational data sets; and
2. In a more practical sense, as the study will provide empirical evidence if changing the sampling posterior geometries could (could not) benefit the performance of MCMC methods and therefore the inferences, under IRT models.

Finally, it is important to mention, that the computational implementation of the method will be developed in **Stan** [72] and **R** [54, 71].

1.3 Organization

Chapter 2 will motivate the GLLAMM for dichotomous outcomes, and define its components. Chapter 3 will describe the Bayesian framework, its benefits and shortcomings. Furthermore, it will outline the evidence behind the change in posterior sampling geometries, and the computational implementation of the model. Chapter 4 will show the results of an empirical simulation study designed to assess the benefits of the re-parametrization, proposed in the previous chapter. Chapter 5 will describe the instruments, the data collection process, and scales under analysis, for a large standardized educational assessment. In addition, the chapter will show the conclusions achieved by the application of the model in the said data. Finally, Chapter 6, will discuss the conclusion for the research, and it will outline the path of future research topics that can be derived from the present effort.

Chapter 2

The GLLAMM for dichotomous outcomes

The Generalized Linear Latent and Mixed Model (GLLAMM) is a framework that unifies a wide range of latent variable models. Developed by Rabe-Hesketh and colleagues [57, 59, 58, 69, 60], the method was motivated by the need of a Multilevel Structural Equation Model (MSEM) that accommodated for unbalanced data, noncontinuous responses and cross-level effects among latent variables. The authors focused its development mainly from the frequentist perspective, however, they offered a general guidance on implementing the model under the bayesian framework (see Skrondal and Rabe-Hesketh [69]).

2.1 Model motivation

Consider a large standardized assessment composed of three sub-test designed to evaluate the reading comprehension, mathematical reasoning, and pedagogical knowledge of teachers; where each sub-test has several dichotomously scored items.

Focusing on the first sub-test, the items were designed to measure only one of the three hierarchically nested sub-dimensions of reading comprehension: literal, inferential, and reflective abilities. Furthermore, it is assumed the three sub-dimensions are all that is needed to measure the reading comprehension ability, effectively making this scale, the highest level latent variable in the model, similar to a hierarchical Confirmatory Factor Analysis (CFA). Finally, the items were bundled in groups of five to a common text or passage, i.e. testlets, that provided the stimulus over which the individual is assessed. Figure 2.1 shows the path diagram of the hypothesized dimensional structure, for the hierarchical cross-classified IRT model corresponding with the instrument. The figure represents the responses of one person on 12 items.

With the purpose of providing an easier motivation of the model, we will not consider yet the cluster effects; however, later in the presentation we will show how easy it is to introduce them in the model. Just for future reference, under this example, one expects to observe clustering effects, because individuals from different regions did not have the same educational opportunities, effectively causing differences among them at a regional level.

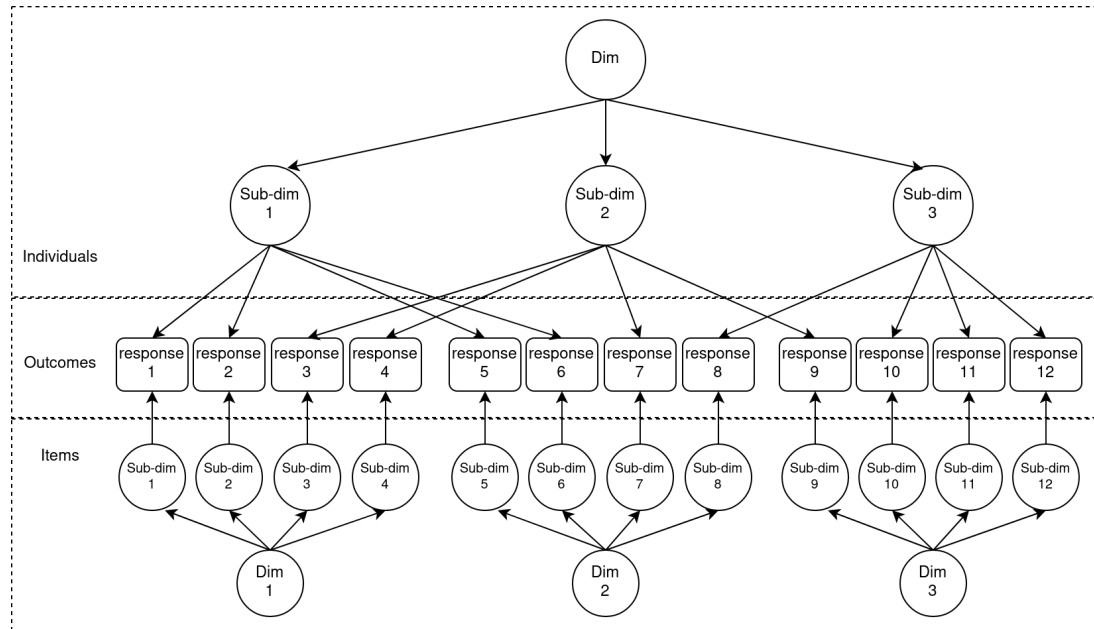


Figure 2.1: Path diagram of the dimensional structure for a hierarchical cross-classified IRT model. Squares represent dichotomous manifest variables, and circles represent latent variables. The figure is based on a reduced set of items, while the errors and scales of the latent variables are not represented. Different sub-dimensions at the individuals block represent the literal, inferential and reflective abilities, while at the items blocks represent the items' difficulties. The dimensions at the individuals block represent the reading comprehension ability, while at the items block represent the multiple testlets.

2.2 Model definition

Following Rabe-Hesketh et al. [57, 59], we continue defining the GLLAMM in two parts: (i) the response model, and (ii) the latent structure.

In case the reader is interested in outcomes different than the dichotomous case, refer to Rabe-Hesketh et al. [57, 59, 58], Skrondal and Rabe-Hesketh [69], and Rabe-Hesketh et al. [60].

2.2.1 Response model

Conditional to all regression parameters β , loadings Λ , latent variables Θ , and structural parameters Ψ and Γ , i.e. $\Omega = \{\beta, \Lambda, \Theta, \Psi, \Gamma\}$; and the “stacked” vector of covariates for the first level (\mathbf{X}) and the structural part (\mathbf{W}); the response model can be represented by a Generalized Linear Model (GLM) [49, 43] with a distributional and a systematic part. The latter composed of a linear predictor and a link function.

For the distributional part, the outcome y_{jkd} is modeled at the first level (level-1) by a Bernoulli probability mass function $f(\cdot)$, in the following form:

$$f(y_{jkd} = 1 | \mathbf{X}, \mathbf{W}, \Omega) = \pi_{jkd}^n (1 - \pi_{jkd})^{1-n} \quad (2.1)$$

where individuals are indexed by $j = 1, \dots, J$, with J representing the total number of individuals in the sample; the items are indexed by k , with d being the dimension the

items are set to measure; and n denotes the endorsement of the item in the Bernoulli trial. On the other hand, for the systematic part, the probability of endorsing the item π_{jkd} is linked to a linear predictor v_{jkd} through an inverse-link function $h(\cdot)$, in the following form:

$$P(y_{jkd} = 1 \mid \mathbf{X}, \mathbf{W}, \boldsymbol{\Omega}) = \pi_{jkd} = h(\tau_k + v_{jkd}) \quad (2.2)$$

where τ_k is k 'th item threshold, assumed to be zero for the binary case [57], while the inverse-link function can be defined in three ways:

$$h(x) = \begin{cases} \exp(x)[1 + \exp(x)]^{-1} \\ \Phi(x) \\ \exp(-\exp(x)) \end{cases} \quad (2.3)$$

corresponding to the logistic, standard normal $\Phi(x)$, and Gumbel (extreme value type I) cumulative distributions, respectively. It is usual to report the last in terms of link functions $g(\cdot) = h^{-1}(\cdot)$. In that case, these corresponds to the well known logit, probit and complementary log-log, respectively. Finally, the linear predictor is defined by:

$$v_{jkd} = \sum_{p=1}^P x_{jp} \beta_p + \sum_{m=2}^{M+1} \sum_{k=1}^{K_{(m)}} \eta_k^{(m)} \alpha_k^{(m)} + \sum_{l=2}^{L+1} \sum_{d=1}^{D_{(l)}} \theta_{jd}^{(l)} \lambda_d^{(l)} \quad (2.4)$$

where β_p denotes regression parameter for the x_{jp} explanatory variable with $p = 1, \dots, P$, and P denoting the total number of level-1 response explanatory variables, e.g. time to answer the item, the number of alternatives, among others. $\eta_k^{(m)}$ is the k th item latent dimension at level m with loading $\alpha_k^{(m)}$, where $k = 1, \dots, K_{(m)}$, $K_{(m)}$ denotes the number of dimensions at level $m = 2, \dots, M + 1$, and M represents the number of levels in the items block. It is important to keep in mind, the model also contemplates that not all the item are set to measure all the individual's dimension; however, we decided to not to show such information in the form of an index in equation (2.4), to avoid making the notation heavier. Nevertheless, equation (2.5) is more clear on this assumption, as the design block matrices show. $\theta_{jd}^{(l)}$ denotes the individual's d th latent dimension at level l with loading $\lambda_d^{(l)}$, where $d = 1, \dots, D_{(l)}$, $D_{(l)}$ represents the number of dimensions at level $l = 2, \dots, L + 1$, and L denotes the number of levels in the individuals block. Notice that since the responses are modeled at the first level, the hierarchies for the latent dimensions need to start from the second level onward.

Additionally, equation (2.4) can be re-written in matrix form in the following way:

$$v_{jkd} = \mathbf{X}_j \boldsymbol{\beta} + \sum_{m=2}^{M+1} \boldsymbol{\eta}^{(m)} \boldsymbol{\alpha}^{(m)} \mathbf{A}_j^{(m)} + \sum_{l=2}^{L+1} \boldsymbol{\theta}_j^{(l)} \boldsymbol{\lambda}^{(l)} \mathbf{B}_j^{(l)} \quad (2.5)$$

where \mathbf{X}_j represents the individual's design matrix of explanatory variables that maps the parameter vector $\boldsymbol{\beta}$ to the linear predictor; and $\mathbf{X} = [\mathbf{X}_1^T, \dots, \mathbf{X}_J^T]^T$ the “stacked” design matrix of \mathbf{X}_j . Moreover, $\boldsymbol{\eta}^{(m)} = [\eta_1^{(m)}, \dots, \eta_{K_{(m)}}^{(m)}]^T$, and $\boldsymbol{\alpha}^{(m)} = [\alpha_1^{(m)}, \dots, \alpha_{K_{(m)}}^{(m)}]^T$ are the vectors of the item's latent dimensions with corresponding loadings at level m , mapped by a block matrix $\mathbf{A}_j^{(m)}$. Similarly, $\boldsymbol{\theta}_j^{(l)} = [\theta_{j1}^{(l)}, \dots, \theta_{jD_{(l)}}^{(l)}]^T$, and $\boldsymbol{\lambda}^{(l)} = [\lambda_1^{(l)}, \dots, \lambda_{D_{(l)}}^{(l)}]^T$ are

the vectors of the individual's latent dimensions with corresponding loadings at level l , mapped by a block matrix $\mathbf{B}_j^{(l)}$.

Finally, in order to have a more concise representation of the model, we can re-express equation (2.5) in the following way:

$$\begin{aligned} v_{jkd} &= \mathbf{X}_j \boldsymbol{\beta} + \boldsymbol{\eta} \boldsymbol{\alpha} \mathbf{A}_j + \boldsymbol{\theta} \boldsymbol{\lambda} \mathbf{B}_j \\ &= \mathbf{X}_j \boldsymbol{\beta} + \boldsymbol{\Theta} \boldsymbol{\Lambda} \mathbf{H}_j \end{aligned} \quad (2.6)$$

where $\boldsymbol{\alpha} = [\boldsymbol{\alpha}^{(2)T}, \dots, \boldsymbol{\alpha}^{(M+1)T}]^T$ and $\boldsymbol{\lambda} = [\boldsymbol{\lambda}^{(1)T}, \dots, \boldsymbol{\lambda}^{(L+1)T}]^T$ represent all the loadings corresponding to the items and individuals dimensions at all levels; whereas $\boldsymbol{\eta} = [\boldsymbol{\eta}^{(2)T}, \dots, \boldsymbol{\eta}^{(M+1)T}]^T$ and $\boldsymbol{\theta} = [\boldsymbol{\theta}^{(2)T}, \dots, \boldsymbol{\theta}^{(L+1)T}]^T$ represent the latent dimensions and sub-dimensions of items and individuals at all levels, respectively. Consequently, \mathbf{A}_j and \mathbf{B}_j are their mapping block matrices. Furthermore, $\boldsymbol{\Lambda} = [\boldsymbol{\alpha}^T, \boldsymbol{\lambda}^T]^T$ and $\boldsymbol{\Theta} = [\boldsymbol{\eta}^T, \boldsymbol{\theta}^T]^T$ to represent the “stacked” vector of loadings, and dimensions, respectively; and \mathbf{H}_j its mapping block matrix.

Considering figure 2.1 as reference, we would have an empty level-1 covariates matrix \mathbf{X}_j , as we do not have any response explanatory variable ($P = 0$). Moreover, we have $M = 2$ levels at the items block, with $K_2 = 12$ and $K_3 = 3$. Consequently, $\boldsymbol{\eta}^{(2)} = [\eta_1^{(2)}, \dots, \eta_{12}^{(2)}]^T$ and $\boldsymbol{\eta}^{(3)} = [\eta_1^{(3)}, \eta_2^{(3)}, \eta_3^{(3)}]^T$ denotes the items' difficulties and testlet effects, respectively. As stated in previous paragraphs, to avoid the use of even heavier notation, the item's indexes do not reflect that not all the items are set to measure all the individual's dimensions; however, the reader needs to keep that in mind. On the other hand, we have $L = 2$ levels in the individuals block, with $D_2 = 3$ and $D_3 = 1$. Therefore, $\boldsymbol{\theta}^{(2)} = [\theta_1^{(2)}, \theta_2^{(2)}, \theta_3^{(2)}]^T$ which denotes the literal, inferential and reflective abilities; whereas $\boldsymbol{\theta}^{(3)} = \theta_1^{(3)}$ represent the reading comprehension latent variable. Furthermore, since we are trying to express an IRT model, it makes sense to put some restrictions to the parameter set. In this case, we establish $\boldsymbol{\alpha}^{(2)} = -\boldsymbol{\lambda}^{(2)}$ with $\boldsymbol{\lambda}^{(2)} = [\lambda_1^{(2)}, \dots, \lambda_{12}^{(2)}]^T$ representing the item's discriminatory parameter, where $\boldsymbol{\lambda}^{(2)} > \mathbf{0}$. This resemble to a multidimensional generalization of the linear predictor observed in the archetypical Rasch [62], or 2PL [39] models, i.e. $\lambda_d^{(2)}(\theta_{jd}^{(2)} - \eta_k^{(2)})$, where $|\lambda_d^{(2)}| = |\alpha_k^{(2)}|$ denotes the discriminatory power of item k , $\eta_k^{(2)}$ its difficulty, and $\theta_{jd}^{(2)}$ the ability of the individual at dimension d . In addition, $\boldsymbol{\lambda}^{(3)} = [\lambda_1^{(3)}, \lambda_2^{(3)}, \lambda_3^{(3)}]^T$ would represent the loadings from reading comprehension to their respective sub-dimensions; whereas $\boldsymbol{\alpha}^{(3)} = [\alpha_1^{(3)}, \alpha_2^{(3)}, \alpha_3^{(3)}]^T$ would represent the item-specific loadings from the testlets, usually set as $[1, 1, 1]^T$, indicating they explain directly the items difficulties at the lower level.

Finally, notice that through the use of \mathbf{A}_j and \mathbf{B}_j design block matrices, and more generally with \mathbf{H}_j , the model departs from the traditional multivariate framework for formulating structural models, i.e. a wide data format; and adopts a univariate approach, i.e. a long data format. The former stores the subject's repeated outcomes in a single row, with multiple response vectors and explanatory variables appended column-wise to the outcome data. The later stores the subject's repeated outcomes in a single “stacked” response vector with as many rows as there are repeated measurements, and explanatory variables appended column-wise to the outcome data, distinguished from each other, by a design block matrix.

Cluster effects

Considering the previous, we can see that modeling individual clustering just involves the addition of more random effects, to the linear predictor defined in equation (2.4):

$$\begin{aligned} v_{jkdc} &= v_{jkd} + \sum_{c=1}^C \delta_c \\ &= v_{jkd} + \boldsymbol{\delta} \mathbf{Z}_j \end{aligned} \quad (2.7)$$

where $c = 1, \dots, C$, which denotes the number of clusters, v_{jkd} is defined as in equation (2.4), and \mathbf{Z}_j is a design block matrix.

2.2.2 Latent structure

The structural model for the latent variables is represented in the following form:

$$\boldsymbol{\Theta} = \boldsymbol{\Psi} \boldsymbol{\Theta} + \boldsymbol{\Gamma} \mathbf{W} + \boldsymbol{\zeta} \quad (2.8)$$

where $S = K + D$, $K = \sum_m K_m$, and $D = \sum_l D_l$. Furthermore, $\boldsymbol{\Psi}$ and $\boldsymbol{\Gamma}$ are parameter matrices that map the relationship between the latent variables $\boldsymbol{\Theta}$, and the “stacked” vector of covariates \mathbf{W} , respectively; while $\boldsymbol{\zeta}$ is a vector of errors or disturbances. It is important to indicate that \mathbf{W} considers a different set of covariates from \mathbf{X} , as we hypothesize they explain the variability in the latent variables at different levels.

Notice equation (2.8) is the generalization of a single-level Structural Equation Models (SEM) to a multilevel setting, however, the main difference in the GLLAMM representation is that the latent variables may vary at different levels.

Additionally, considering that $\boldsymbol{\Theta}$ has no feedback effects, is permuted, and sorted according to the levels of interest, then $\boldsymbol{\Psi}$ will be a strictly upper triangular matrix. In this regard, (i) the absence of feedback loops imply the method deals with non-recursive models, i.e. none of the latent variables are specified as both causes and effects of each other [36]; and (ii) the strictly upper triangular structure reveals the GLLAMM does not allow latent variables to be regressed on lower level latent or observed variables, implying the method deals with reflective measurement¹[5]. For a more detailed explanation on the topic see Edwards and Bagozzi [12].

However, notice that because in the IRT framework $\boldsymbol{\eta}$ and $\boldsymbol{\theta}$ should be orthogonal to each other by design, we can further decompose equation (2.8) in the following form:

$$\boldsymbol{\eta} = \boldsymbol{\Psi}_\eta \boldsymbol{\eta} + \boldsymbol{\Gamma}_\eta \mathbf{W}_\eta + \boldsymbol{\zeta}_\eta \quad (2.9)$$

$$\boldsymbol{\theta} = \boldsymbol{\Psi}_\theta \boldsymbol{\theta} + \boldsymbol{\Gamma}_\theta \mathbf{W}_\theta + \boldsymbol{\zeta}_\theta \quad (2.10)$$

where $\boldsymbol{\Psi}_\eta$, $\boldsymbol{\Psi}_\theta$, $\boldsymbol{\Gamma}_\eta$, and $\boldsymbol{\Gamma}_\theta$ are the dimension-specific parameter matrices that map the relationship between the corresponding latent variables $\boldsymbol{\eta}$ and $\boldsymbol{\theta}$; with $\boldsymbol{\zeta}_\eta$ and $\boldsymbol{\zeta}_\theta$ being the dimension-specific vector of disturbances. Finally, the matrices \mathbf{W}_η and \mathbf{W}_θ would be the dimension-specific covariates.

¹A latent variable is considered reflective when it is thought to be the cause of the lower level latent or manifest variables.

Considering figure 2.1 as reference, we did not specified any structural relationships Ψ ; nor declare any additional covariates \mathbf{W} . However, chapter 4 and 5 will show an implementation where we hypothesized a set of covariates explain the variability on some of the latent variables.

2.3 Model assumptions

Following Skrondal and Rabe-Hesketh [69], the framework has two main assumptions: (i) complete latent space, and (ii) local or conditional independence.

(M1) Complete latent space. The latent space is considered complete if all the latent variables, that we hypothesize affect the outcomes, are considered in the model [26]. In the GLLAMM representation, these would be all latent variables Θ at levels $l > 1$ and $m > 1$, as the outcomes are modeled at the first level.

(M2) Local Independence, also known as conditional independence, is defined in the following form:

$$f(\mathbf{y} = \mathbf{1} | \mathbf{X}, \mathbf{W}, \boldsymbol{\Omega}) = \prod_{j=1}^J \prod_{d=1}^D \prod_{k=1}^K f(y_{jkd} = 1 | \mathbf{X}, \mathbf{W}, \boldsymbol{\Omega}) \quad (2.11)$$

where $f(\mathbf{y} = \mathbf{1} | \mathbf{X}, \mathbf{W}, \boldsymbol{\Omega})$ denotes the level-1 conditional likelihood, and \mathbf{y} the vector of all responses at the first level.

Notice the approach also assumes local or conditional independence, as their non-hierarchical IRT model counterparts. Nevertheless, its independence is conditional on all the latent dimensions and covariates, at different hierarchical levels; effectively modeling all the observed dependencies.

Finally, it is important to point out that equation (2.11) results from the union of two more specific assumptions, local item and individual independence [64, 3, 27]:

(a) **Local item independence**, which entails the individual's response to an item does not affect the probability of endorsing another item, after conditioning on the individual's ability. This is expressed in the following mathematical form:

$$f(y_{j..} = 1 | \mathbf{X}, \mathbf{W}, \boldsymbol{\Omega}) = \prod_{d=1}^D \prod_{k=1}^K f(y_{jkd} = 1 | \mathbf{X}, \mathbf{W}, \boldsymbol{\Omega}) \quad (2.12)$$

where $y_{j..} = [y_{j1}, \dots, y_{jKD}]$ is the vector of all items for individual j and, as previously defined, $K = \sum_m K_m$ and $D = \sum_l D_l$.

(b) **Local individual independence**, which entails that an individual's response to an item is independent of another person's response to that same item. The assumption is expressed in the following form:

$$f(y_{.kd} = 1 | \mathbf{X}, \mathbf{W}, \boldsymbol{\Omega}) = \prod_{j=1}^J f(y_{jkd} = 1 | \mathbf{X}, \mathbf{W}, \boldsymbol{\Omega}) \quad (2.13)$$

where $y_{.kd} = [y_{1kd}, \dots, y_{Jkd}]$ is the vector of all individuals endorsing item k from dimension d .

Chapter 3

Bayesian estimation

The practical use the GLLAMM developed in chapter 2 requires the estimation of all of the items and individuals' dimensions, loadings, regression and structural parameters. These can be obtained within two frameworks: the frequentist and bayesian.

The current chapter center its attention on describing the bayesian estimation procedure, using the Markov Chain Monte Carlo method (MCMC). For a full development of GLLAMM under the frequentist framework refer to Rabe-Hesketh and colleagues [57, 59, 69, 60].

3.1 Benefits and shortcomings

3.1.1 Why Bayesian?

The reasons on why bayesian statistics is attractive to perform the parameters' estimation of any model, and especially for the GLLAMM developed in chapter 2, are:

1. It is built on a simulation-based estimation method, therefore, it can handle all kinds of priors and data-generating processes [14]. This is especially useful with highly complex and over-parameterized models, where other methods are unfeasible or work poorly [2, 35].
2. While the likelihood functions are used to define the posterior sampling distributions, they can also be used in a generative way. The likelihood for the data, and priors for the parameters, form the basis to produce samples from the posterior distribution. However, they can also be used to simulate observations, allowing us to test the ability of the method/data to recover the parameters of interest [44].
3. The bayesian estimates are at least as good as its frequentist counterparts [2, 75, 30]. This is true when the method uses uninformative 'flat' priors. However, because the procedure allow us to integrate prior knowledge about the parameters, beyond the observed responses, it can produce results even in scenarios where the Maximum Likelihood methods (ML) have issues of non-convergence or improper estimation [69, 14, 44]. Examples of such are:
 - (a) when we have small sample sizes.

- (b) when individuals have null scores or aberrant response patterns [27, 1]. The latter happens when examinees answered some relatively difficult and discriminating items correctly, while answering some of the easiest incorrectly.
- (c) when parameters need to be confined to a permitted space, e.g. the estimation of positive unique factors variances [42].
- (d) when we need to estimate parameters under sparse data, where the asymptotic theory is unlikely to hold [14];

3.1.2 Are you sure there's nothing wrong?

Off course the bayesian framework has shortcomings, among them:

1. It exposes the user to somewhat-arbitrary decisions about the running of the chains, in order to ensure a proper performance, e.g. how many iterates does the chain need to achieve precise estimates?, what is the right size for the burn-in and warm-up phases?, how should the thinning procedure be performed, if any?, should we follow the same procedure for all parameters of interest?, among others [69].
2. The user can include all type of information through the priors distributions, apparently making their elicitation convenient for manipulation, towards the use of highly informative priors.
3. Multiple options are available to evaluate the performance of the method, and most of them are visual, making it hard to assess if a proper posterior investigation have been made [23]. More specifically, the user has multiple options to assess if the chain achieves the three requirements of a good performance: stationarity, convergence, and good mixing [44].
4. The procedure makes it hard to discover parameters' lack of identification [69]. Inadequate mixing of the chain could lead us to think unidentified parameters have been estimated with precision, when in fact what we have are 'flat' posteriors [33].
5. Oftentimes the posterior sampling geometry of the model makes it hard to find proper solutions for the parameter space, no matter the rotation/rescaling of the parameter, or the amount of data [6]. This is especially true in complex hierarchical models.
6. The greater the complexity of the model, the harder it is to communicate/share the implementation with other scientist. This is especially true, when researcher re-parameterize the model to solve the previous shortcoming [44].
7. The procedure usually requires more time to achieve a proper solution, compared to the classical methods. This is especially true in models with high complexity [73, 65].

Although some of the previous shortcomings have made the Bayesian procedure a "controversial" implementation, most of them already have acceptable solutions.

For the first point, a popular approach is to use a large number of iterates, burn-in and thinning processes. This is mostly applicable under the Metropolis-Hastings and

Gibbs sampling algorithms. However, recent solutions, like the Hamiltonian Monte Carlo (HMC) [6], is less reliant on the decision of selecting these features, as it implements a different sampling mechanism (see section 3.3.1).

On the second point, the literature has indicated that priors can be used in a subjective manner¹. However, as McElreath [44] indicated, because they can be considered a part of the model assumptions, they can be chosen, evaluated, and revised as any other component of the model, through the use of prior predictive simulations and/or sensitivity analysis (see section 3.3.5).

About the third point, the literature on bayesian analysis acknowledge that the visual assessment of stationarity and convergence is easier, and these procedures usually has additional support from statistics like `Rhat` [22]. On the contrary, a visual evaluation of ‘good’ mixing remains as a hard task. Recent approaches have taken a more proactive stance on the latter, seeking to increase the possibility of a well mixed chain by changing the posterior sampling geometry of the model [50, 51, 6, 44] (see section 3.4).

On the fourth point, the most common solution is to use regularizing priors, i.e. priors that are more ‘skeptical’ of wider parameter spaces [44]. However, it is important to mention, there are scenarios where one achieves poor parameter estimates, even in the presence of ‘enough’ data and regularizing priors, but this shortcoming is also applicable to the classical estimation procedures, e.g. the estimation of the variance parameters in random effects models [69].

About the fifth point, as it was mentioned in previous paragraphs, a recent approach to solve the issue is to change the posterior sampling geometry of the model. This means to re-parameterize the model in a way that removes the dependence of the parameters on other sampled parameters; or even, produce sample mechanisms located in a continuous between a centered (CP) and non-centered parametrization (NCP), e.g. Interleaved HMC (iHMC) and/or Variational Inference (VI) [18, 19, 50, 51, 6, 25] (see section 3.4).

Finally, the sixth and seventh points can be considered the ‘price’ a scientist has to pay, to be able to fit models that conforms better with the observed data generating processes. Although, recent developments are striving to improve upon reducing the latter, i.e. the required running time.

3.2 Bayesian GLLAMM for dichotomous outcomes

3.2.1 Posterior distribution

Denoting \mathbf{Y} as the observed data and $\boldsymbol{\Omega} = \{\boldsymbol{\beta}, \boldsymbol{\Lambda}, \boldsymbol{\Theta}, \boldsymbol{\Psi}, \boldsymbol{\Gamma}\}$, i.e. all the parameters declared in section 2.2.1 and 2.2.2, the posterior distribution is obtained using the Bayes theorem, in the following way:

$$P(\boldsymbol{\Omega} | \mathbf{Y}) = \frac{P(\mathbf{Y} | \boldsymbol{\Omega}) P(\boldsymbol{\Omega})}{\int P(\mathbf{Y} | \boldsymbol{\Omega}) P(\boldsymbol{\Omega}) d\boldsymbol{\Omega}} \quad (3.1)$$

this is possible since the Bayesian approach makes no distinction between latent variables and parameters. All of them are considered random quantities [69]. Furthermore, since inference only requires representing the likelihood of the data $P(\mathbf{Y} | \boldsymbol{\Omega})$ and the prior

¹see McElreath [44] (Chapter 2, pp. 36), Rethinking section “Prior, prior pants on fire”, for an interesting stance contrary to this statement.

distribution $P(\Omega)$; and because the denominator is just a (hard to calculate) constant, the posterior can be determined up to a normalizing constant, without loss of generality:

$$P(\Omega | \mathbf{Y}) \propto P(\mathbf{Y} | \Omega) P(\Omega) \quad (3.2)$$

3.2.2 Prior distributions

Similar to Patz and Junker [52], we use an independent distributional structure for the joint priors of the parameters. Therefore, at the highest level of the GLLAMM we have:

$$\begin{aligned} P(\Omega) &= P(\beta, \Lambda, \Theta, \Psi, \Gamma) \\ &= P(\beta) P(\Lambda) P(\Theta) P(\Psi) P(\Gamma) \\ &= P(\beta) [P(\alpha) P(\lambda)] [P(\eta) P(\theta)] [P(\Psi_\eta) P(\Psi_\theta)] [P(\Gamma_\eta) P(\Gamma_\theta)] \end{aligned} \quad (3.3)$$

However, giving the hierarchical and cross-classified structure of the model, the lower level priors will also depend on further parameters², e.g. variances and covariances of the latent variables. These are known as *hyper-parameters*, and their prior distributions as *hyper-priors*. Because of the previous, we are not going to detail their lower level representation, as they are highly dependent on the specifics of the model.

Section 3.3.5 details the process of prior predictive investigation for prior elicitation. On the other hand, chapter 4 and 5 will show the elicitation of priors, in the context of a simulated and real data set, respectively.

3.2.3 Likelihood

Following Rabe-Hesketh et al. [57], the likelihood function is build in a recursive way. First, we replace the structural model (2.8) into the linear predictor (2.6):

$$v_{jkd} = \mathbf{X}_j \beta + (\mathbf{I} - \Psi)^{-1} [\Gamma \mathbf{W} + \zeta] \Lambda \mathbf{H}_j \quad (3.4)$$

Second, the linear predictor and inverse-link function (2.3) are used to construct the systematic part of the response (2.2), i.e. its expected value. Here we use a logit link for pedagogical purposes:

$$\pi_{jkd} = \frac{\exp(\tau_k + v_{jkd})}{1 + \exp(\tau_k + v_{jkd})} = \frac{\exp(v_{jkd})}{1 + \exp(v_{jkd})} \quad (3.5)$$

Third, the expected value is used in the distributional part (2.1), in the following form:

$$f(y_{jkd} = 1 | \mathbf{X}, \mathbf{W}, \Omega) = \pi_{jkd}^n (1 - \pi_{jkd})^{1-n} \quad (3.6)$$

Fourth, considering assumptions (M1) and (M2) described in section 2.3, we produce the level-1 likelihood:

$$f(\mathbf{y} = \mathbf{1} | \mathbf{X}, \mathbf{W}, \Omega) = \prod_{j=1}^J \prod_{d=1}^D \prod_{k=1}^K f(y_{jkd} = 1 | \mathbf{X}, \mathbf{W}, \Omega) \quad (3.7)$$

²Because of this sequential model specification, it is said the priors also have a “hierarchical” structure.

Fifth, we define the marginal likelihood at levels l and m , conditional on the latent variables at levels $l + 1$ and $m + 1$, in the following form:

$$f_{(m)}^{(l)}(\mathbf{y} = \mathbf{1} | \mathbf{X}, \mathbf{W}, \boldsymbol{\Omega}) = \int \left[\prod f_{(m-1)}^{(l-1)}(\mathbf{y} = \mathbf{1} | \mathbf{X}, \mathbf{W}, \boldsymbol{\Omega}) \right] P(\boldsymbol{\Theta}_{(m)}^{(l)}) d\boldsymbol{\Theta}_{(m)}^{(l)} \quad (3.8)$$

where the product inside the brackets is over all units in level $(l - 1)$ and $(m - 1)$, the first level is defined as in equation (3.7), and $P(\boldsymbol{\Theta}_{(m)}^{(l)})$ are the prior distributions for the latent variables at level l and m , with $\boldsymbol{\Theta}_{(m)}^{(l)} = [\boldsymbol{\eta}^{(m)}, \boldsymbol{\theta}^{(l)}]$. Finally, we define the likelihood as:

$$\mathcal{L}(\mathbf{X}, \mathbf{W}, \boldsymbol{\Omega}) = \prod_{m=2}^{M+1} \prod_{l=2}^{L+1} f_{(m)}^{(l)}(\mathbf{y} = \mathbf{1} | \mathbf{X}, \mathbf{W}, \boldsymbol{\Omega}) \quad (3.9)$$

and the log-likelihood as:

$$\ell(\mathbf{X}, \mathbf{W}, \boldsymbol{\Omega}) = \log \mathcal{L}(\mathbf{X}, \mathbf{W}, \boldsymbol{\Omega}) \quad (3.10)$$

3.2.4 Model identification

As indicated by Rabe-Hesketh et al. [57], in order to fully specify the model and provide a scale for the latent variables, we have to make assumptions for either the distribution of the disturbances $\boldsymbol{\zeta}$, or the distribution of one or more of the latent variables $\boldsymbol{\Theta}$. On the other hand, as point out by Fujimoto [15] and several others authors, we could also set restrictions for one or more of the loadings in $\boldsymbol{\Lambda}$. The last is more prevalent in frequentist software packages like Winsteps [38].

Furthermore, as it is hinted by equation (3.9), it is assumed the latent variables at different levels are independent from each other, whereas latent variables at the same level may present dependency. In case of the latter, we presume the latent variables at the same level have a multivariate normal distribution with a mean and covariance structure determined by equations (2.9) and (2.10). In the case of the covariance matrices, these are determined by the covariance of the specific disturbances $\boldsymbol{\zeta}$.

Chapter 4 and 5 will show the model identification strategy in the context of a simulated and real data set, respectively.

3.3 Computational implementation

3.3.1 Hamiltonian Monte Carlo

For years the state-of-the-art platform for Bayesian statistical modeling have been the BUGS³ project [41, 40], with its WinBUGS and OpenBUGS implementations. However, a more recent participant JAGS⁴ [53] has gain traction, due to its cross-platform capabilities. In any case, both platforms are not that different from each other. Both use two of the most popular and successful algorithms for performing MCMC: the Metropolis-Hastings [45, 28] and Gibbs Sampling [24] algorithms.

In general lines, the Metropolis algorithm follows a two-step procedure: (i) it produces a new proposal for a parameter's value, and (ii) it evaluates the proposal against the

³Bayesian inference Using Gibbs Sampling

⁴Just Another Gibbs Sampling

current, accepting the new value if it is more likely under the posterior distribution. On the other hand, the Gibbs sampling uses a similar procedure, but it gains efficiency by exploiting the knowledge behind the target distribution. The latter improvement catapulted the Gibbs sampler into the workhorse of high dimensional Bayesian computing.

However, both methods remain as highly random procedures, and because of it, they still have important limitations. The most important of them all is that they do not yield independent and identically distributed samples (*iid*). This in turn means, the exploration of the posterior is made through a series of (sometimes highly dependent) values, causing the MCMC chain to converge to the target distribution only in the long run, i.e. when the number of iterations approach infinity ($t \rightarrow \infty$) [22]. It is important to mention that while the non-fulfillment of *iid* samples is a critic of all simulation based method, in no algorithms is more relevant than in the previous two.

In this setting three solutions have been proposed within the context of these algorithms, and oftentimes the aforementioned software packages use them in conjunction. The first consist on improving the sampling mechanism by using a Hybrid MCMC method. A good example is the “Metropolis-within-Gibbs” algorithm [46]. The second consist on setting a warm-up phase that seeks to adapt the proposal distributions to favor the exploration of the posterior. Finally, the third consist on defining the number of iterates, burn-in and thinning processes in a way that it reduces the serial dependencies in the samples.

Nevertheless, the aforementioned solutions, while useful, do not solve all issues related to the MCMC chain’s performance, as these can remain biased in subtle ways, that are more harder to identify [44]. Therefore, researchers have decided instead to propose new improved algorithms.

Is in this context were the Hamiltonian Monte Carlo or Hybrid Monte Carlo (HMC) was proposed by Duane et al. [11], using the theory of Hamiltonian Dynamics. While the full representation of method is out of the scope of this research, we can still make a high-level description of its process, with purpose of point out its benefits and shortcomings.

Assuming we have continuous distributions and the partial derivatives of the log-density function (the gradient) exists, the method iterates the updating of two vector spaces of a particle [48, 44]. First, it samples new values for the particle’s momentum vector, independent of the current values of its position vector, i.e. it gives the particle a random “flick”. In the second iteration, using Hamiltonian dynamics, a Metropolis update is performed to propose a new position vector for the particle. In this sense, one can say the HMC runs a small physics simulation, where the position of the particle denotes the current parameter values in the Markov chain, the momentum denotes the proposed path to a new set of values, and the log-posterior provides the “friction-less” surface over which the particle moves, where the gradient defines its curvature [44].

In principle, because HMC produce “more informed” proposals, it will accept all of them. In practice, however, HMC uses a rejection criterion, that inform us when the method was not able to maintain the “balance” of the system, producing a bad numeric approximation (see section 3.4 for an example). For more on the background theory on Hamiltonian Dynamics and specifics about the HMC algorithm refer to Neal [48] and Betancourt and Girolami [6].

All of this just tells us that HMC is a highly complex algorithm. However, as McElreath [44] point out, the Gibbs strategy got its improvement over the Metropolis-Hastings by being less random, not more. And in that sense, HMC pushes this principle to a greater

length, but manages to improve the efficiency of the MCMC procedure. This is especially true in cases where ordinary Metropolis or Gibbs sampling cannot make a proper exploration of the parameter space, e.g. with highly correlated parameters or with models with hundreds or thousands of parameters, like complex hierarchical models. Moreover, as HCM is more efficient, it requires less number of iterations to make a proper posterior investigation [44, 22]

Off course, this comes with a cost. The methods is more computationally intensive than the previous. However, because of the efficiency improvement and the need of less number of iterations, the method requires less computer time in total, even when each individual sample needs more.

3.3.2 Where can I find this magical software?

Stan [72] is the software package that will provide us with the machinery of HMC. Furthermore, the results produced from the software will be analyzed with **R** [54, 71], and its integration packages.

3.3.3 What about burn-in and thinning?

Since HMC uses a different approach and produces more informative proposals, setting specific burn-in and thinning processes is no longer necessary.

However, the method does require to perform a warm-up procedure to adapt sampling, and to tune in two parameters of the algorithm: the number of steps (leapfrogs), and the step size [72]. These parameters are used to make a discrete approximation of the momentum vector, i.e. the path of the particle [48, 6].

Notice, this phase is similar to a procedure performed in JAGS, where the proposal distribution gets “tuned up” to improve the posterior investigation. However, the similarities end there. The warm-up samples in HMC are not representative of the target posterior distribution, no matter how long the iterations continue [44]. Finally, after the warm-up is finished, and assuming the adaption was successful, the method will sample directly from the target distribution.

In the current research, we will use a total 3,000 effective iterations, coming from 3 chains of 2,000 iterations each, where 1,000 of them will be spend on warm-up. Notice this departs (by far) from most of the literature on bayesian IRT models, e.g. Fujimoto [16] used chains with 60,000 iterations, where 15,000 were discarded and the remaining were thinned in jumps of 3; while Fujimoto [15] used 225,000 iterations, with burn-in of 30,000 and thinning with jumps of 15; just to mention a few.

3.3.4 Initial starts

Since the method requires starting values for the parameters, the author decided to allow the software to sample these from the priors defined in the model.

3.3.5 Prior elicitation

As stated in section 3.1.2, because priors can be considered a part of the model assumptions, they can be chosen, evaluated, and revised as any other component of the model

[44]. On the other hand, as recommended by several authors the priors will be mildly informative [44, 17, 73, 32, 1, 75], model-specific, and determined by a prior predictive investigation.

Multiple studies have pointed out the benefits of using mildly informative priors to reduce over-fitting, while allowing the model to learn regular features of the data, e.g. McElreath [44], Gelman et al. [21] and Jaynes [31]. In contrast, the literature has emphasized the unintended consequences on the posterior, resulting from using highly uninformative priors, e.g. Seaman et al. [66], and Gelman [20].

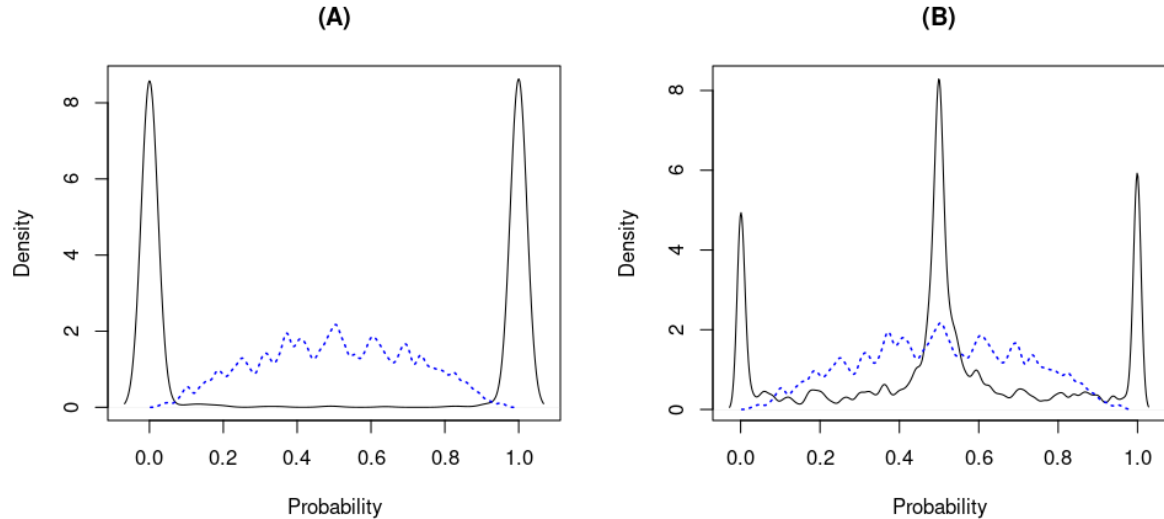


Figure 3.1: Prior predictive simulation. Examples of uninformative and mildly informative priors. The panels show the density for the probability of a binary outcome under: (A) uninformative prior on equation (3.11) and mildly informative prior on equation (3.13); and (B) uninformative prior on equation (3.12) and mildly informative prior on equation (3.14). Uninformative (black continuous lines), and mildly informative (blue discontinuous lines).

In the case pertaining our implementation, the reasons why we are using mildly informative priors, can be understood with a simple illustration. Consider an example similar to one outlined by Seaman et al. [66] and McElreath [44], where a simple latent model is defined as follows:

$$\begin{aligned} \theta &\sim N(0, 100) \\ p &= \frac{\exp(\theta)}{1 + \exp(\theta)} \end{aligned} \tag{3.11}$$

where θ denotes a latent dimension, and p denotes the probability of a binary outcome, defined by the logit-link function. For pedagogical purposes, we did not declare the distribution of the responses, as we wanted to see what this prior implied for their probability, i.e. the expected value of an outcome with a Bernoulli distribution.

Panel (A), from figure 3.1, shows the uninformative prior in equation (3.11) forces an unintended assumption on the expected value of the outcome (black continuous line), i.e.

the model is now highly ‘skeptical’ of probabilities that are not zero or one. Moreover, this means that we are effectively using highly regularizing priors, but opposite on how they are supposed to be used, i.e. to avoid visiting non-likely parameter spaces.

The scenario only gets equally bad with the presence of hyper-parameters, and even less extreme assumptions. Consider the following example:

$$\begin{aligned} v &\sim \log N(0, 3) \\ \theta &\sim N(0, v) \\ p &= \frac{\exp(\theta)}{1 + \exp(\theta)} \end{aligned} \tag{3.12}$$

where v is distributed as a log-normal distribution ($v > 0$). Figure 3.1, panel (B), shows the uninformative priors in equation (3.12) forces another unintended assumption on the expected value of the outcome (black solid line), i.e. the model is now highly ‘skeptical’ of probabilities that are not $p = \{0, 0.5, 1\}$. Again is like using regularizing priors but “in reverse”.

Luckily, these extreme priors can be overcome with enough data. However, that does not discard the need to address the issue of the unintended assumptions, resulting from using uninformative priors.

In that sense, the use mildly informative priors can help alleviate the concern. Mildly/weakly informative priors are prior distributions that are not supplying any controversial information, that are consistent with the likelihood, and are strong enough to pull the data away from inappropriate inferences [22]. Consider the following change to equation (3.11):

$$\begin{aligned} \theta &\sim N(0, 1) \\ p &= \frac{\exp(\theta)}{1 + \exp(\theta)} \end{aligned} \tag{3.13}$$

where θ has a prior that is not only consistent with common IRT applications, but it also does not force the expected value of the outcome to be as extreme as in the uninformative case. Notice in panel (A) on figure 3.1 (blue discontinuous line vs black solid line), the probability can be in the $[0, 1]$ space, where extreme probability values are assumed less likely.

Similarly, in the presence of hyper-parameters we can set mildly informative priors in the following form:

$$\begin{aligned} v &\sim \log N(0, 0.5) \\ \theta &\sim N(0, v) \\ p &= \frac{\exp(\theta)}{1 + \exp(\theta)} \end{aligned} \tag{3.14}$$

where the blue discontinuous line on panel (B) of figure 3.1 shows its transformation into the expected value scale.

One can imagine the procedure of prior elicitation will get more complicated with a larger number of parameter and hyper-parameters. Therefore, the use of prior predictive simulation will be a tool of high value for complex models, as in our current implementation.

3.4 To center or not to center

As pointed out by Betancourt and Girolami [6], even the most simple hierarchical models present formidable pathologies, that no simple correction can be performed to visit the posterior distribution properly. This is true no matter the rotation/rescaling of the parameter, or the amount of data.

A great example of this is what McElreath [44] dubbed the Devil's funnel (depicted in figure 3.3), where the author shows that you do not need a complex model to start observing these issues. Consider the following joint distribution:

$$\begin{aligned} v &\sim N(0, 3) \\ \theta &\sim N(0, \exp(v)) \end{aligned} \tag{3.15}$$

where v is the *hyper-parameter* of θ , and θ is dependent on the samples of v . The latter is what the literature dubbed as the centered parametrization (CP).

This joint distribution might seem familiar, as bayesian hierarchical model practitioners often use it to ensure the standard deviation remains into the permitted parameter space ($\sigma \geq 0$). Similar types of requirements permeate IRT models. Moreover, it seems that any MCMC procedure would not have any issues exploring the posterior distribution of these parameters, as they are normally distributed and there are only two of them, but we would be wrong. The reader can find the `stan` and `jags` implementations for these examples in Appendix B.1.1. The `stan` implementation replicates the example stated by Betancourt and Girolami [6] and McElreath [44].

Figure 3.2 show the chains resulting from implementing the model on equation (3.15), through HMC (`stan`). For pedagogical purposes, the example was run without data, as the author wanted to emphasize the pathologies are present even before we feed the data to our model. However, its easy to extrapolate that these issues will remain present when data is available.

As one can see from the figure, the joint posterior distribution is not explored properly. The chains show no sign of achieving ergodicity [45], i.e. they do not show stationarity or convergence (top panels), nor a good mixing (middle and bottom panels). This is further supported by the `Rhat`, and effective sample sizes estimates `n_eff` [22]. The `Rhat` for all parameters did not approach 1 properly (most of them were above 1.05), indicating the chains did not achieve convergence: the between-chain variability was larger than the within-chain variability. Furthermore, the effective samples sizes were 34 and 293 for v and θ , respectively; indicating the values of the chains remained highly correlated (see bottom panels). This is striking as one expects effective sample sizes closer to the actual number of iterations 3,000 (3 chains with 1,000 samples each, after warm-up).

3.4.1 Wasn't HMC the solution to this?

HMC is a powerful MCMC algorithm, and its benefits stand the test of other scenarios, as detailed by multiple authors [44, 22]. However, the issue with this example goes a little bit farther than what the algorithm can actually overcome, and this is true also for the Metropolis and Gibbs sampler. Nevertheless, we will see HMC still manages to be efficient within the constraints of the problem.

Figure 3.3 shows the posterior sampling geometry of the model in equation (3.15), for the HMC algorithm (`stan`, left) and Metropolis/Gibbs sampler (`jags`, right).

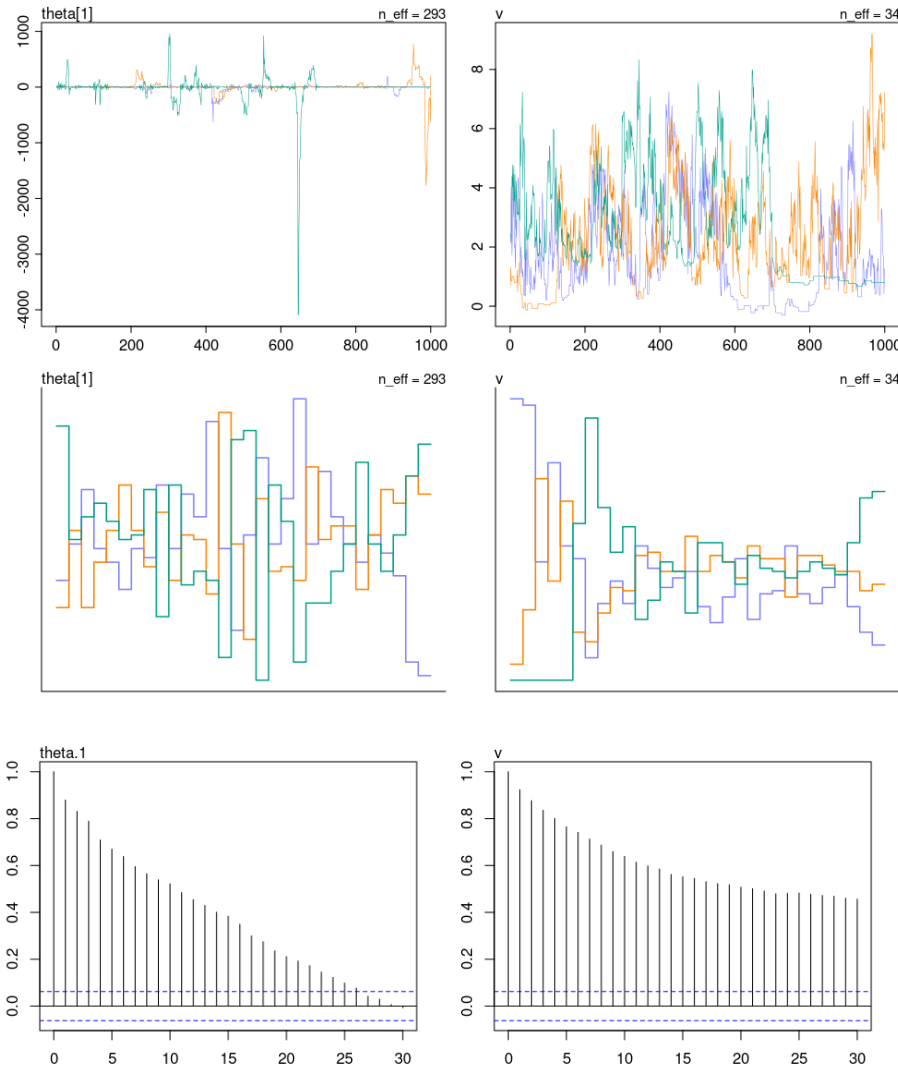


Figure 3.2: The Devil’s funnel. Centered Parametrization. (Top) Trace plots for the iterations on three chains. (Middle) Trank plots for the same data. (Bottom) Auto-correlation Functions (ACF) plot for the iterations.

The first thing to notice is the complexity of the joint posterior geometry, with a steep funnel shape as the values of v gets smaller and smaller. This makes sense, as the exponential of larger negative values, force the standard deviation of θ to be narrower and narrower around its mean (zero).

The second thing to notice is that HMC (left panel) still manages to successfully explore the steep parameter space of v and θ . This can be observed through the blue points that are scattered in most of the geometry, albeit some parts are less visited (area where $\theta > 0$). This does not happen under the Gibbs sampler. In fact, `jags` did not managed to escape the narrow funnel shape, no matter the number of iterations used in the adaptation, burn-in and sampling procedures⁵ (panel B). Moreover, as shown in figure

⁵`stan` used 3 chains with 1,000 iterations for adaptation, and 1,000 iterations for sampling. `jags` used 3 chains with 5,000 iterations for adaptation, 5,000 iterations for burn-in, and 5,000 iterations for sampling.

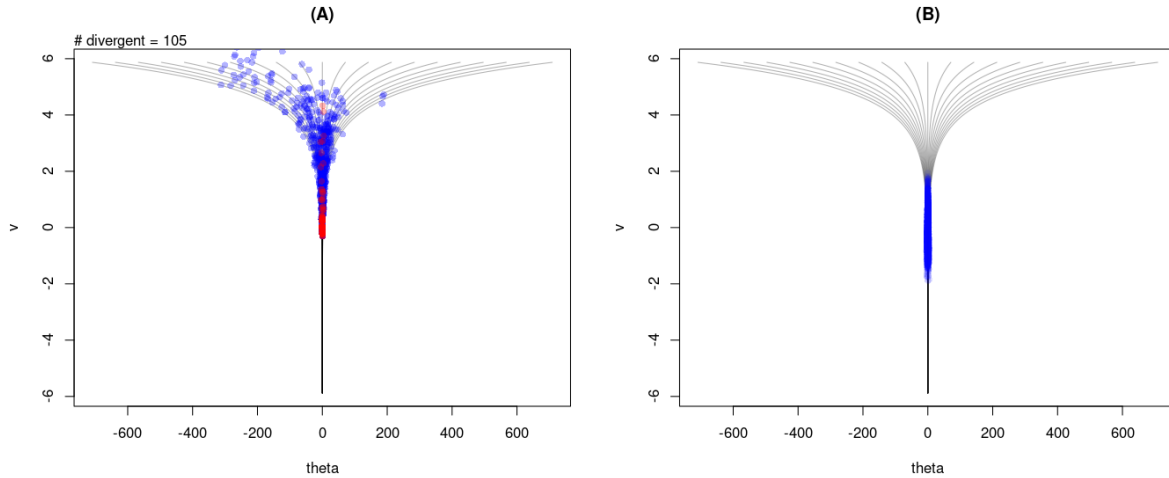


Figure 3.3: Posterior sampling geometry. Centered Parametrization. (A) HMC exploration, blue points are accepted samples, red points denote divergent transitions. (B) Metropolis/Gibbs exploration, blue points are samples.

A.1 (appendix), the traceplots indicate the chains are “healthy”, ignoring the clear lack of exploration of the joint distribution.

Finally, although HMC did not fully explore the joint distribution, at least the method let us know which parts of the distribution did not manage to visit appropriately (see red points indicating divergent transitions). The last is important, because HMC gives us the opportunity to identify where can we improve our parametrization, something that is not available on Metropolis or Gibbs.

3.4.2 So, how can we solve this?

There are two proposed solutions for this issue: (i) use regularizing priors, and (ii) change the posterior sampling geometry. This section will outline the geometrical perspective of the first, as it is already a well study result; while is going to advocate for the benefits of the second, in the context of IRT models.

Regularizing priors

It turns out that the benefits of using regularizing priors can also be explained from a geometrical perspective. Consider the following change to equation (3.15):

$$\begin{aligned} v &\sim N(0, 1) \\ \theta &\sim N(0, \exp(v)) \end{aligned} \tag{3.16}$$

notice now we have chosen a weakly informative prior for v .

Figure 3.4 shows the joint posterior sampling geometry of equation (3.16), for the HMC algorithm (`stan`, left) and Metropolis/Gibbs sampler (`jags`, right).

The first thing to notice from the figure is that the geometry available for exploration seems more broad. However, what is actually happening is that by adding information

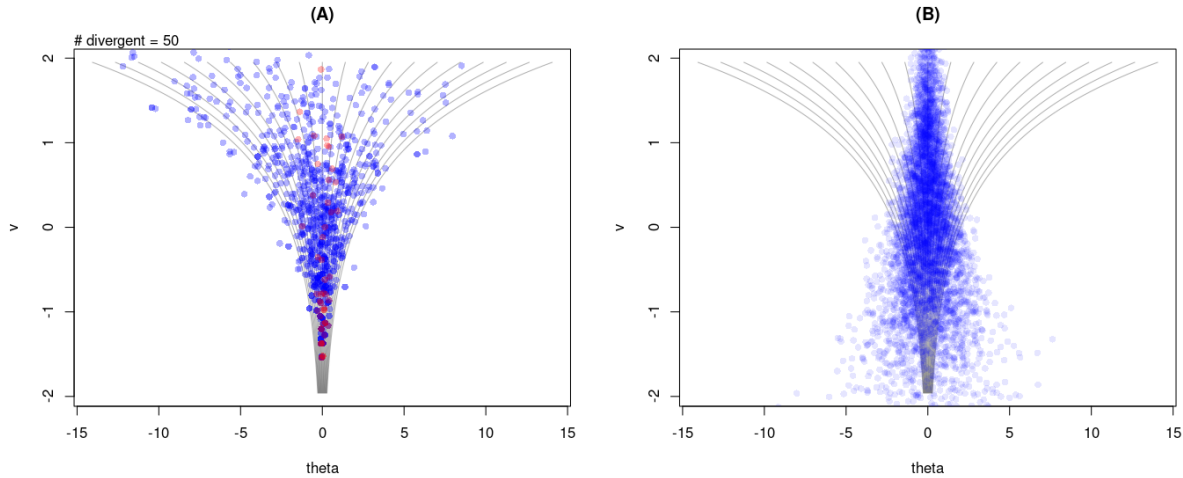


Figure 3.4: Posterior sampling geometry. Centered Parametrization with mildly informative priors. (A) HMC exploration, blue points are accepted samples, red points denote divergent transitions. (B) Metropolis/Gibbs exploration, blue points are samples.

about v , we are “zooming” into the posterior geometry observed in figure 3.3, according to the range of the new priors. This further benefits the exploration of the posterior, as extreme ranges don’t have to be visited from the start, e.g. the narrow funnel in the range $[-6, -2]$ of v from figure 3.3.

The second thing one can notice is that HMC does not “lose time” exploring sections of the posterior distribution that are not needed. Surprisingly in contrast, the Gibbs sampler explore non-useful sections and leaves the useful ones unexplored. Again, this is true no matter the number of iterations used in the adaptation, burn-in and sampling procedures⁶. Moreover, the chains in figure A.2 (appendix) seem to be ergodic, ignoring the clear lack of exploration of the joint distribution, as in the previous example.

Third, we see that using regularizing priors reduced the number of `stan`’s divergent transitions from 150 (in the previous example) to 50. Although we still observe them in the steepest part of the geometry. Such information is not provided by `jags`.

Finally, we notice a mild improvement on the trace, tranks and ACF plots in figure 3.5, compared to figure 3.2 in the previous example.

Non-Centered Parametrization

It would seem that increasing the regularizing power of the priors, is the answer to get rid of the sampling issues raised by a complex posterior sampling geometry. However, there is a limit on the information a prior can contain, without imposing strong assumptions about the parameters (see section 3.3.5 for an example). Furthermore, sometimes researchers want the information on the data dominates the posterior parameter space. In those cases, imposing even mildly informative priors is a solution that is out of the picture.

In this context, Betancourt and Girolami [6] indicated that prior information can be included in the model, not only through the prior distributions, but also by encoding it

⁶the author used the same settings as in the previous example.

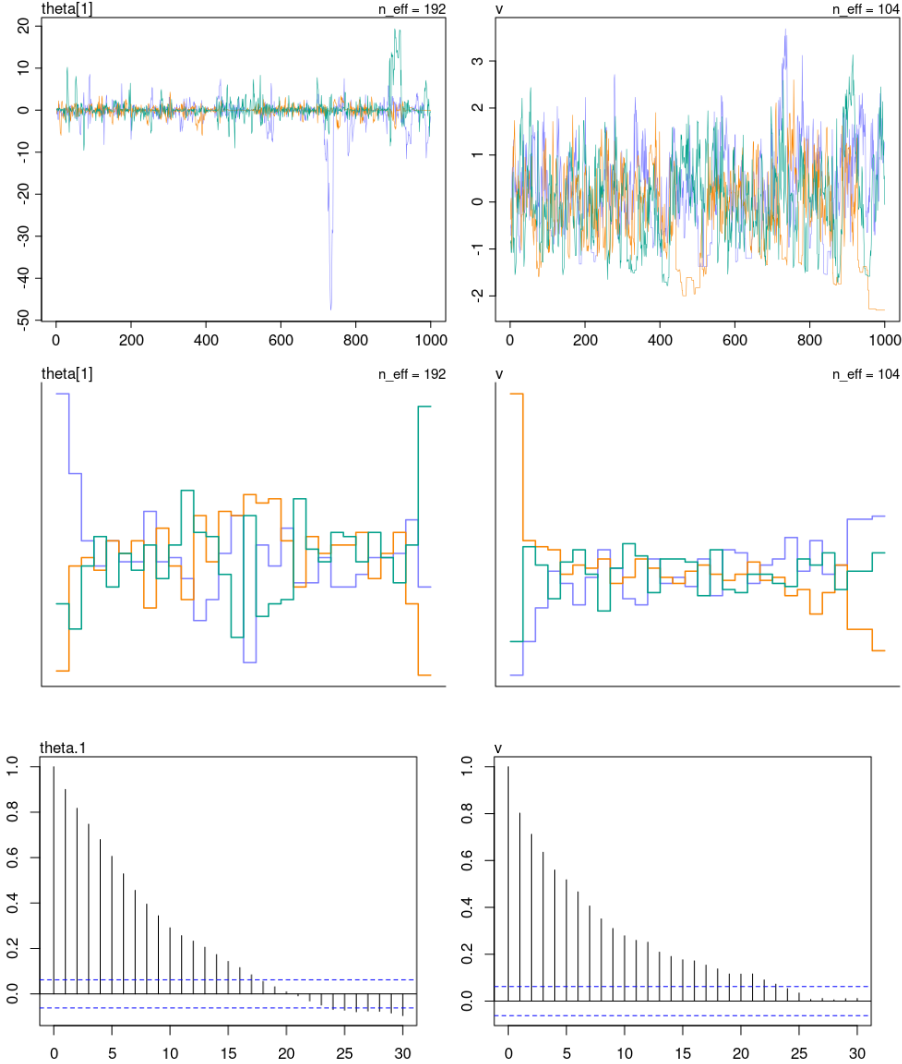


Figure 3.5: The Devil’s funnel. Centered Parametrization with mildly informative priors. (Top) Trace plots for the iterations on three chains. (Middle) Trank plots for the same data. (Bottom) Auto-correlation Functions (ACF) plot for the iterations.

in the model itself, taking advantage of the hierarchical structure explicitly, i.e. change the posterior sampling geometries.

Following Papaspiliopoulos et al. [50, 51], and Betancourt and Girolami [6], under the Bayesian framework, a change in geometry consist on a re-parameterization of a model that seeks to remove the dependence of parameters on other sampled parameters, therefore favoring the performance of the MCMC chains. This is what the literature has dubbed as the non-centered parametrization (NCP).

In our case, changing the posterior sampling geometry means to modify equation (3.15) in the following way:

$$\begin{aligned} v &\sim N(0, 3) \\ z &\sim N(0, 1) \\ \theta &= \exp(v) z \end{aligned} \tag{3.17}$$

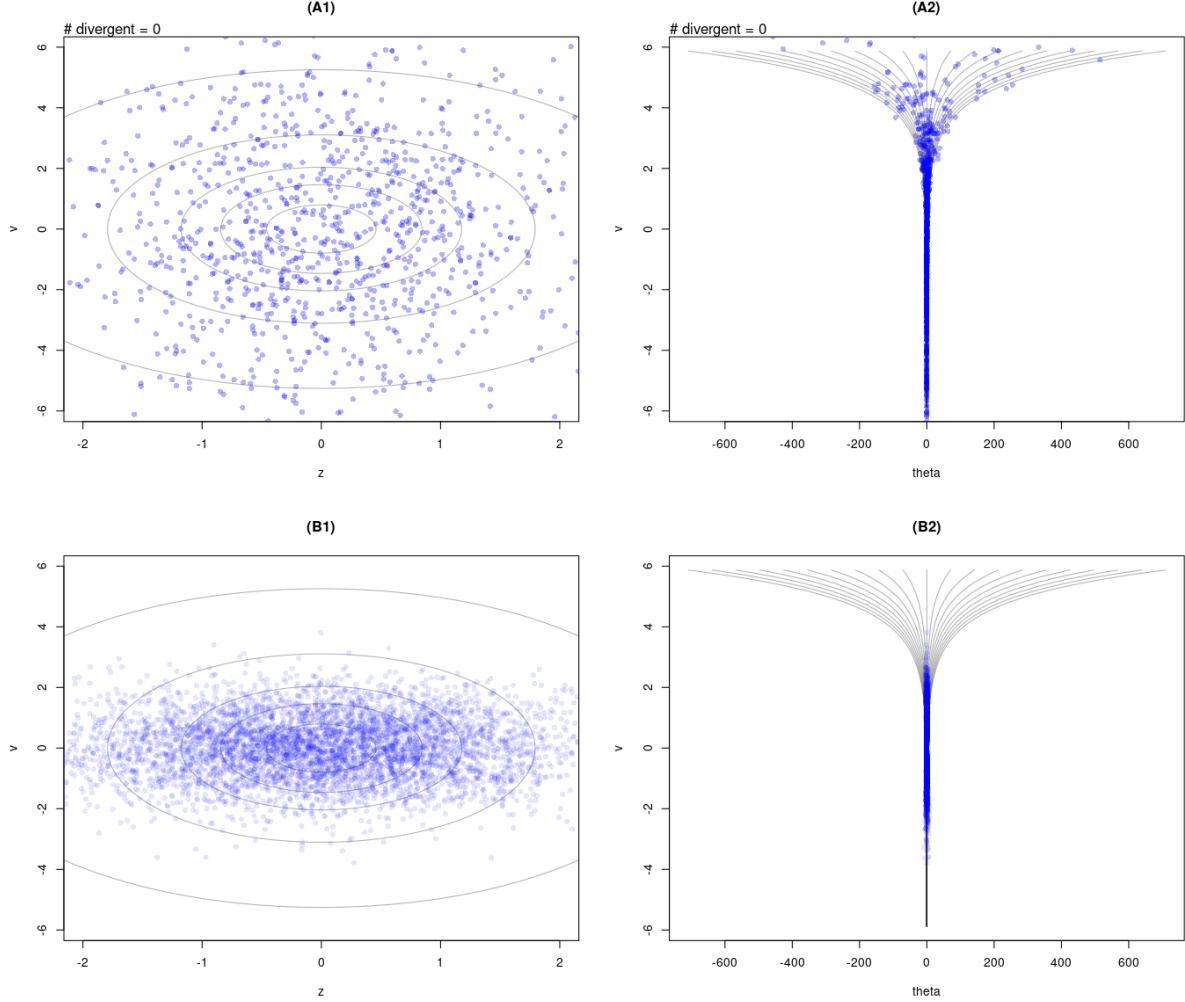


Figure 3.6: Posterior sampling geometry. Non-Centered Parametrization. (A1, B1) geometry defined by the independent parameters v and z . (A2, B2) Original sampling geometry defined by v and θ . (A1, A2) HMC algorithm (`stan`). (B1, B2) Metropolis/Gibbs sampler (`jags`). Blue points are accepted samples. Red points denote divergent transitions.

notice v has the original assumed variability, but now θ is defined in a way, that is no longer sample dependent on v , i.e. we no longer sample θ directly but z , and transform it back.

The motivation for this re-parametrization have seeds in the calculation of the standard score (z-score). Notice that if $\theta \sim N(\mu_\theta, \sigma_\theta)$ where $\sigma_\theta = \exp(v)$, then $(\theta - \mu_\theta)/\sigma_\theta = z$ and $z \sim N(0, 1)$. Using this process in reverse, we notice $\theta = \mu_\theta + \sigma_\theta z = \exp(v) z$ when $\mu_\theta = 0$, then $\theta \sim N(0, \exp(v))$. As the previous, there are transformation that can be done for other distributions, and they can even be extended to the multivariate normal case, through the use of the Cholesky decomposition [44].

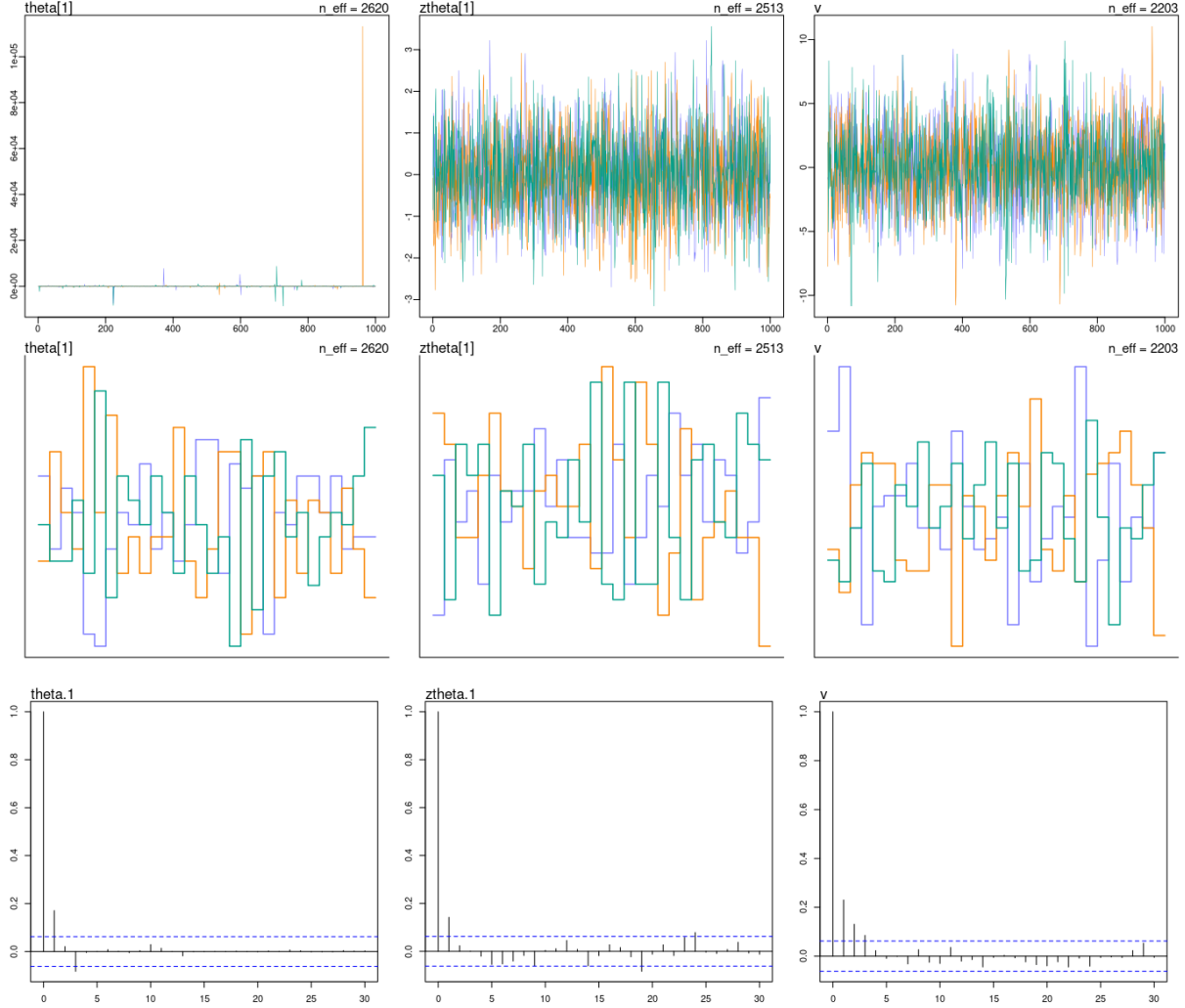


Figure 3.7: The Devil’s funnel. Non-centered Parametrization. (Top) Trace plots for the iterations on three chains. (Middle) Trank plots for the same data. (Bottom) Auto-correlation Functions (ACF) plots for the iterations.

For our current application, however, figure 3.6 show the posterior sampling geometry for the HMC and Gibbs sampler. Notice, under the re-parametrization, both algorithms manage to explore more successfully the posterior distribution, although HMC does it a bit better on the extremes of v . Moreover, HMC shows no divergent transitions, meaning the posterior is “visited” without issues. The latter can be as seen on figure 3.7, where the chains show clear signs of stationarity, convergence and good mixing.

Finally, Papaspiliopoulos et al. [51] indicated that the success of the NCP strategy is largely dependent on the specifics of the model, i.e. neither CP or NCP is more “optimal” than the other. The author pointed out that the natural CP showed better performance when conditional conjugacy was present, i.e. when the posterior distribution belonged to the same parametric family as the likelihood or prior distribution. On the other hand, the NCP worked as its complement, excelling when the previous requirement was not present. Therefore it makes sense that recent advancements on the topic are focused on producing sample mechanisms located in a continuous between CP and NCP, as greater

performance improvements can be obtained by leveraging on the “best of both worlds”, e.g. Interleaved HMC (iHMC) or Variational Inference (VI) [18, 19, 50, 51, 25].

Chapter 4 and 5 will show the application of NCP in the context of an IRT model.

Chapter 4

Simulation Study

4.1 Conditions

A simulation study was conducted to assess three attributes of the bayesian implementation of the GLLAMM for dichotomous outcomes:

1. **Performance.** The study assessed the performance of the MCMC chains in terms of achieving ergodicity, under the centered (CP) and non-centered parametrization (NCP), respectively.
2. **Recovery capacity.** The study evaluated the capacity to recover the parameters of interest, e.g. regression parameters, latent variables and loadings. However, it centered its focus on the recovery of the regression parameters, as they are highly relevant for making appropriate inferences at the individual level.
3. **Retrodictive accuracy.** The study appraised the capacity of the implementation to retrodict the data of interest, according to a set of aggregation dimensions.

In this context, a fully crossed design with $3 \times 2 \times 2$ experimental conditions was proposed.

First, the author used three different samples sizes to generate the data under analysis: 500, 250, and 100. The literature on IRT models present several implementations with samples sizes above 250, however, few present samples lower than that. The author decided to use a sample size of a 100 to fill in this gap. Moreover, the decision was also supported by the notion that the change of the posterior sampling geometries could benefit the performance, and recovery capacity of the implementation, under this setting.

Second, as expected, the author used two parametrization of the models: CP and NCP. To the author's knowledge, the IRT literature has not evaluated the change of posterior sampling geometries, as an alternative to improve the performance of the bayesian implementation of said models. This study is set to fill in part of this gap.

Third, the author evaluated the performance, recovery capacity and retrodictive accuracy of a first-order and second-order latent variable models (FOLV and SOLV, respectively). The decision was based on the literature of Confirmatory Factor Analysis (CFA), where before fitting a SOLV model (figure 4.2), the researcher need to asses if the correlation structure at the first level of the FOLV model (figure 4.1) justifies the decision.

Therefore, ten (10) data sets were generated for each study condition, following the algorithm in section 4.2. Each data set resembled responses to 25 binary scored items,

conforming to the SOLV model defined in figure 4.2. The model was motivated by the hypothesized structure for the reading comprehension sub-test, from the Peruvian public teaching career national assessment (see chapter 5). The latent structure, regression parameters, and loadings remained unchanged throughout the simulation replicas, to reduce experimental error [34].

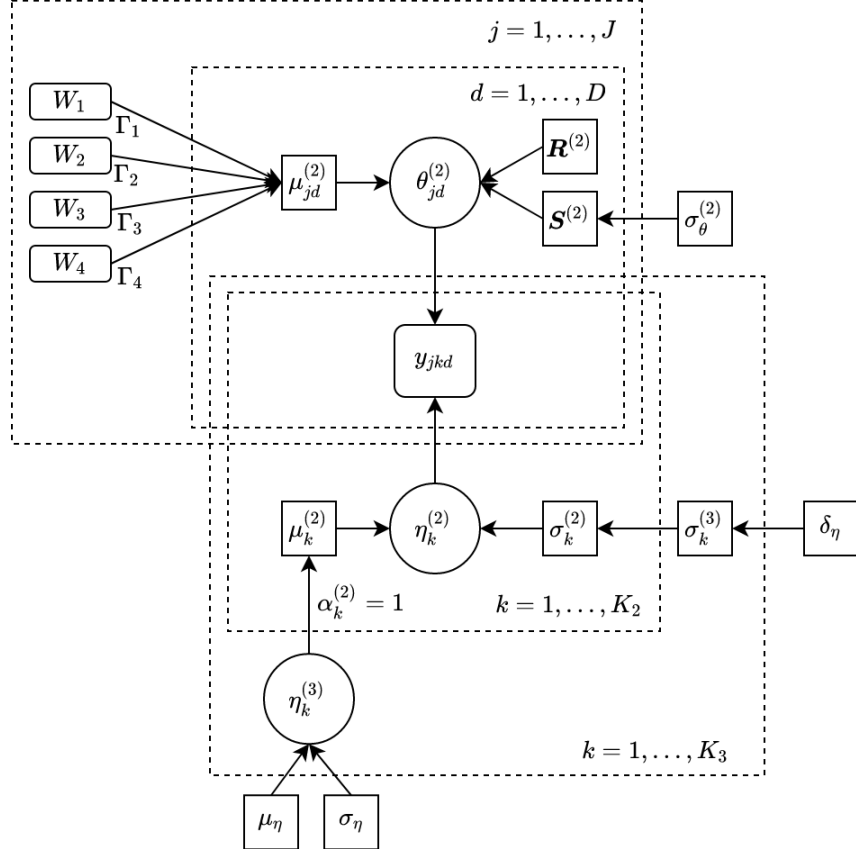


Figure 4.1: Directed Acyclic Graph (DAG). First Order Latent Variables model (FOLV). Circles represent latent variables. Squares represent parameters or parameters for priors. Large Squares represent nesting in specific units.

4.2 Algorithm

Each data replication was simulated following a six-step procedure. First, the author randomly simulated a collection of pseudo-covariates $\mathbf{W}_\theta = [W_1, W_2, W_3, W_4]$, motivated by a similar information set present in the reading comprehension sub-test. The generated covariates were: (i) a binary “gender” variable (W_1), describing males and females, (ii) an integer “age” variable (W_2) with range [30, 65], the latter corresponding to the age of retirement, (iii) a three-level categorical “education” variable (W_3), indicating the type of education the individual received: institute only, university only, or both; and finally (iv) a four-level categorical “experience” variable (W_4), denoting the individual’s years of work experience, where the higher the category, the higher the years of experience. Associated with these, the author defined their regression parameters $\boldsymbol{\Gamma}_\theta = [\Gamma_0, \Gamma_1, \Gamma_2, \Gamma_3, \Gamma_4]$ where: (i) $\Gamma_0 = 0$, indicating the absence of an intercept; (ii) $\Gamma_1 = [\gamma_m, \gamma_f] = [0, 1]$, for males and

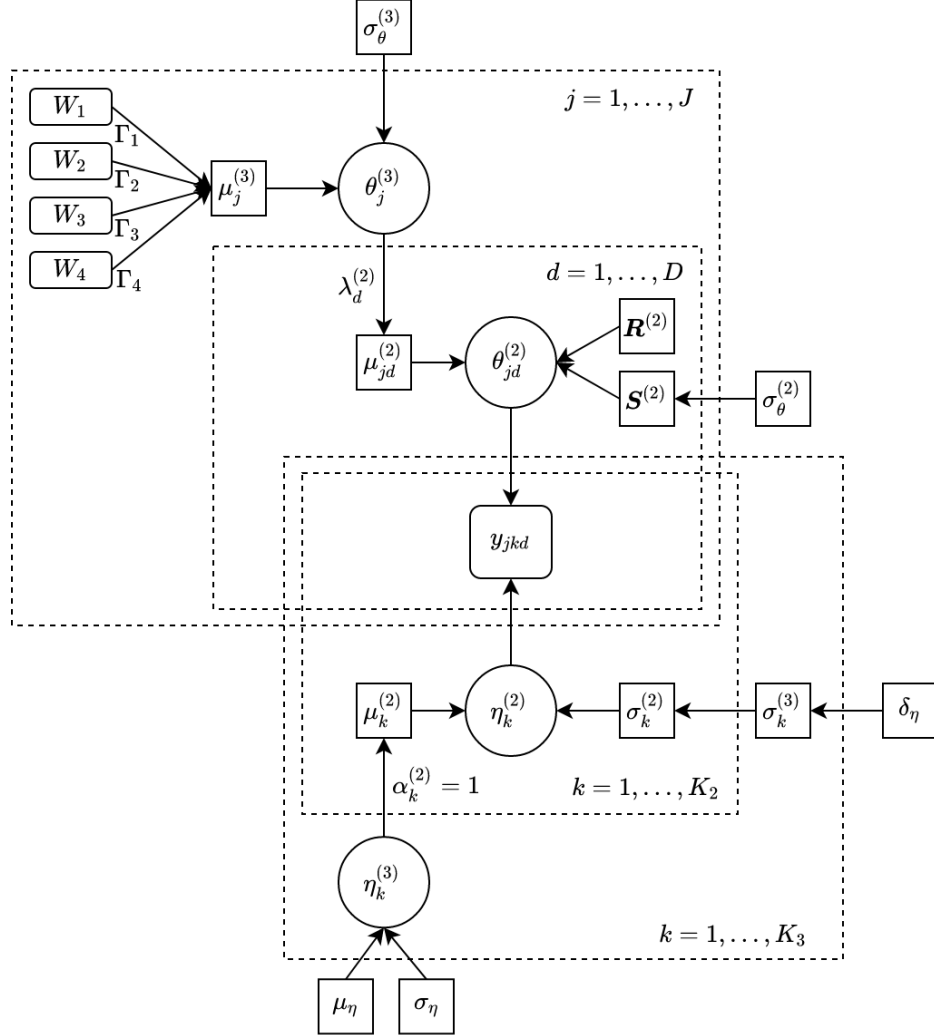


Figure 4.2: Directed Acyclic Graph (DAG). Second Order Latent Variables model (SOLV). Circles represent latent variables. Squares represent parameters or parameters for priors. Large Squares represent nesting in specific units.

females, respectively; (iii) $\Gamma_2 = -0.01$, indicating the individuals loose ability with age, in a linear manner; (iv) $\Gamma_3 = [\gamma_{io}, \gamma_{uo}, \gamma_b] = [-0.5, 0.5, 0]$, assuming individuals with only university degree have better ability levels, followed by individuals with both educations, and individuals with only institute degrees; and lastly (v) $\Gamma_4 = [\gamma_{0y}, \gamma_{5y}, \gamma_{10y}, \gamma_{11+y}] = [-0.5, 0, 0.35, 0.5]$, implying experience has decreasing returns on abilities.

Second, the study simulated the second- and first-order latent variables, corresponding to the reading comprehension ability and its three sub-dimensions: literal, inferential and reflective. Reading comprehension ($\theta_j^{(3)}$) was generated from a normal distribution $N(\mu_j^{(3)}, \sigma_\theta^{(3)})$, with $\mu_j^{(3)} = \boldsymbol{\Gamma}_\theta \mathbf{W}_\theta$, i.e. the linear combination of the simulated covariates and its corresponding regression parameters, and $\sigma_\theta^{(3)} = 0.5$. On the other hand, the three sub-dimensions were generated from a multivariate normal distribution $MVN(\boldsymbol{\mu}_j^{(2)}, \boldsymbol{\Sigma}^{(2)})$, with $\boldsymbol{\mu}_j^{(2)} = [\mu_{j1}^{(2)}, \mu_{j2}^{(2)}, \mu_{j3}^{(2)}] = [\lambda_1^{(2)}\theta_j^{(3)}, \lambda_2^{(2)}\theta_j^{(3)}, \lambda_3^{(2)}\theta_j^{(3)}]$, and $\boldsymbol{\Sigma}^{(2)} = \mathbf{S}^{(2)} \cdot \mathbf{R}^{(2)} \cdot \mathbf{S}^{(2)}$. In order to ensure the FOLV model in figure 4.1 lead us to the SOLV in figure 4.2, the

author assumed loadings $\boldsymbol{\lambda}^{(2)} = [\lambda_1^{(2)}, \lambda_2^{(2)}, \lambda_3^{(2)}] = [0.95, 0.95, 0.95]$. Using Wright's tracing rules [5], the latter implies the sub-dimension would have an approximate unconditional correlation of $0.95 \times 0.94 = 0.9025$. Lastly, $\mathbf{S}^{(2)} = \boldsymbol{\sigma}_{\theta}^{(2)} \mathbf{I}$, i.e. a diagonal standard deviation matrix with $\boldsymbol{\sigma}_{\theta}^{(2)} = [0.5, 0.5, 0.5]$; whereas $\mathbf{R}^{(2)} = \mathbf{I}$, i.e. an identity correlation matrix, implying the sub-dimensions are independent after accounting reading comprehension.

Third, the author defined five (5) common stimulus or texts for the items, where the mean difficulty for the texts $\boldsymbol{\eta}^{(3)} = [\eta_1^{(3)}, \eta_2^{(3)}, \eta_3^{(3)}, \eta_4^{(3)}, \eta_5^{(3)}] = [-1.50, -0.75, 0, 0.75, 1.50]$; whereas the deviation from said mean difficulties were $\sigma_k^{(3)} = 0.5$ for all texts.

Fourth, 25 items were randomly generated from independent normal distributions $N(\mu_k^{(2)}, \sigma_k^{(2)})$, with $\mu_k^{(2)} = \boldsymbol{\eta}^{(3)} \boldsymbol{\alpha}^{(2)} \mathbf{A}$ and $\sigma_k^{(2)} = \sigma_k^{(3)}$; where $\boldsymbol{\alpha}^{(2)} = \mathbf{1}$, indicating the difficulty of the common stimulus directly explained the difficulty of the items, and \mathbf{A} was a block design matrix that maps the items to its corresponding passage, defined in the previous step. Lastly, the dimensions the items were designed to measure were also generated at random.

Fifth, the author calculated the linear predictor v_{jkd} and probability of endorsing an item π_{jkd} , for each individual j on item k (belonging to dimension d), according to equations (2.5), (2.2), and (2.3), respectively; where the probability was calculated using the logistic inverse-link function.

Sixth and last, the outcome y_{jkd} was simulated from a Bernoulli distribution as in equation (2.1), with a probability of success calculated as in the previous step.

The code associated with the full simulation process can be found in Appendix B.2.1.

4.3 Parameter estimation

4.3.1 Models and identification

As stated in previous sections, we analyze two models: (i) the FOLV model depicted in figure 4.1, and (ii) the SOLV model depicted in figure 4.2. We proceed to enumerate the likelihood functions, and the full set of priors and hyper-priors used.

First, as stated in equations (3.6), (3.4) and (3.5), the distributional and systematic part of both models was defined as follows:

$$y_{jkd} \sim \text{Bernoulli}(\pi_{jkd}) \quad (4.1)$$

$$\text{logit}(\pi_{jkd}) = v_{jkd} \quad (4.2)$$

$$v_{jkd} = \theta_{jd}^{(2)} - \eta_k^{(2)} \quad (4.3)$$

Notice the linear predictor can be considered as a multilevel-multidimensional extension of the well known Rasch IRT model [62]. As stated in previous chapters, the reader should keep in mind that in order to avoid the use of heavy notation, the items' indexes did not reflect the fact that some items are set to measure specific individual's dimensions.

Second, the first-order latent variables and prior parameters were defined as follows:

$$\boldsymbol{\theta}_j^{(2)} = [\theta_{j1}^{(2)}, \theta_{j2}^{(2)}, \theta_{j3}^{(2)}] \quad (4.4)$$

$$\boldsymbol{\theta}_j^{(2)} \sim \text{MVNormal}(\boldsymbol{\mu}_j^{(2)}, \boldsymbol{\Sigma}^{(2)}) \quad (4.5)$$

where $\Sigma^{(2)}$ is defined by:

$$\Sigma^{(2)} = \mathbf{S}^{(2)} \cdot \mathbf{R}^{(2)} \cdot \mathbf{S}^{(2)} \quad (4.6)$$

$$\mathbf{S}^{(2)} = \boldsymbol{\sigma}_\theta^{(2)} \mathbf{I} = \begin{pmatrix} \sigma_1^2 & 0 & 0 \\ 0 & \sigma_2^2 & 0 \\ 0 & 0 & \sigma_3^2 \end{pmatrix} \quad (4.7)$$

$$\mathbf{R}^{(2)} = \begin{pmatrix} 1 & \rho_{12} & \rho_{13} \\ \rho_{21} & 1 & \rho_{23} \\ \rho_{31} & \rho_{32} & 1 \end{pmatrix} \quad (4.8)$$

while $\mu_j^{(2)}$ can be defined in two ways, depending on the model we are fitting. For the FOLV model depicted in figure 4.1, the mean vector would be defined as follows:

$$\boldsymbol{\mu}_j^{(2)} = [\mu_{j1}^{(2)}, \mu_{j2}^{(2)}, \mu_{j3}^{(2)}] \quad (4.9)$$

$$\mu_{jd}^{(2)} = \beta_G G_j + \beta_A (A_j - A_{\min}) + \beta_E E_j + \beta_X X_j \quad (4.10)$$

notice the regression parameters are not dimension specific. On the other hand, for the SOLV model depicted in figure 4.2, $\boldsymbol{\mu}_j^{(2)}$ would be defined by:

$$\boldsymbol{\mu}_j^{(2)} = [\mu_{j1}^{(2)}, \mu_{j2}^{(2)}, \mu_{j3}^{(2)}] \quad (4.11)$$

$$\boldsymbol{\lambda}^{(2)} = [\lambda_1^{(2)}, \lambda_2^{(2)}, \lambda_3^{(2)}] \quad (4.12)$$

$$\mu_{jd}^{(2)} = \lambda_d^{(2)} \theta_j^{(3)} \quad (4.13)$$

where d denotes the individual's dimension. Lastly, because the SOLV contemplates an additional level, corresponding to the reading comprehension ability, an additional set of parameters is defined as follows:

$$\theta_j^{(3)} \sim \text{Normal}(\mu_j^{(3)}, \sigma_\theta^{(3)}) \quad (4.14)$$

$$\mu_j^{(3)} = \beta_G G_j + \beta_A (A_j - A_{\min}) + \beta_E E_j + \beta_X X_j \quad (4.15)$$

Third, turning now our attention to the items' parameters $\eta_k^{(2)}$, for both models we have:

$$\eta_k^{(2)} \sim \text{Normal}(\mu_k^{(2)}, \sigma_k^{(2)}) \quad (4.16)$$

$$\mu_k^{(2)} = \boldsymbol{\eta}^{(3)} \mathbf{A} \quad (4.17)$$

$$\sigma_k^{(2)} = \boldsymbol{\sigma}^{(3)} \mathbf{A} \quad (4.18)$$

where $k = 1, \dots, 25$ items, $\boldsymbol{\eta}^{(3)} = [\eta_1^{(3)}, \eta_2^{(3)}, \eta_3^{(3)}, \eta_4^{(3)}, \eta_5^{(3)}]$ represent the texts difficulties, $\boldsymbol{\sigma}^{(3)} = [\sigma_1^{(3)}, \sigma_2^{(3)}, \sigma_3^{(3)}, \sigma_4^{(3)}, \sigma_5^{(3)}]$ the text deviations from such difficulties; and \mathbf{A} is the block matrix that maps the items with its corresponding passage. In addition, $\eta_k^{(3)}$ and $\sigma_k^{(3)}$ are distributed as:

$$\eta_k^{(3)} \sim \text{Normal}(\mu_\eta, \sigma_\eta) \quad (4.19)$$

$$\sigma_k^{(3)} \sim \text{Exponential}(\delta_\eta) \quad (4.20)$$

Fourth, we declared all the hyper-priors required:

$$\mathbf{R}^{(2)} \sim \text{LkjCorrelation}(2) \quad (4.21)$$

$$\beta_G \sim \text{Normal}(0, 0.5) \quad (4.22)$$

$$\beta_A \sim \text{Normal}(0, 0.5) \quad (4.23)$$

$$\beta_E \sim \text{Normal}(0, 1) \quad (4.24)$$

$$\beta_X \sim \text{Normal}(0, 0.5) \quad (4.25)$$

where $\text{LkjCorrelation}(\cdot)$ denotes the Lewandowski, Kurowicka, and Joe correlation distribution [37].

Finally, in order to fully specify the model and provide a scale for the latent variables, the current research decided to set the scale of the higher order dimension and sub-dimensions to one, i.e. $\sigma_\theta^{(3)} = 1$, and $\mathbf{S}^{(2)} = \boldsymbol{\sigma}_\theta^{(2)} \mathbf{I}$ with $\boldsymbol{\sigma}_\theta^{(2)} = [1, 1, 1]^T$, commonly known as the unit variance identification scheme (UVI). Moreover, to identify the texts' and items' parameters we set $\mu_\eta = 0$, $\sigma_\eta = 1$, $\delta_\eta = 2$.

Notice we need to set the scales for all the dimensions equal to one, because otherwise the latent structure would not be identified. At the level of the FOLV (level-2), we would have $(3 \times 4)/2 = 6$ pieces of information available, corresponding to the variances and covariances of the FOLV. The information then will need to estimate 10 parameters, i.e. 3 loadings, 4 variances corresponding to the FOLV and SOLV, and 3 correlations among sub-dimensions. Therefore, by restricting the variances to one, we have enough information to estimate the other parameters of interest (loadings and correlations). Additionally, this is further justified by the fact that latent variables have no inherent unit in which they are measured, consequently, setting their scale is an arbitrary decision [5].

4.3.2 Prior predictive investigation

As it was outlined in section 3.3.5, we will use prior predictive investigation to assess and visualize the consequences of our prior assumptions. The implications will be assessed from two perspectives: the IRT and the outcome space perspective. For the former, we will investigate what the set of priors imply for the item characteristic curves (ICC), and item information function (IIF). For the latter, we will examine how the prior assumption translate onto the outcome space.

First, it will be useful to define the ICC and IIF functions. Hambleton and Swaminathan [26] defined the ICC as the mathematical function that relates the probability of success on an item, to the ability measured by that same item. In our current implementation, such function would correspond to the systematic part of the GLLAMM, as defined in equations (2.2) and (2.3):

$$\text{ICC} = \pi_{jkd} = \frac{\exp(v_{jkd})}{1 + \exp(v_{jkd})} \quad (4.26)$$

where the linear predictor v_{jkd} contains the items' dimensions $\eta_k^{(m)}$ and the individuals' abilities $\theta_{jd}^{(l)}$, as defined in equation 2.4. As previously mentioned, the ICC of our current implementation can be considered as the multilevel-multidimensional extension to the Rasch model's ICC.

On the other hand, the same authors defined the IIF as a function that measured the amount of information provided by an item. In this setting, “information” is understood as the reduction of uncertainty, resulting from using an item to measure the ability of an individual. Given the above, the IIF for the GLLAMM will be defined as in its Rasch counterpart, in the following form:

$$\text{IIF} = \pi_{jkd} (1 - \pi_{jkd}) \quad (4.27)$$

Figure 4.3 shows the ICC and IIF for the FOLV (figure 4.1), resulting from the assumptions integrated by the priors detailed in the previous section. From panel (A), we can notice the difficulty of the items match a wide range of the individuals’ abilities (see multiple black solid lines). This means that the model expect items’ difficulties to be in any part of the continuous range of abilities, with no restriction. Furthermore, the latter imply the priors allow the model to obtain information about individuals, located in the full significant range of the abilities, as seen in panel (B) of the same figure. All of this just means that no unintended assumption has “creep” into the model, at least from the IRT perspective. A similar result can be seen for the SOLV (figure A.4, appendix).

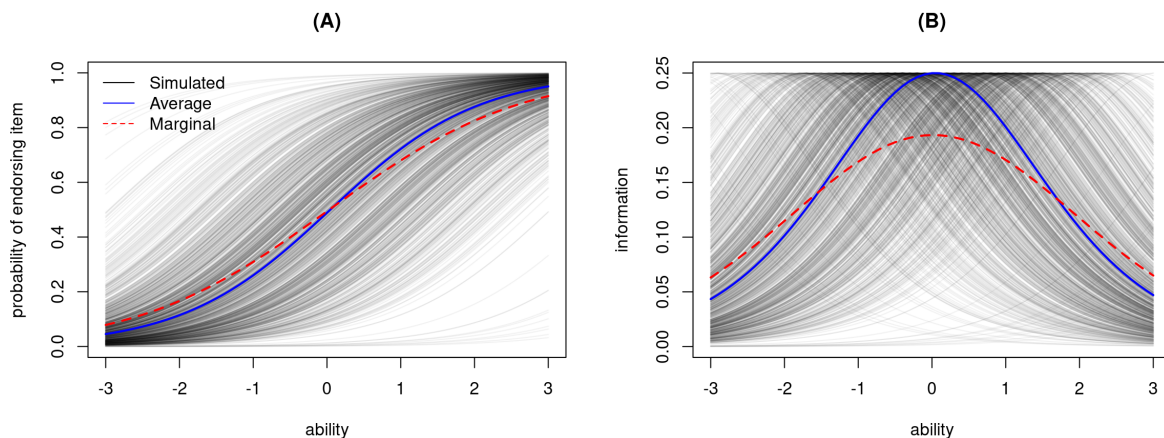


Figure 4.3: First-Order latent variable model (FOLV). (A) Item Characteristics Curve, ICC. (B) Item Information Function, IIF.

Finally, from figure 4.4 and 4.5, we notice that no unintended assumption has been translated to the outcome space of the FOLV either. Panel (A) from figure 4.4 shows the individuals’ proportion of correctly answered items, can be present in the full range of possibilities. Furthermore, panel (B) of the same figure, shows the proportion of individuals endorsing an item, for any item, can also be present in the full range of possibilities. Lastly, panels (C) and (D) convey similar information aggregated by texts and dimensions. On the other hand, from all panels in figure 4.5, we can observe the priors did not force the model to assume any apriori tendency in the covariates. A similar result can be seen for the outcome space of the SOLV (figures A.5 and A.6, appendix).

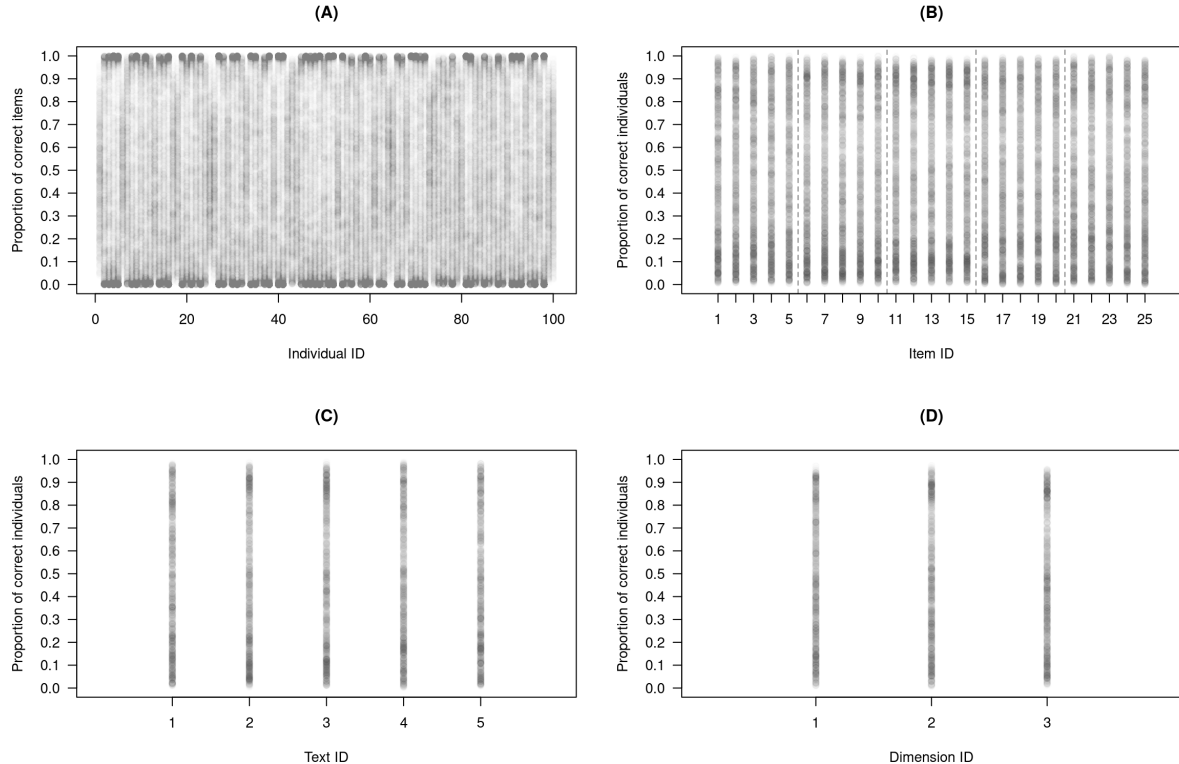


Figure 4.4: First-Order latent variable model (FOLV). Aggregated endorsement rate per: (A) individuals, (B) items, (C) text or passage, and (D) measured dimension.

4.4 Evaluation criteria

As stated in section 4.1, the study was set to evaluate the performance, recovery capacity, and retrodictive accuracy of the bayesian implementation.

First, to assess the performance of the MCMC chains, in terms of achieving stationarity, convergence and good mixing, the author followed the usual visual approach. The approach involved the visual evaluation of (i) trace plots, for stationarity and convergence, and (ii) trunk and autocorrelation plots (ACF), for good mixing. Moreover, the assessment of convergence and good mixing were supported by the `Rhat` and `n_eff` statistics developed in Gelman et al. [22] (pp. 284 – 287).

Second, to evaluate the recovery capacity for all parameters $\Omega = \{\beta, \Lambda, \Theta, \Psi, \Gamma\}$, the author used the root mean squared error (RMSE), i.e. the extent of the deviation the posterior means exhibited from the true generating values, in all replicate simulations. Notice, in the case of the FOLV model no loading recovery can be assessed; however, using Wright's tracing rules, we evaluated the implied correlation structure between the sub-dimensions, resulting from having a second-order latent variable. The RMSE for each parameter of interest was defined as follows:

$$RMSE(\eta_k^{(m)}) = \sqrt{\frac{1}{R} \sum_{r=1}^R (\hat{\eta}_{kr}^{(m)} - \eta_k^{(m)})^2} \quad (4.28)$$

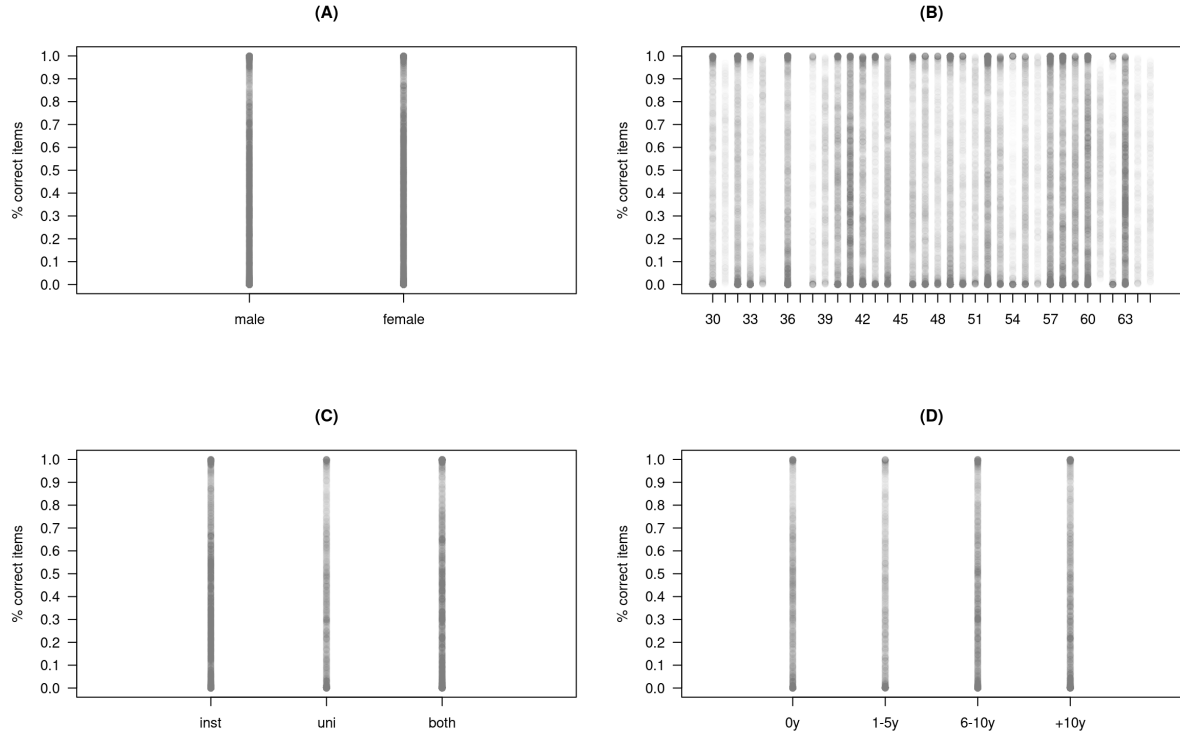


Figure 4.5: First-Order latent variable model (FOLV). Aggregated endorsement rate per simulated covariate: (A) gender, (B) age, (C) education, and (D) experience.

$$RMSE \left(\theta_{jd}^{(l)} \right) = \sqrt{ \frac{1}{R} \sum_{r=1}^R \left(\hat{\theta}_{jdr}^{(l)} - \theta_{jd}^{(l)} \right)^2 } \quad (4.29)$$

$$RMSE \left(\Gamma_w \right) = \sqrt{ \frac{1}{R} \sum_{r=1}^R \left(\hat{\Gamma}_{wr} - \Gamma_w \right)^2 } \quad (4.30)$$

$$RMSE \left(\lambda_d^{(l)} \right) = \sqrt{ \frac{1}{R} \sum_{r=1}^R \left(\hat{\lambda}_{dr}^{(l)} - \lambda_d^{(l)} \right)^2 } \quad (4.31)$$

where the “hat” parameters with index r described the posterior mean in replica $r = 1, \dots, R$, with $R = 10$, and each posterior mean was calculated with 3 chains of 1,000 iterations each.

Finally, since IRT models are known to be invariant to the shift of the linear predictor [4, 7], i.e. the addition/subtraction of a constant to the abilities/difficulties results in the same probability value, it could happen that we observe substantial differences in the recovery of the parameters, that not necessarily implies a classification error [75]. Therefore, to avoid a mistake in the assessment of fit of the model, the current research will use posterior predictive checks, i.e. retrodictive accuracy.

What are they?, at which aggregation dimensions?: for individuals in different dimensions, items, and texts.

4.5 Results

4.5.1 Chain performance

First, the CP and NCP chain performance for the texts' mean difficulties is reported in figures 4.6 and 4.7, respectively. The figures correspond to replica number two of the FOLV model, with a simulated sample size of 100.

From the figures, one can easily notice the parameters under the CP did not show signs of achieving ergodicity. The chains showed a clear lack of stationarity and convergence (left panels). Moreover, the iterations did not explore the posterior distribution appropriately, hinting a lack of good mixing, e.g. the top trace and trunk plots show chains that are "stuck" in specific areas of the distribution. In addition, the ACF plots reveal the chain iterations were highly auto-correlated, again indicating a serious lack of good mixing. All of this is further confirmed by panels (A) and (C) of figure 4.8, where we can see the CP has low effective samples sizes (`n_eff`) and higher than appropriate `Rhat` values, compared to the NCP.

On the contrary, the parameters from the NCP seem to achieve ergodicity. The trace plots show chains that seem to be stationary and convergent. The trunk plots show the rapid exploration of the full range of posterior distribution. And finally, the ACF plots show the iterations were less auto-correlated. Again, this is further confirmed by figure 4.8, where the NCP show greater `n_eff` and appropriate `Rhat` values, versus the CP.

On the other hand, figures A.7 and A.8 (appendix) show the the CP and NCP trace, trunk, and ACF plots for the the difficulties' deviations of the texts. At a simple glance, the plots seem to indicate that both parametrizations achieve a similar level of ergodicity. However, from panels (A) and (C) in figure 4.8, we can notice that while both parametrization show an $Rhat < 1.05$, the CP effectively has sample sizes in a larger range than the NCP, i.e. [35, 2734] and [897, 2587], respectively. The latter just indicates the NCP has less auto-correlated chains, and therefore a bit better mixing.

Furthermore, figures A.9 and A.10 (appendix) show the chain performance for the item difficulties under the CP and NCP, respectively. The trace, trunk and ACF plots show a similar pattern as the one outlined for the difficulty of the texts, albeit more extreme. The CP chains did not achieved stationarity, convergence, nor good mixing; whereas it seems the NCP does. This is further confirmed by panels (B) and (D) of figure 4.8, where one can see the NCP has significantly higher effective sample sizes and $Rhat < 1.05$, in contrast to the CP.

Second, the chain performance for the reading comprehension sub-dimensions, under the CP are reported in figures A.11, A.13, A.15. The figures correspond to replica number six of the FOLV model, with a simulated sample size of 100. The chains also show a lack of ergodicity similar to the texts' difficulties, e.g. the left panels of figure A.15 show chains that did not explore the posterior distribution appropriately (see straight lines in chains). This is further confirmed by panels (A) through (D) in figure A.27, where the CP has effective sample sizes in the range of [8, 527], while an important proportion of the parameters is above the recommended `Rhat` threshold. In contrast, the NCP chains for the sub-dimensions achieve ergodicity, as it is shown in figures A.12, A.14, A.16 and confirmed by the `n_eff` and `Rhat` values in figure A.27.

Third, similar visualizations for the CP and NCP regression parameters are shown in figures A.17 and A.18. With a careful inspection of the CP trace plots, one can notice

we still have chains that are “stuck” in specific part of the posterior distribution (see green lines). As a result, the CP registered lower effective samples sizes than the NCP, as figure A.28 confirms. However, neither of those things prevented the CP achieving convergence, as the `Rhat` in the same figure confirms. In contrast, the NCP parameters seem to achieve stationarity, convergence, and good mixing without any issues, with higher effective sample sizes and `Rhat` values close to one.

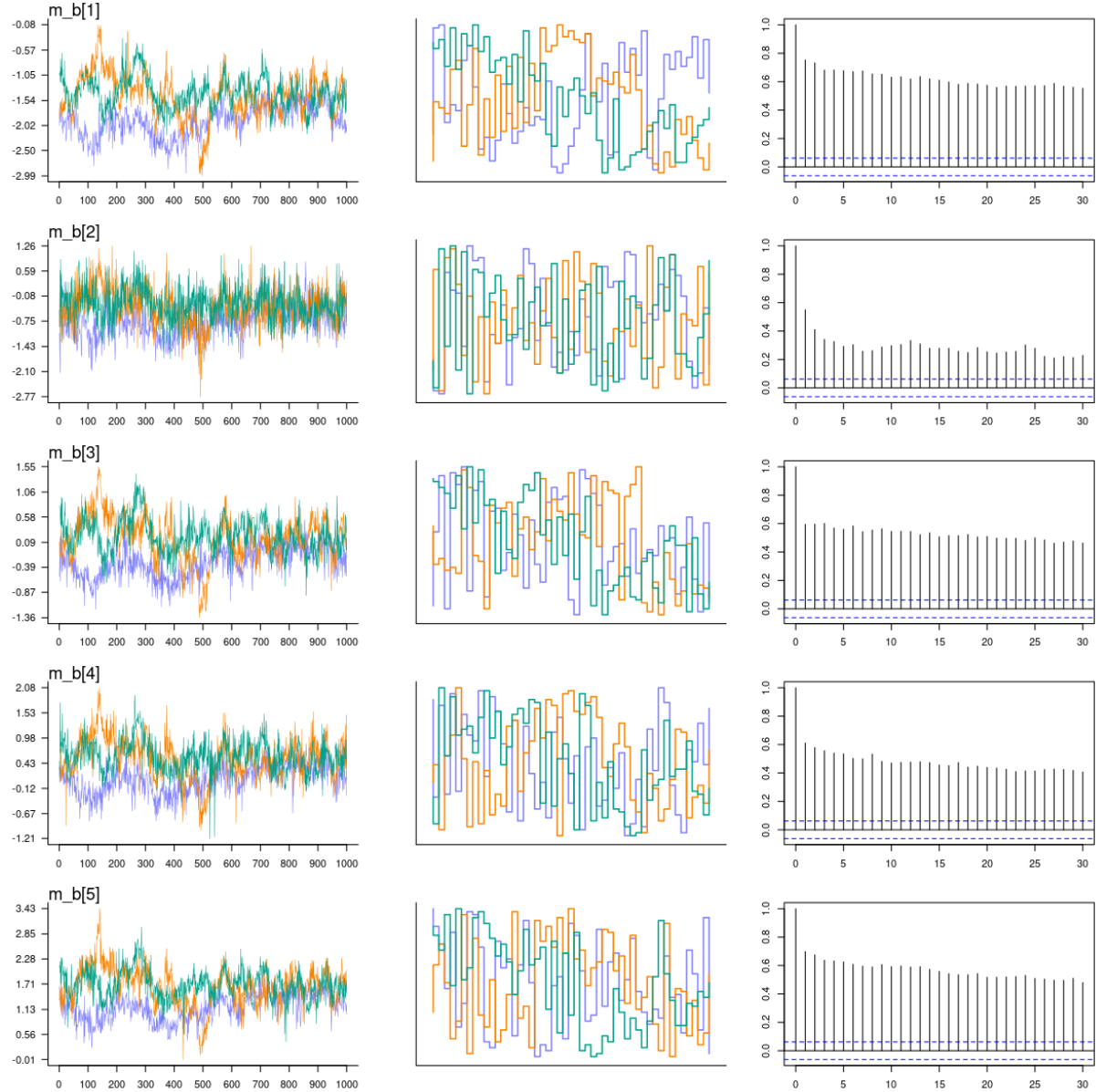


Figure 4.6: First-Order latent variable model (FOLV). Sample size 100, replica number 2. Centered parametrization. Mean difficulty per text: (Left) trace plot, (Middle) trunk plot, (Right) auto-correlation plot.

Lastly, the performance assessment plots for the FOLV sub-dimensions’ correlation are shown in figures A.19 and A.20. In both parametrizations, we observe the correlations seem to achieve stationarity and convergence. However, it also seems they do not achieve

good mixing, i.e. the MCMC procedure does not manage to make a proper investigation of the posterior. This is further confirmed by panels (B) and (D) from figure A.28, where we see observe the parameters' chains remain below the R_{hat} recommended threshold, indicating convergence. Although, the effective sample sizes were low, in the range of [249, 1311] for CP, and [285, 1283] for NCP, indicating highly auto-correlated iterations.

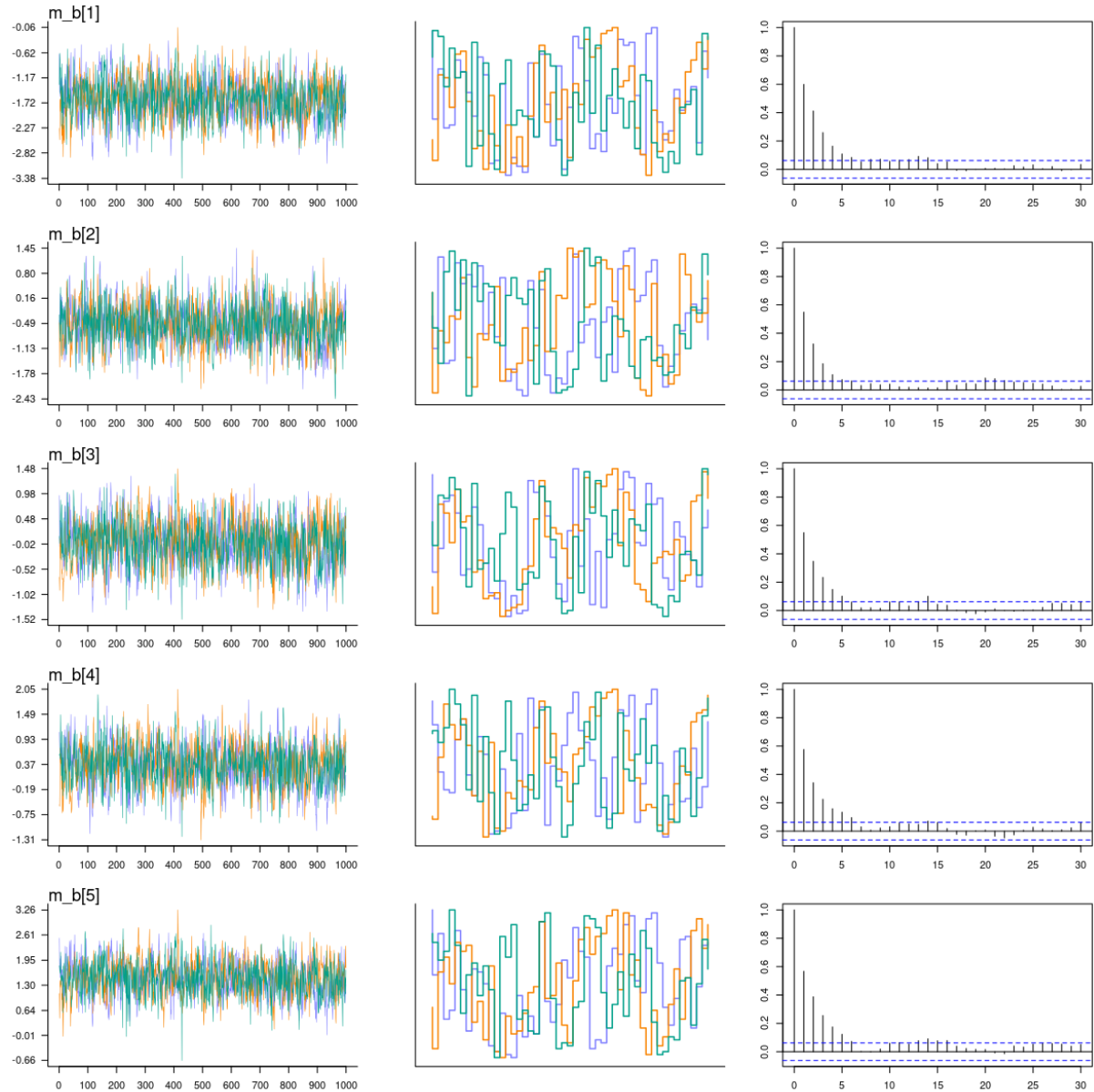


Figure 4.7: First-Order latent variable model (FOLV). Sample size 100, replica number 2. Non-centered parametrization. Mean difficulty per text: (Left) trace plot, (Middle) trunk plot, (Right) auto-correlation plot.

So far we have only assessed specific replicas of the FOLV model, with a simulated sample size of 100, as the previous paragraphs and title of the figures have indicated.

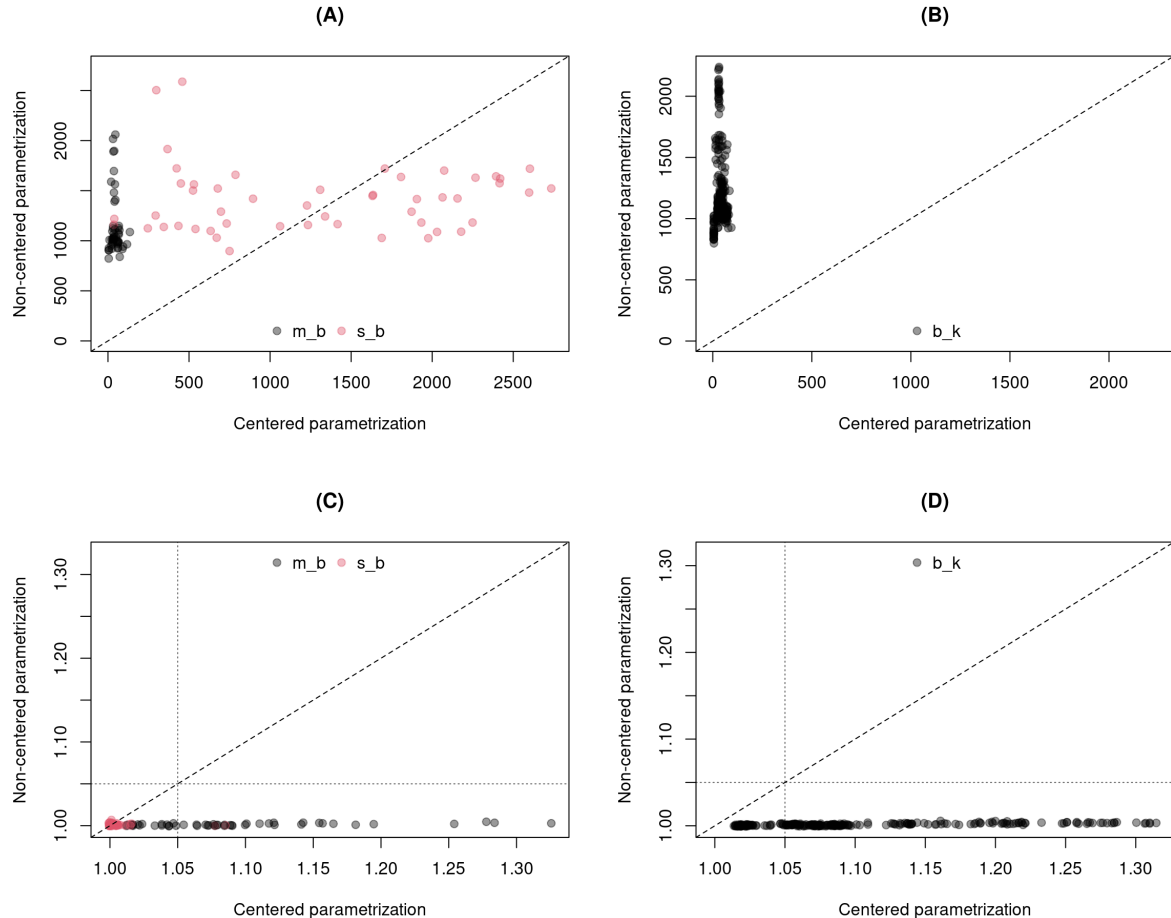


Figure 4.8: First-order latent variable model (FOLV). Sample size 100, all replicas. CP and NCP comparison plot. (A) n_{eff} for texts' mean difficulty and standard deviation of difficulty. (B) n_{eff} for items's difficulties. (C) $Rhat$ for texts' mean difficulty and standard deviation of difficulty. (D) $Rhat$ for items's difficulties. Diagonal discontinuous line describes equality between CP and NCP. Vertical and horizontal discontinuous lines is set at $Rhat = 1.05$.

However, after the inspection of the trace, trank, ACF and comparison plots¹, we notice the preceding patterns of stationarity, convergence and mixing extends to all replicas and simulated sample sizes in the FOLV model. Furthermore, the aforementioned patterns were also observed in the similar parameter set of the SOLV model.

Additionally, for the remaining parameters in the SOLV, i.e. the loadings and reading comprehension higher-order latent variables, we continue observing the recurrent pattern between CP and NCP, detailed in previous paragraphs. Figures A.21 and A.22 show the NCP loadings have chains that seem slightly more stationary, convergent, and well mixed than its CP counterpart. This is further confirmed by panels (B) and (D) of figure A.29. In a similar fashion, figures A.25 and A.26 show the higher-order latent variable

¹To inspect the remaining trace, trank, ACF, and comparison plots follow the github accompanying page detailed in Appendix A.2.2.

is significantly more ergodic under the NCP than the CP, and figure A.30 confirms the hypothesis, by showing it has largely better effective sample sizes, with R_{hat} values always close to one.

Finally, panel (A) of figure A.31 show the pattern of ergodicity for the regression parameters is slightly improved under the SOLV², i.e. the chains have larger effective sample sizes under the NCP versus the CP, indicating less correlation among the iterations, and therefore, better mixing. The result appear to be sensible, if we consider that the SOLV model was the data generating model.

Ultimately, the patterns for this set of parameters is also consistent across replicas and simulated sample sizes. Consequently, all of the above just show the NCP largely improved the performance of the MCMC chains under our implementation, for all models and almost all of the parameters. It is important to point out, the result did not extend to the sub-dimensions' correlation parameters, where no large difference was observed between the CP and NCP. On this matter, the issue was not related to a lack of identification of said parameters, as we were careful of ensuring this requirement.

4.5.2 Recovery capacity

4.5.3 Retrodictive accuracy

4.5.4 Time

Parametrization	Sample	Time		
		mean	min	max
1 CP	100	288.23	113.26	453.67
2 CP	250	470.85	335.86	994.39
3 CP	500	1149.25	1032.27	1351.92
4 NCP	100	116.49	104.35	133.99
5 NCP	250	430.86	406.58	503.91
6 NCP	500	1342.93	1207.00	1717.22

Table 4.1: FOLV running time statistics.

Parametrization	Sample	Time		
		mean	min	max
1 CP	100	242.30	83.54	513.22
2 CP	250	428.00	313.32	689.50
3 CP	500	968.54	867.03	1183.53
4 NCP	100	112.33	97.27	136.72
5 NCP	250	355.01	311.75	407.40
6 NCP	500	994.65	802.05	1095.33

Table 4.2: SOLV running time statistics.

²For the trace, trank and ACF plots refer to the corresponding accompanying page detailed in Appendix A.2.2.

Chapter 5

Application

5.1 Instruments

5.2 Data

5.2.1 Collection

5.2.2 Sample scheme

5.3 Results

All of the preceding suggests one way to navigate overfitting and underfitting: Evaluate our models out-of-sample. using cross validation and information criteria

Pareto-smoothed importance sampling cross-validation (PSIS) and the Widely Applicable Information Criterion (WAIC).

Chapter 6

Conclusion and Discussion

6.1 Discussion

6.2 Conclusions

6.3 Future development

Investigate this, maybe you need to use Variational Inference methods

It is important to point out, the result did not extend to the sub-dimensions' correlation parameters, where no large difference was observed between the CP and NCP. On this matter, the issue was not related to a lack of identification of said parameters, as we were careful of ensuring this requirement.

Appendix A

Additional plots and tables

A.1 Chapter 3: Bayesian estimation

A.1.1 To center or not to center

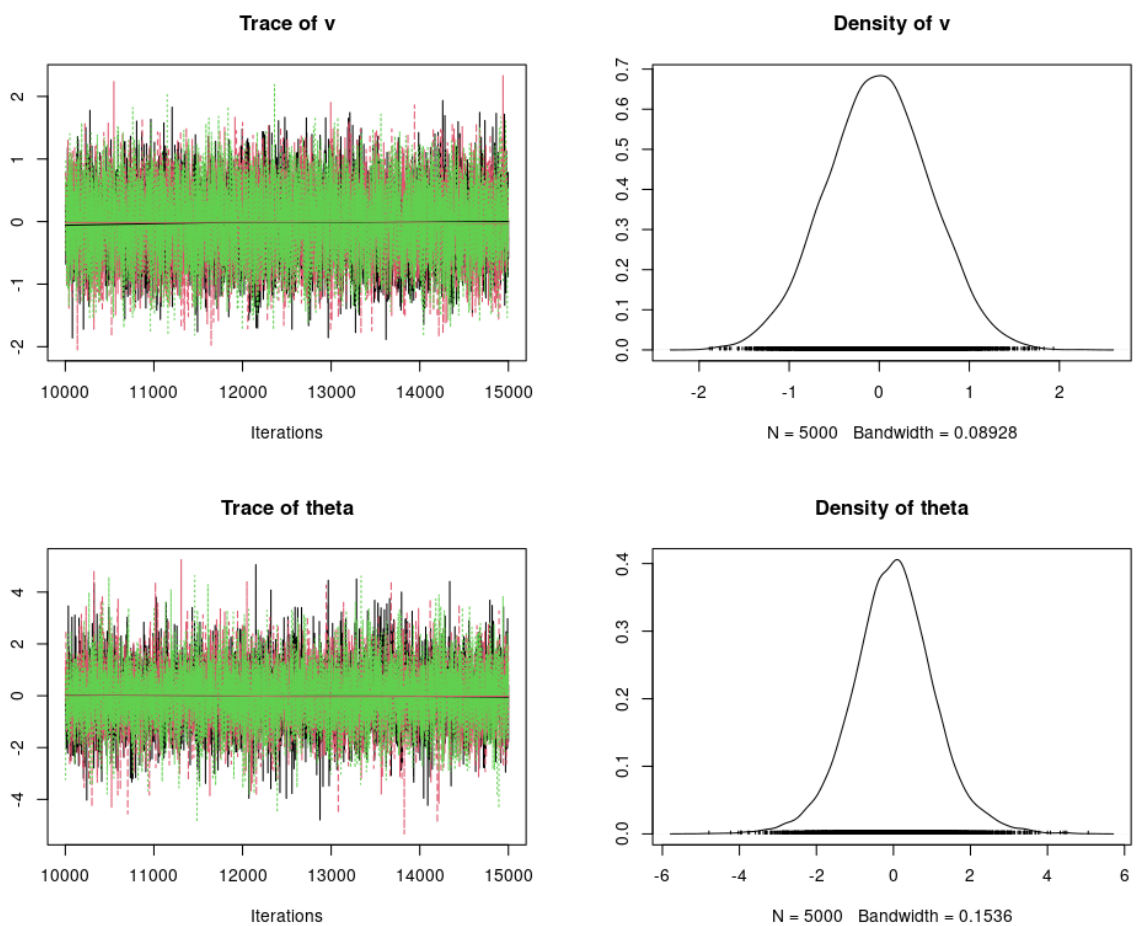


Figure A.1: The Devil's funnel. Centered Parametrization implemented in JAGS. It shows the traceplot and distribution of the parameters of interest.

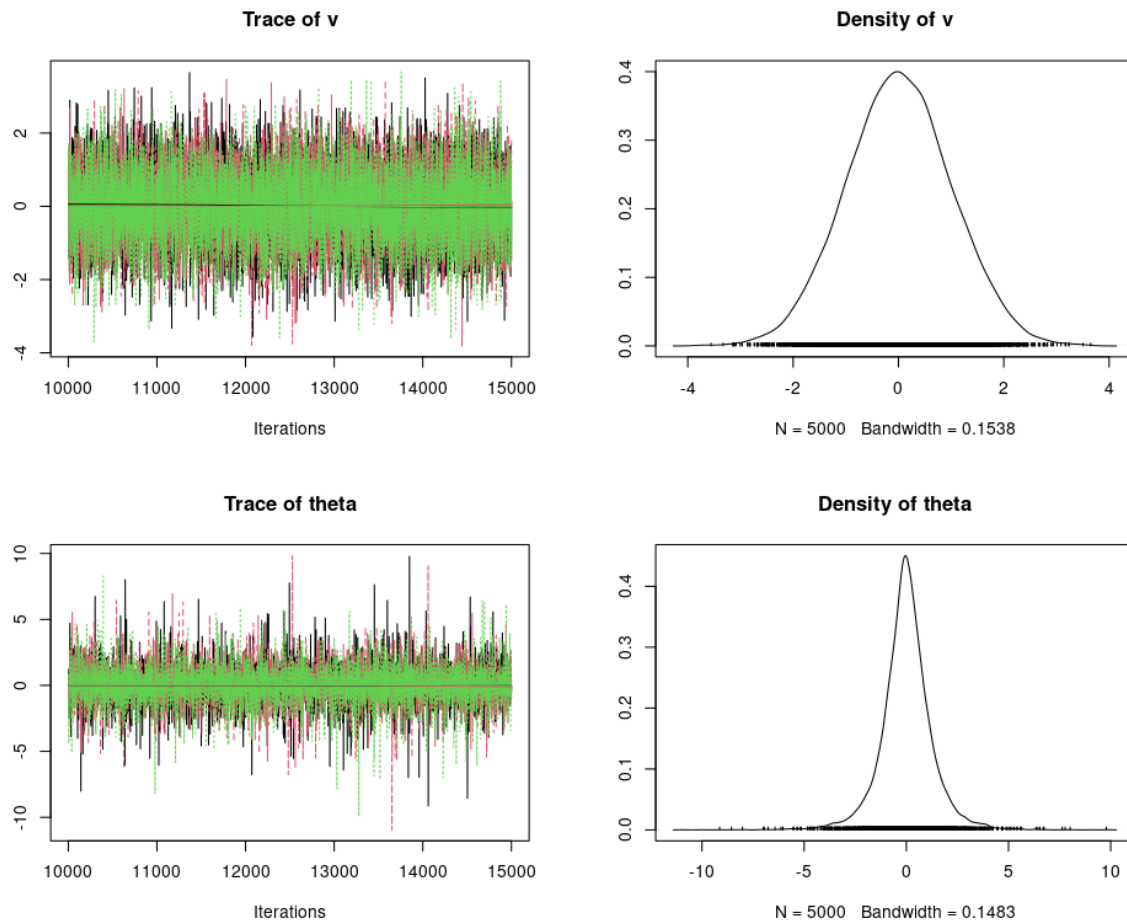


Figure A.2: The Devil's funnel. Centered Parametrization with mildly informative priors implemented in JAGS. It shows the traceplot and distribution of the parameters of interest.

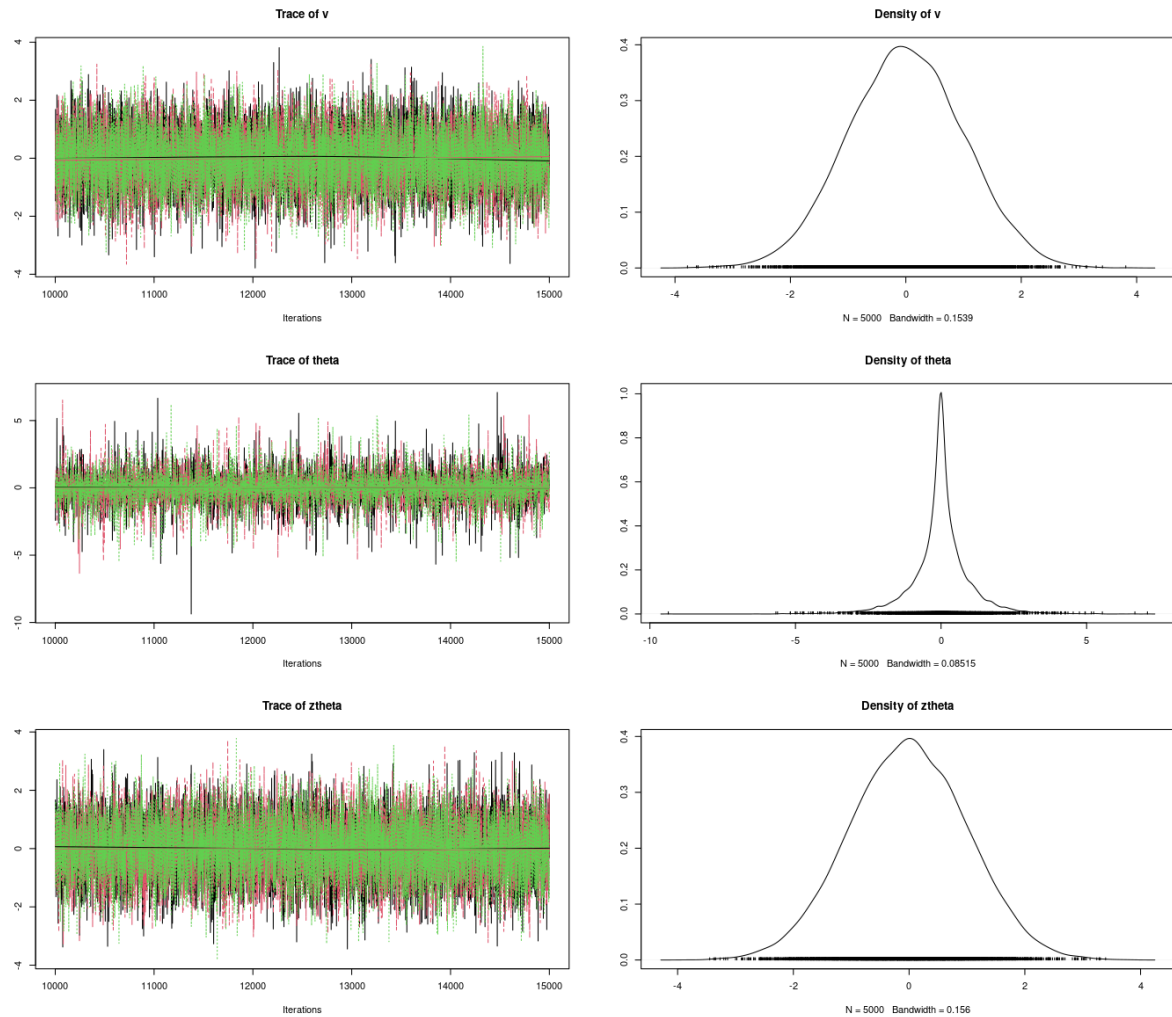


Figure A.3: The Devil's funnel. Non-Centered Parametrization implemented in JAGS. It shows the traceplot and distribution of the parameters of interest.

A.2 Chapter 4: Simulation study

A.2.1 Prior elicitation

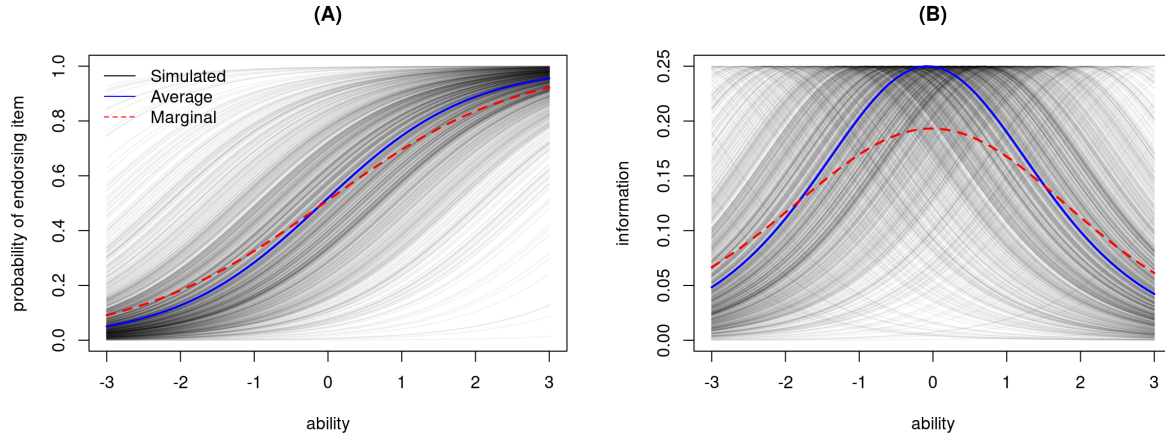


Figure A.4: Second-Order latent variable model (SOLV). (A) Item Characteristics Curve, ICC. (B) Item Information Function, IIF.

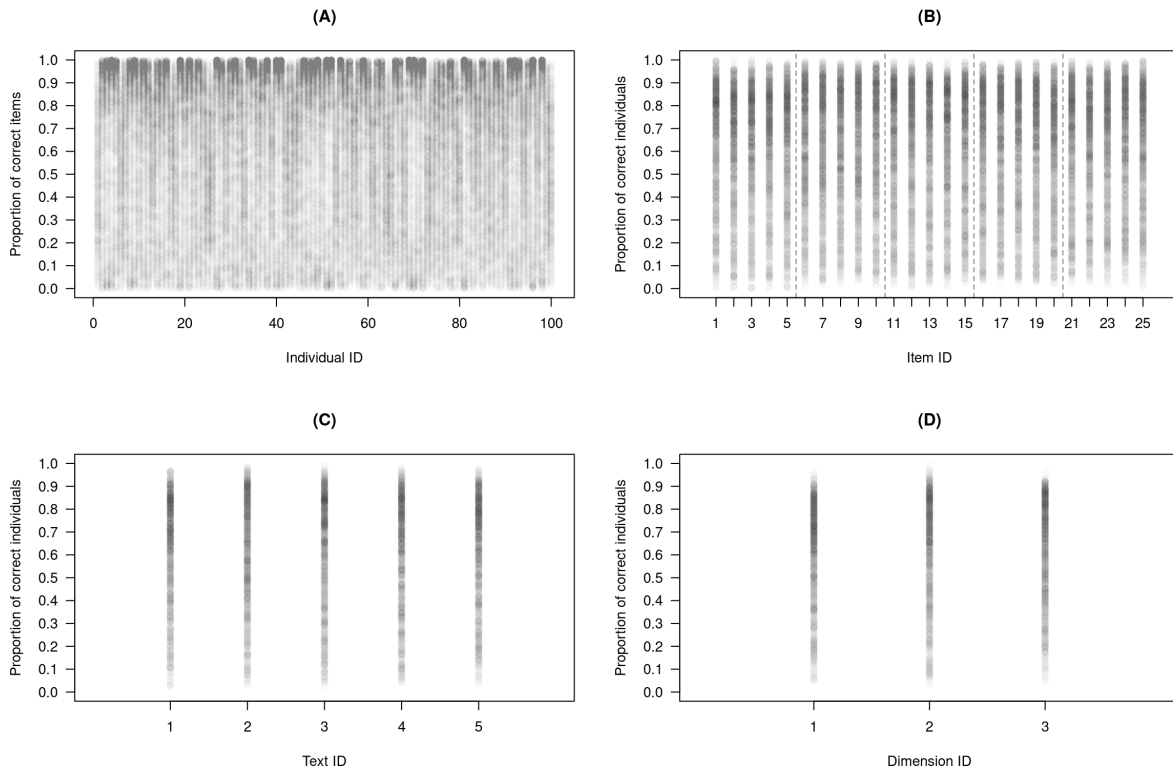


Figure A.5: Second-Order latent variable model (SOLV). Aggregated endorsement rate per: (A) individuals, (B) items, (C) text or passage, and (D) measured dimension.

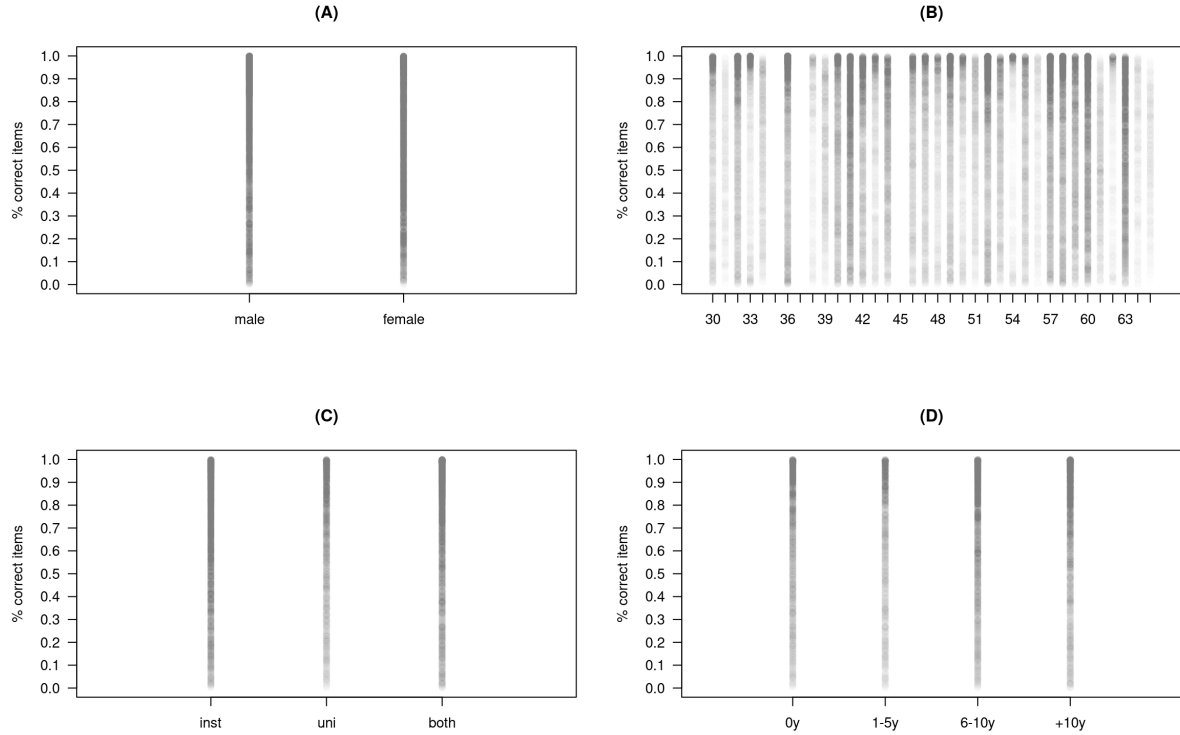


Figure A.6: Second-Order latent variable model (SOLV). Aggregated endorsement rate per simulated covariate: (A) gender, (B) age, (C) education, and (D) experience.

A.2.2 Chain performance

This section only shows a small set of trace, rank and ACF plots for the parameters of interest. For all the plots across parameters, models, parametrizations, and replicas refer to the images section of the accompanying github page:

<https://github.com/jriveraespejo/thesis/tree/master/images/chains>

Similarly, the CP and NCP `n_eff` and `Rhat` comparison plots shown here is a small set of the full available plots. For the set of figures across parameters, models, and replicas refer to the corresponding image section of the accompanying github page:

https://github.com/jriveraespejo/thesis/tree/master/images/chains_stat

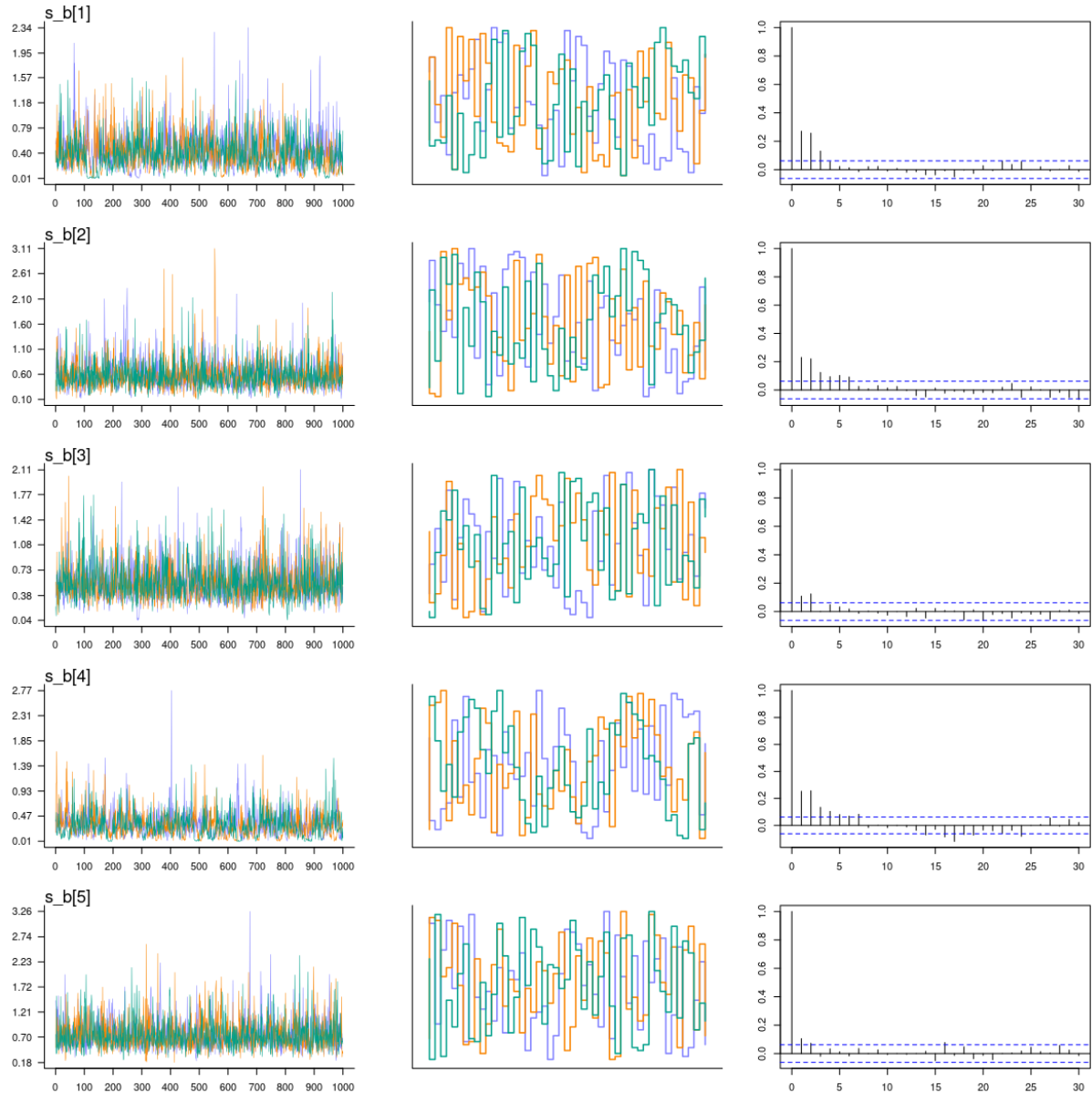


Figure A.7: First-Order latent variable model (FOLV). Sample size 100, replica number 3. Centered parametrization. Difficulty deviation per text: (Left) trace plot, (Middle) trunk plot, (Right) auto-correlation plot.

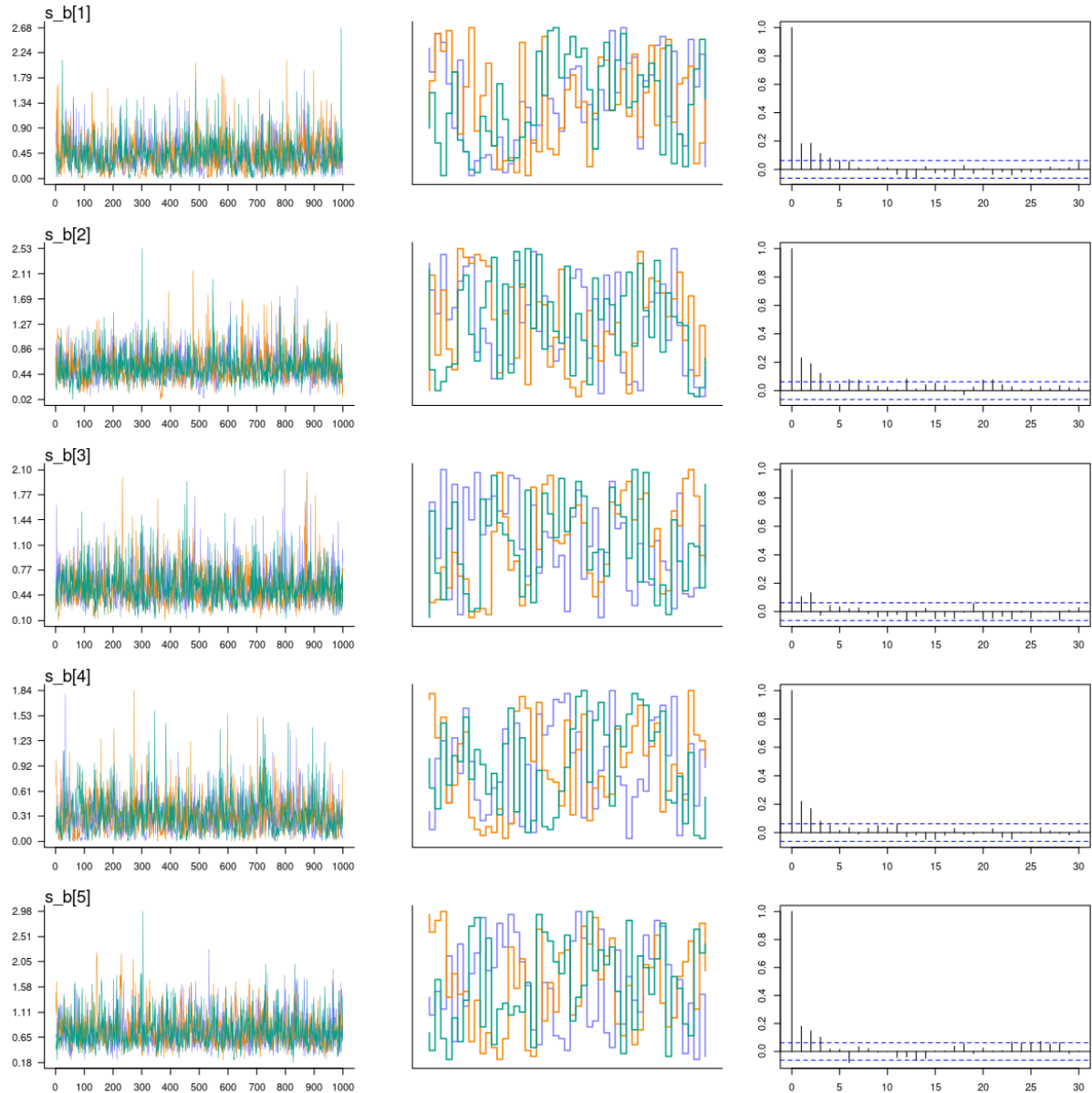


Figure A.8: First-Order latent variable model (FOLV). Sample size 100, replica number 3. Non-centered parametrization. Difficulty deviation per text: (Left) trace plot, (Middle) trunk plot, (Right) auto-correlation plot.

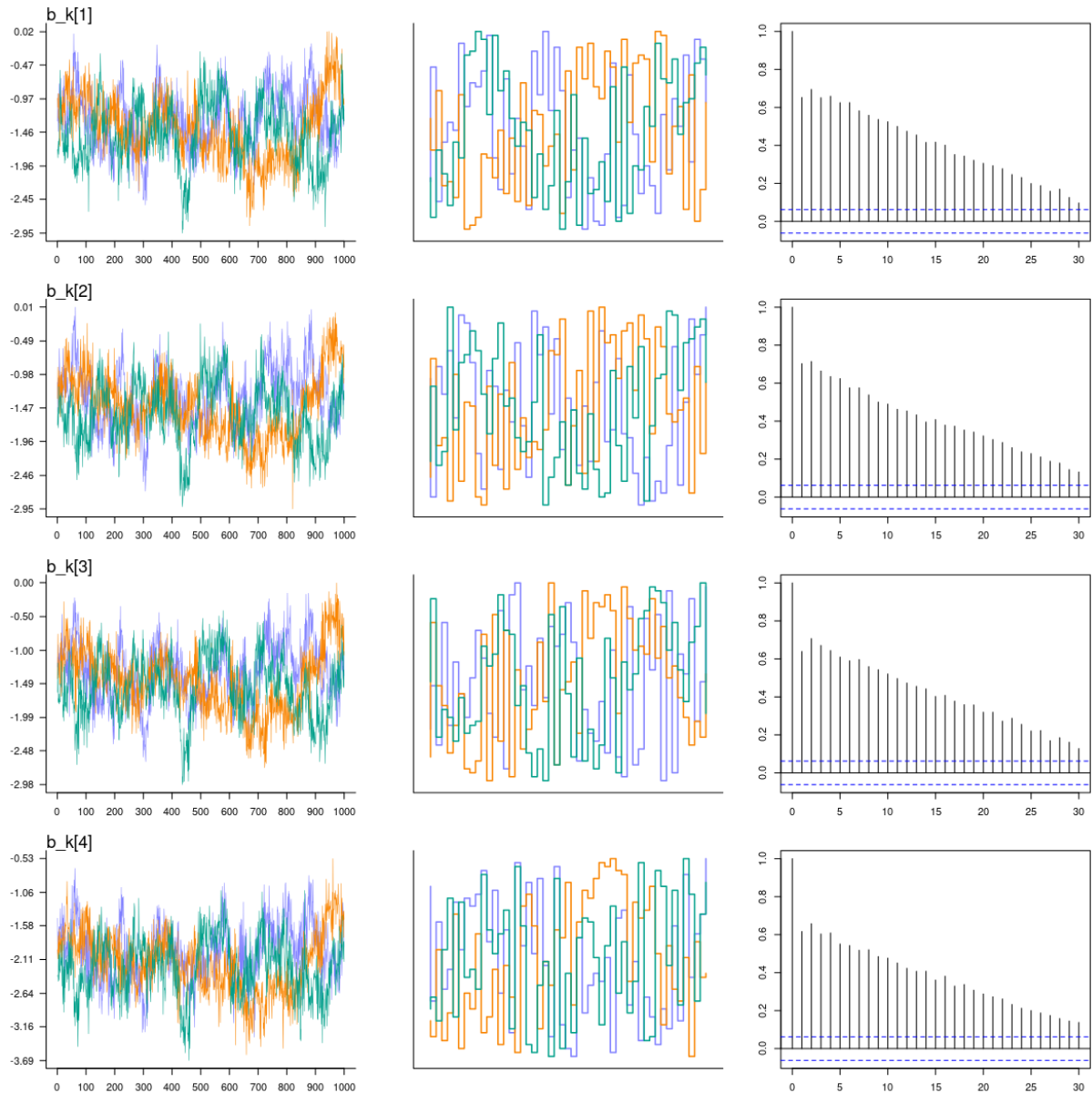


Figure A.9: First-Order latent variable model (FOLV). Sample size 100, replica number 1. Centered parametrization. Difficulty per item: (Left) trace plot, (Middle) trunk plot, (Right) auto-correlation plot.

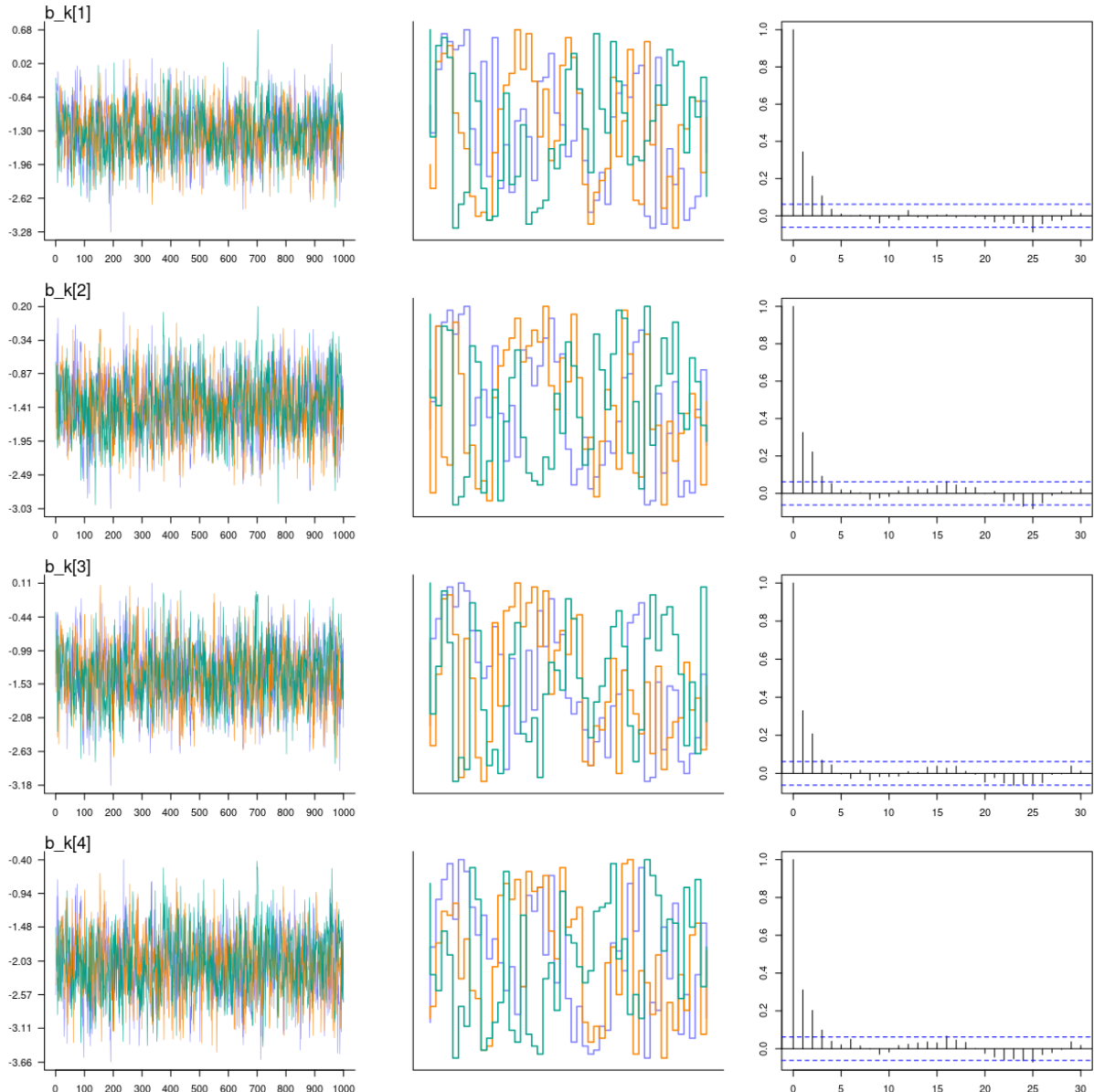


Figure A.10: First-Order latent variable model (FOLV). Sample size 100, replica number 1. Non-centered parametrization. Difficulty per item: (Left) trace plot, (Middle) trunk plot, (Right) auto-correlation plot.

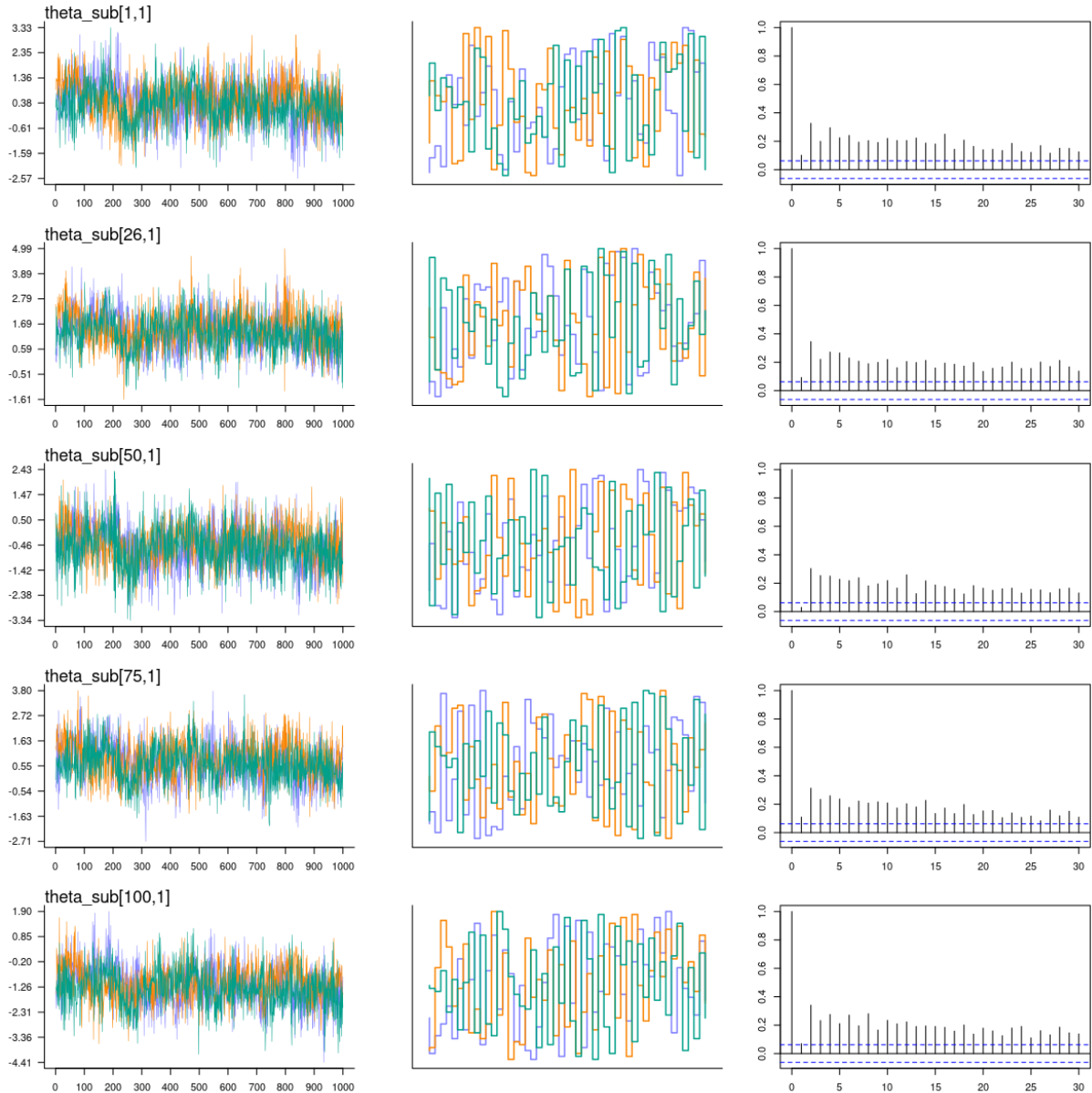


Figure A.11: First-Order latent variable model (FOLV). Sample size 100, replica number 6. Centered parametrization. Individual's first sub-dimension: (Left) trace plot, (Middle) trunk plot, (Right) auto-correlation plot.

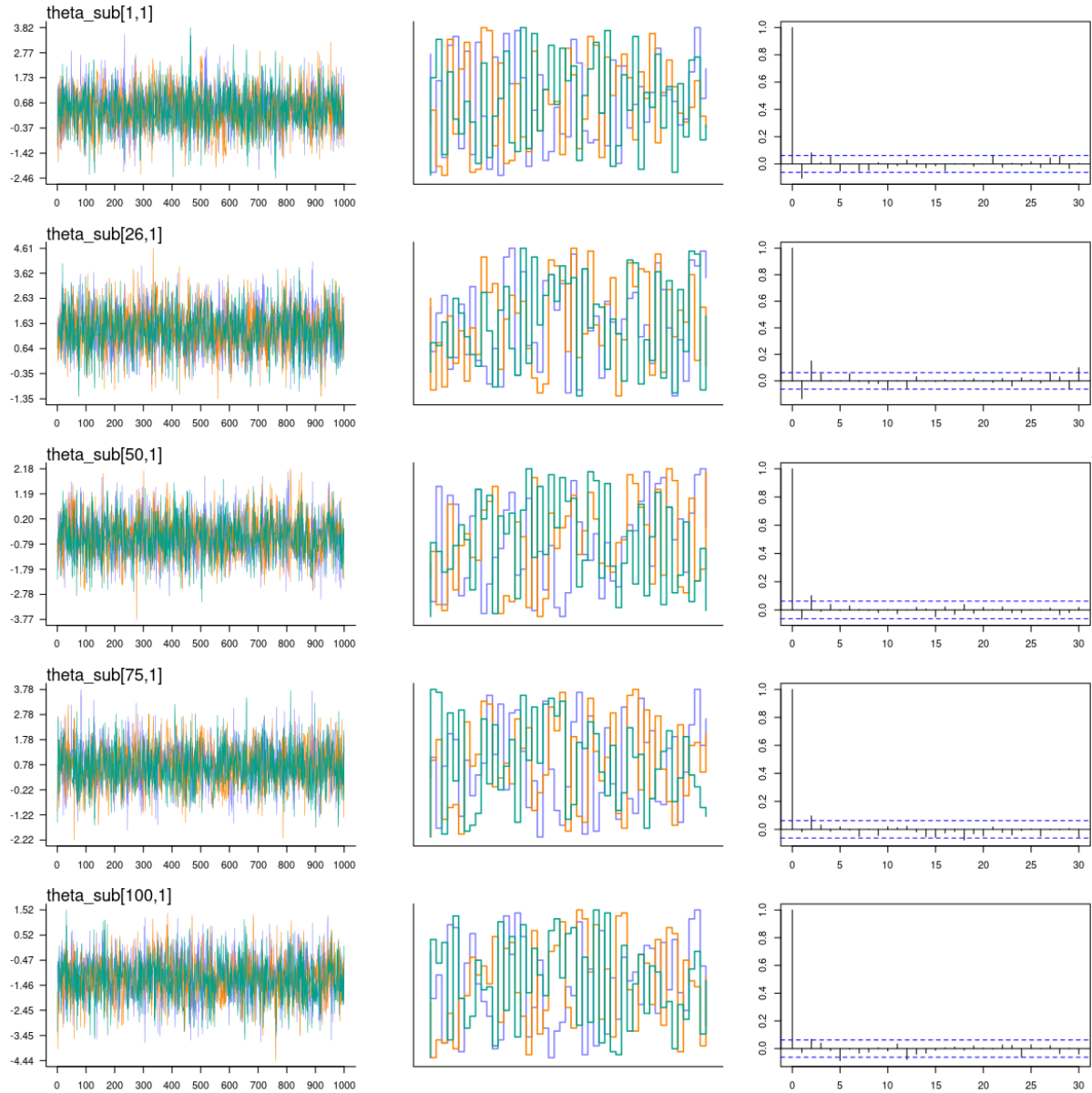


Figure A.12: First-Order latent variable model (FOLV). Sample size 100, replica number 6. Non-centered parametrization. Individual's first sub-dimension: (Left) trace plot, (Middle) trunk plot, (Right) auto-correlation plot.

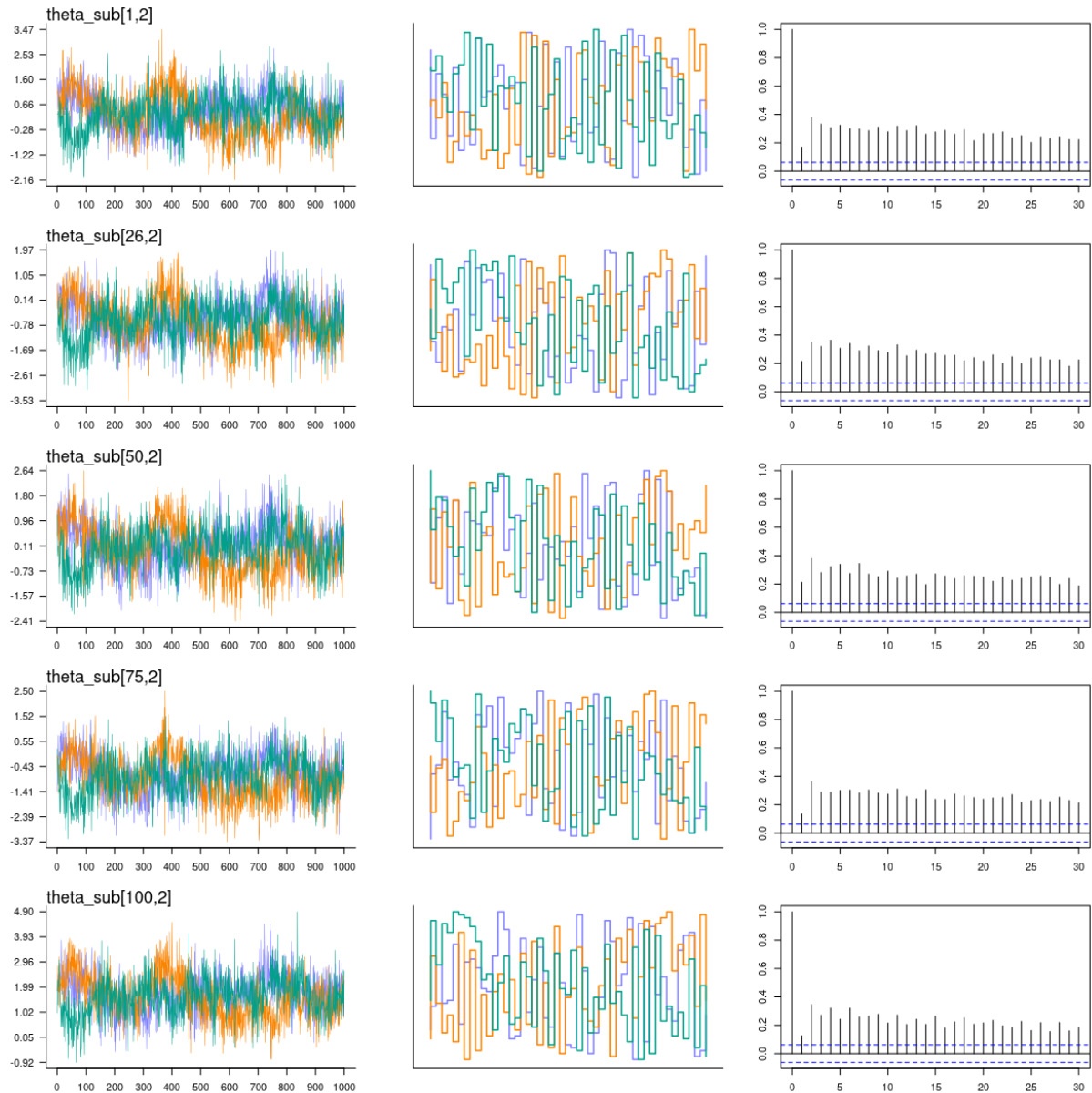


Figure A.13: First-Order latent variable model (FOLV). Sample size 100, replica number 7. Centered parametrization. Individual's second sub-dimension: (Left) trace plot, (Middle) trunk plot, (Right) auto-correlation plot.

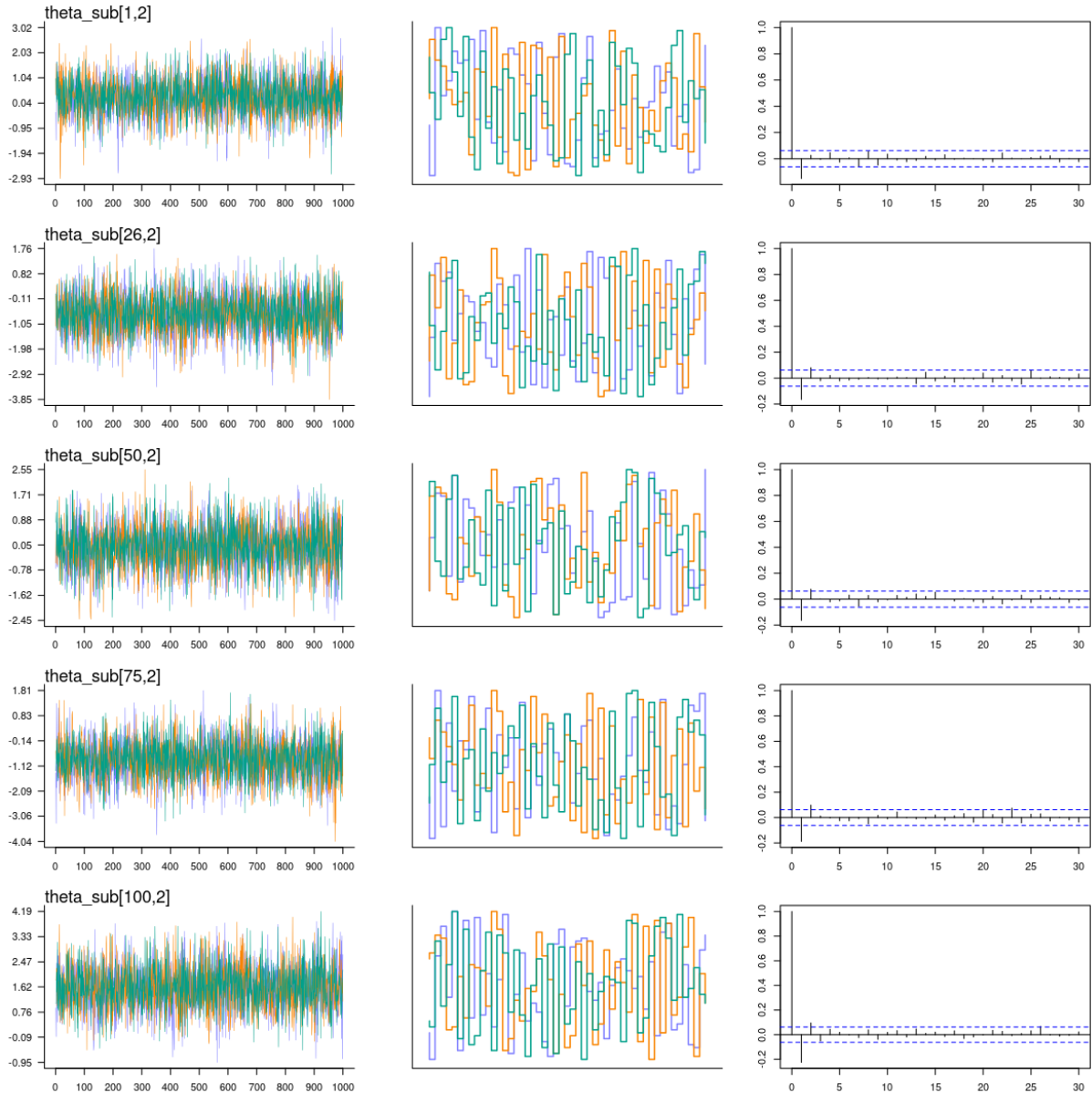


Figure A.14: First-Order latent variable model (FOLV). Sample size 100, replica number 7. Non-centered parametrization. Individual's second sub-dimension: (Left) trace plot, (Middle) rank plot, (Right) auto-correlation plot.

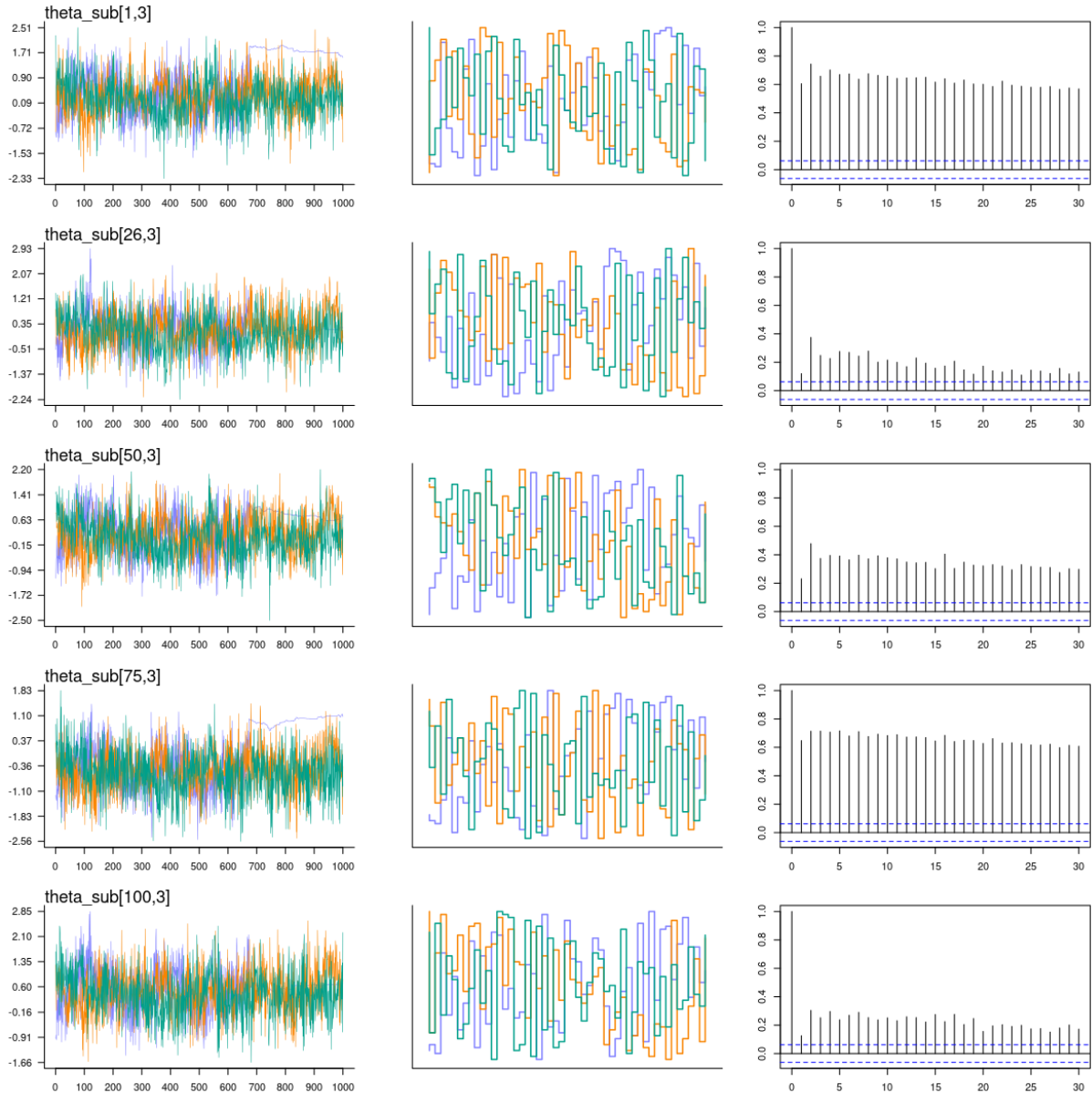


Figure A.15: First-Order latent variable model (FOLV). Sample size 100, replica number 8. Centered parametrization. Individual's third sub-dimension: (Left) trace plot, (Middle) trunk plot, (Right) auto-correlation plot.

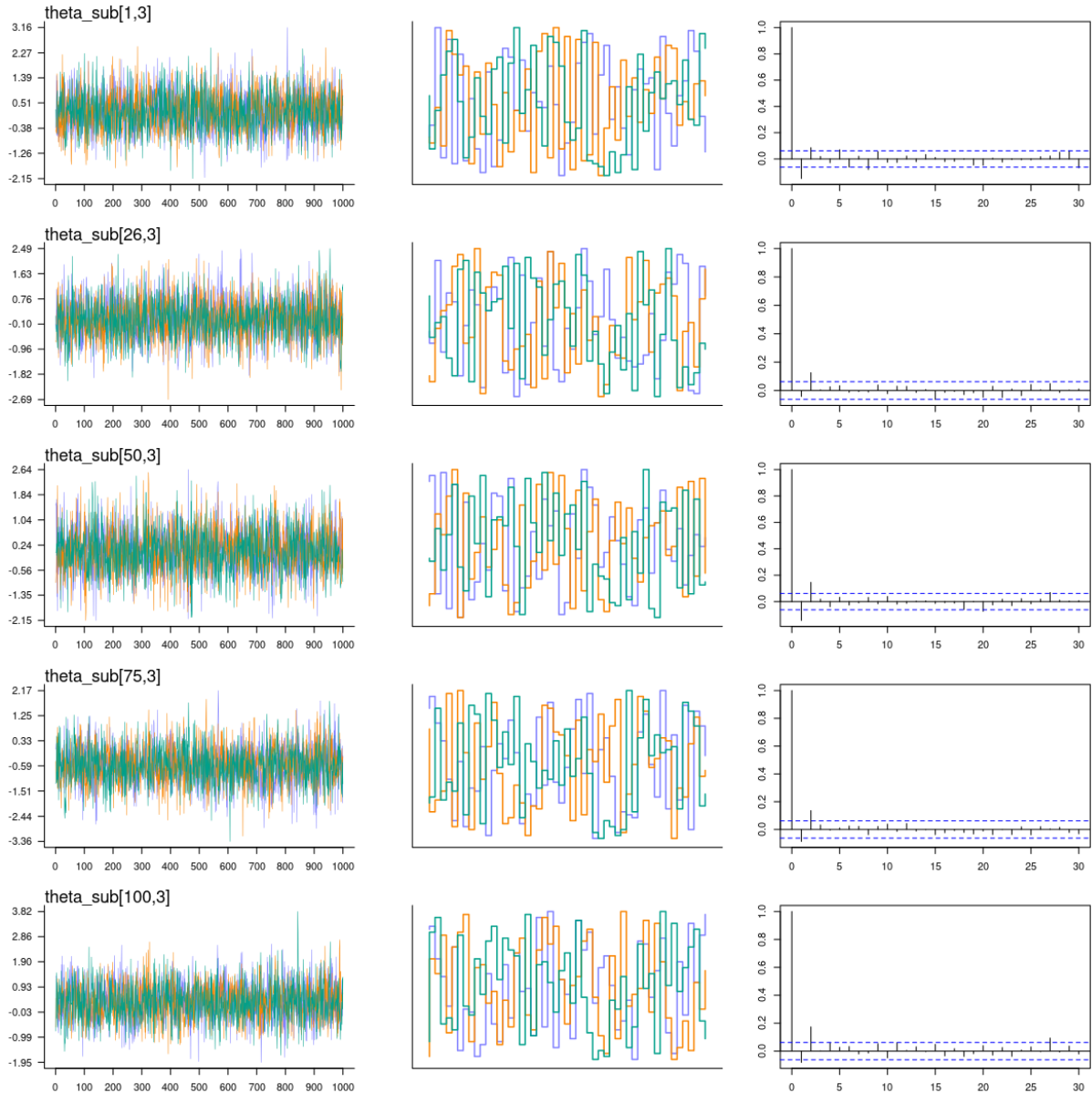


Figure A.16: First-Order latent variable model (FOLV). Sample size 100, replica number 8. Non-centered parametrization. Individual's third sub-dimension: (Left) trace plot, (Middle) trunk plot, (Right) auto-correlation plot.

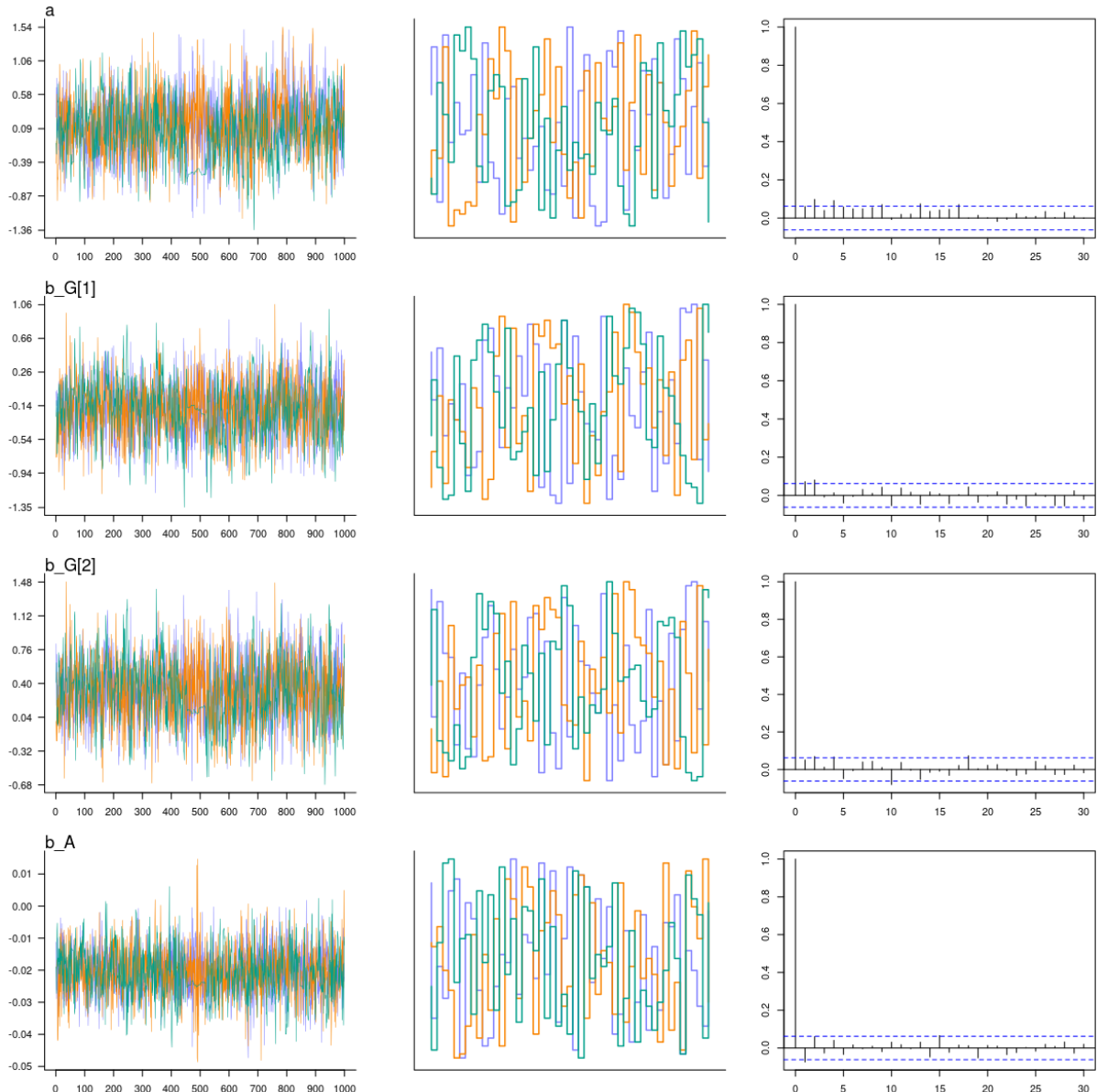


Figure A.17: First-Order latent variable model (FOLV). Sample size 100, replica number 4. Centered parametrization. Regression parameters: (Left) trace plot, (Middle) trunk plot, (Right) auto-correlation plot.

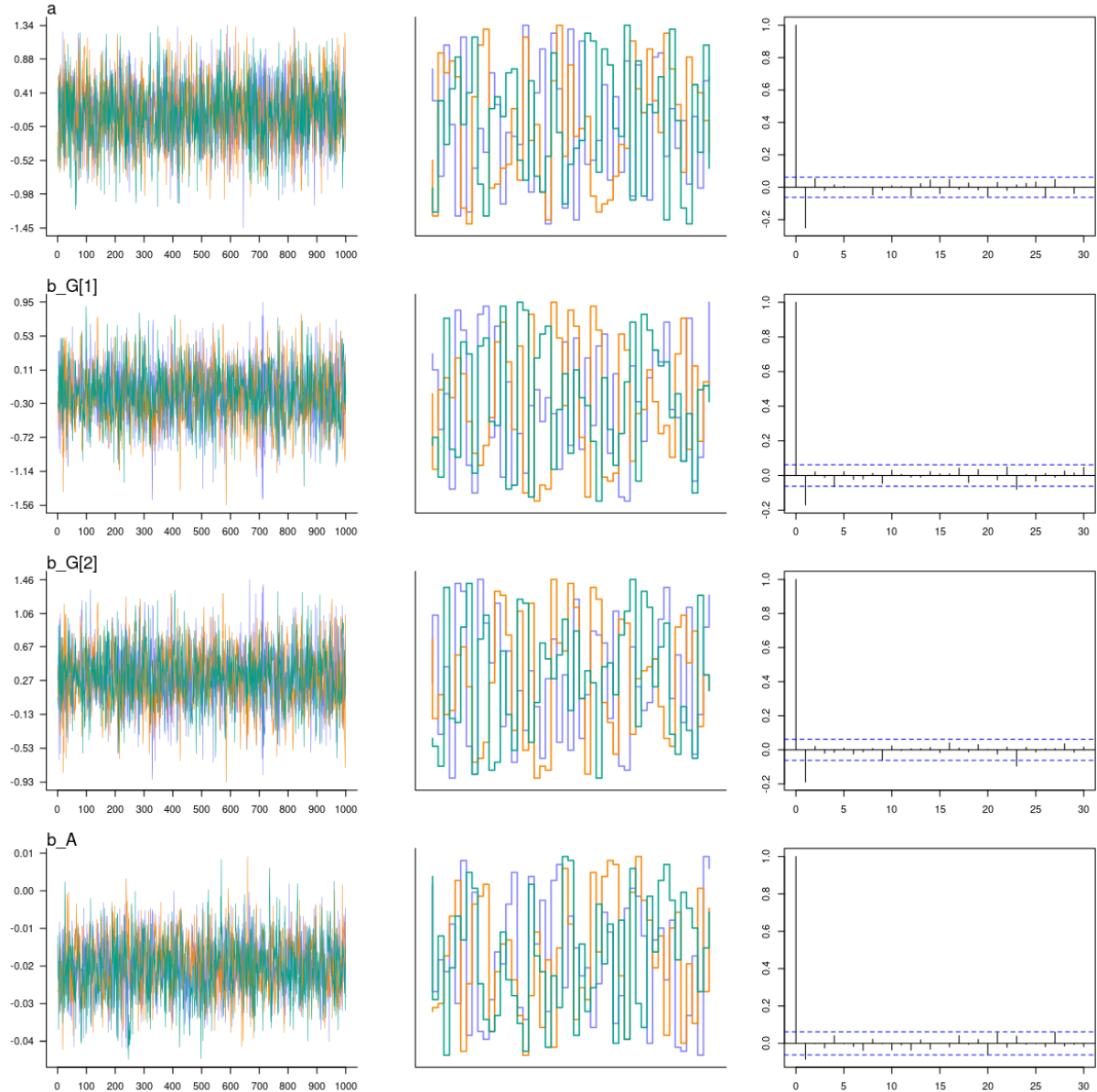


Figure A.18: First-Order latent variable model (FOLV). Sample size 100, replica number 4. Non-centered parametrization. Regression parameters: (Left) trace plot, (Middle) trunk plot, (Right) auto-correlation plot.

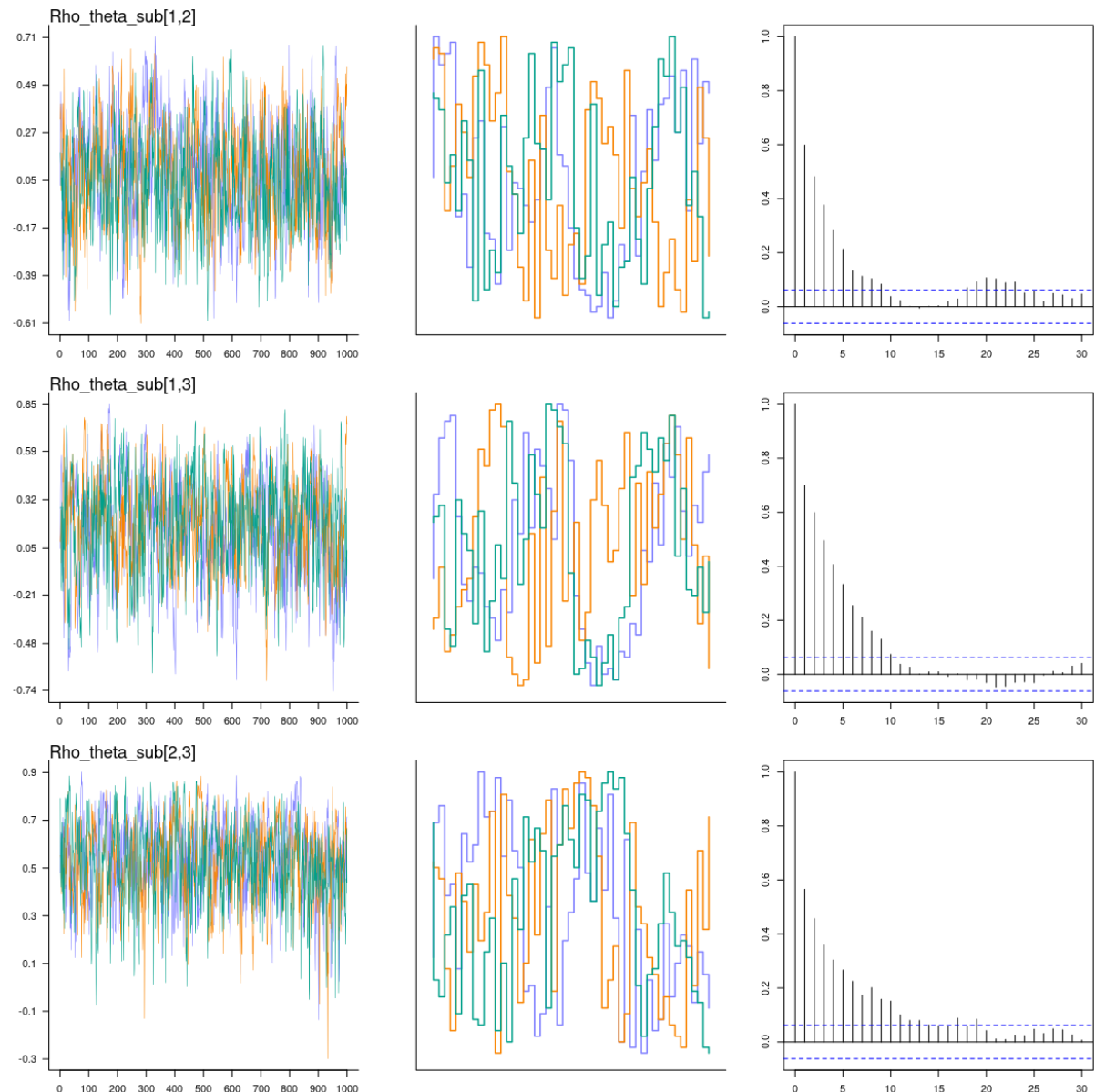


Figure A.19: First-Order latent variable model (FOLV). Sample size 100, replica number 5. Centered parametrization. Correlation of sub-dimensions: (Left) trace plot, (Middle) rank plot, (Right) auto-correlation plot.

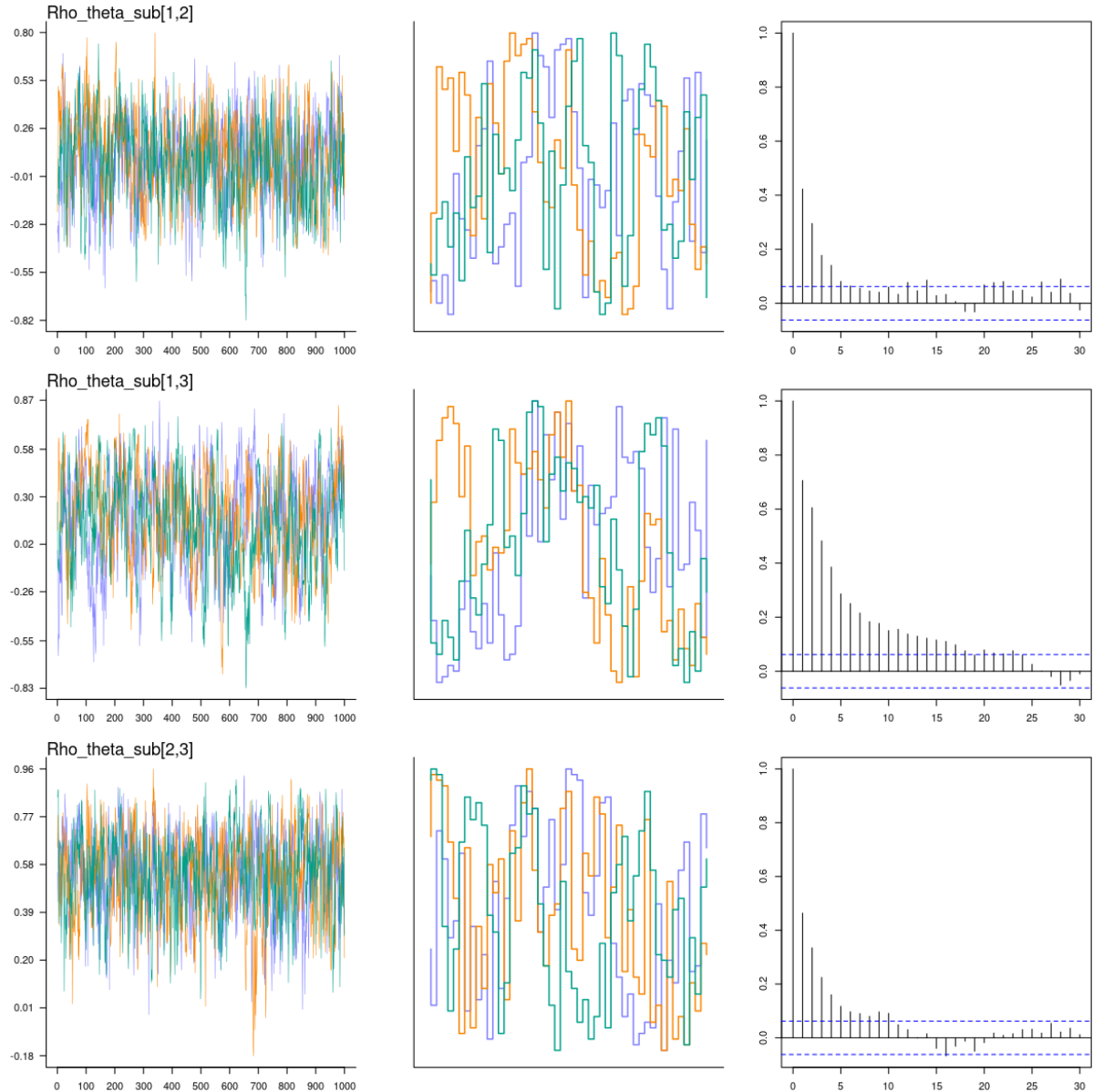


Figure A.20: First-Order latent variable model (FOLV). Sample size 100, replica number 5. Non-centered parametrization. Correlation of sub-dimensions: (Left) trace plot, (Middle) rank plot, (Right) auto-correlation plot.

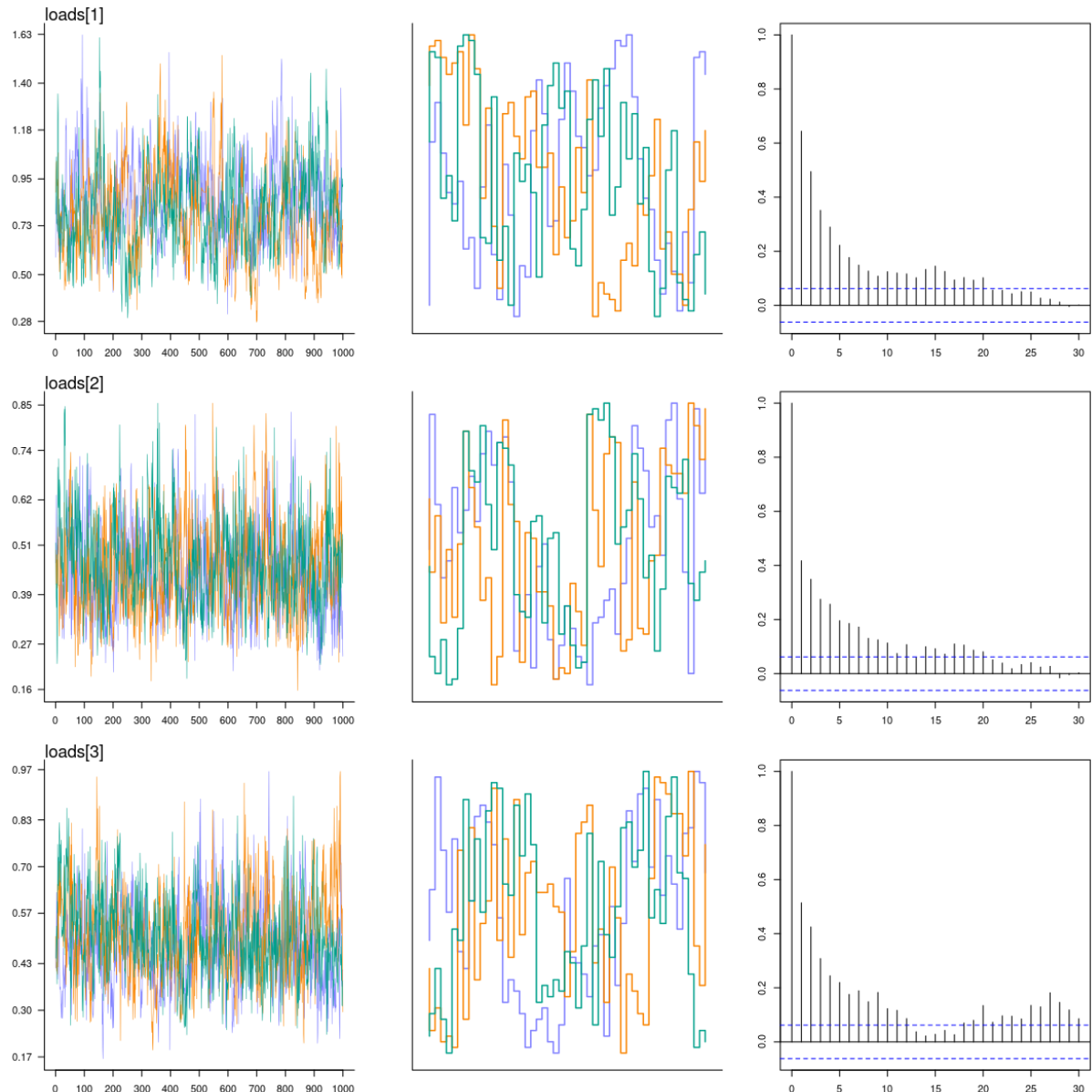


Figure A.21: Second-Order latent variable model (SOLV). Sample size 100, replica number 9. Centered parametrization. Loadings: (Left) trace plot, (Middle) trunk plot, (Right) auto-correlation plot.

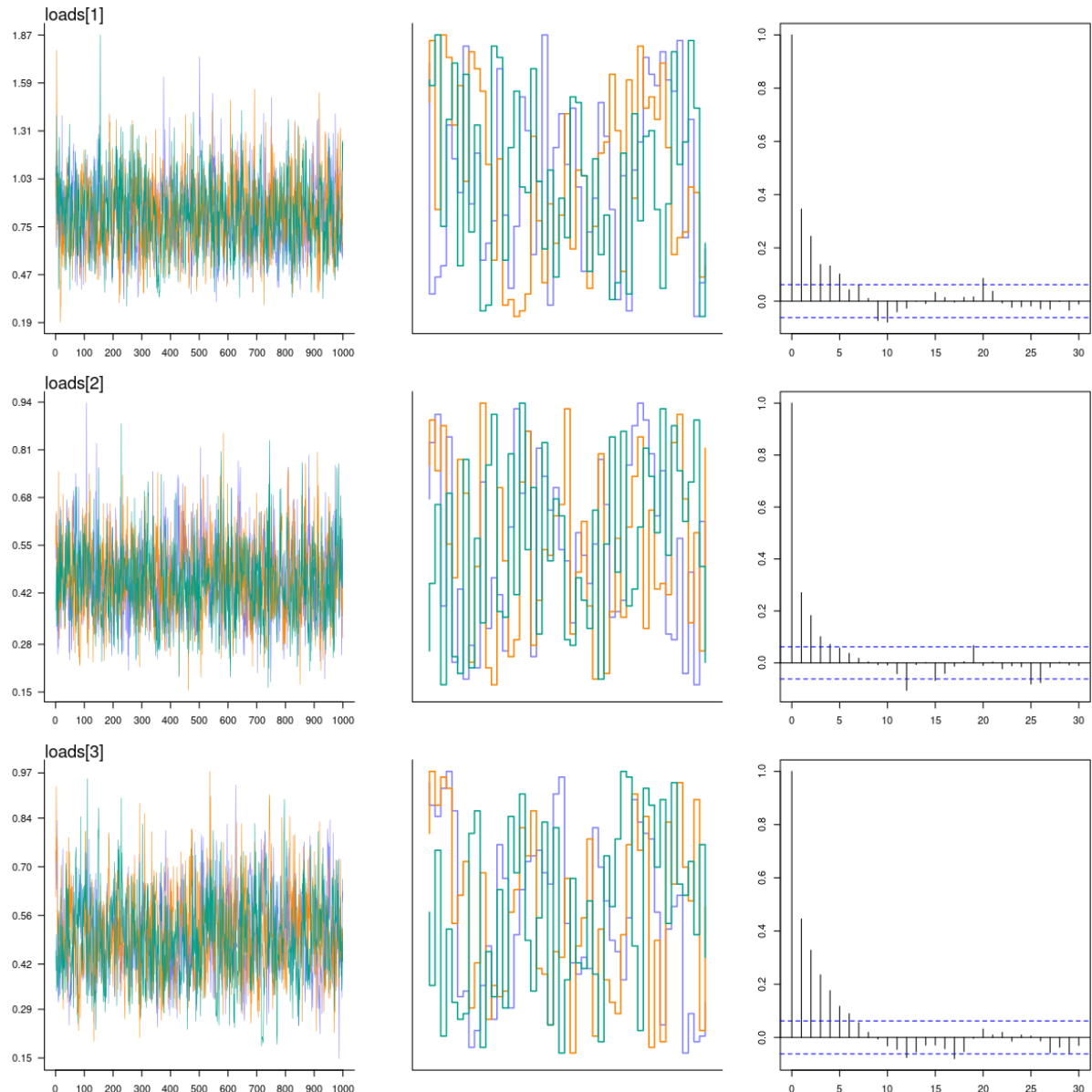


Figure A.22: Second-Order latent variable model (SOLV). Sample size 100, replica number 9. Non-centered parametrization. Loadings: (Left) trace plot, (Middle) trunk plot, (Right) auto-correlation plot.

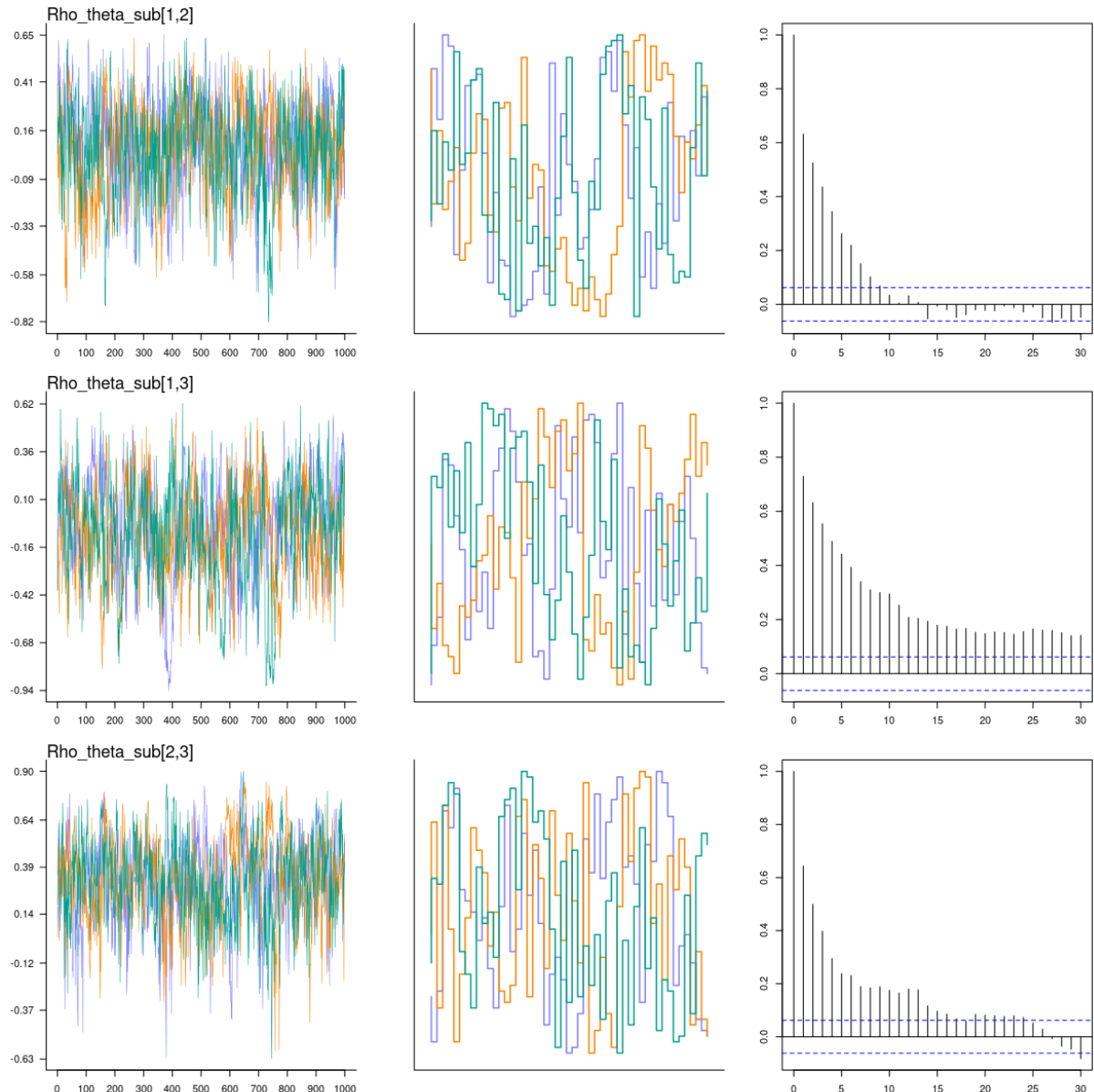


Figure A.23: Second-Order latent variable model (SOLV). Sample size 100, replica number 1. Centered parametrization. Correlation of sub-dimensions: (Left) trace plot, (Middle) trunk plot, (Right) auto-correlation plot.

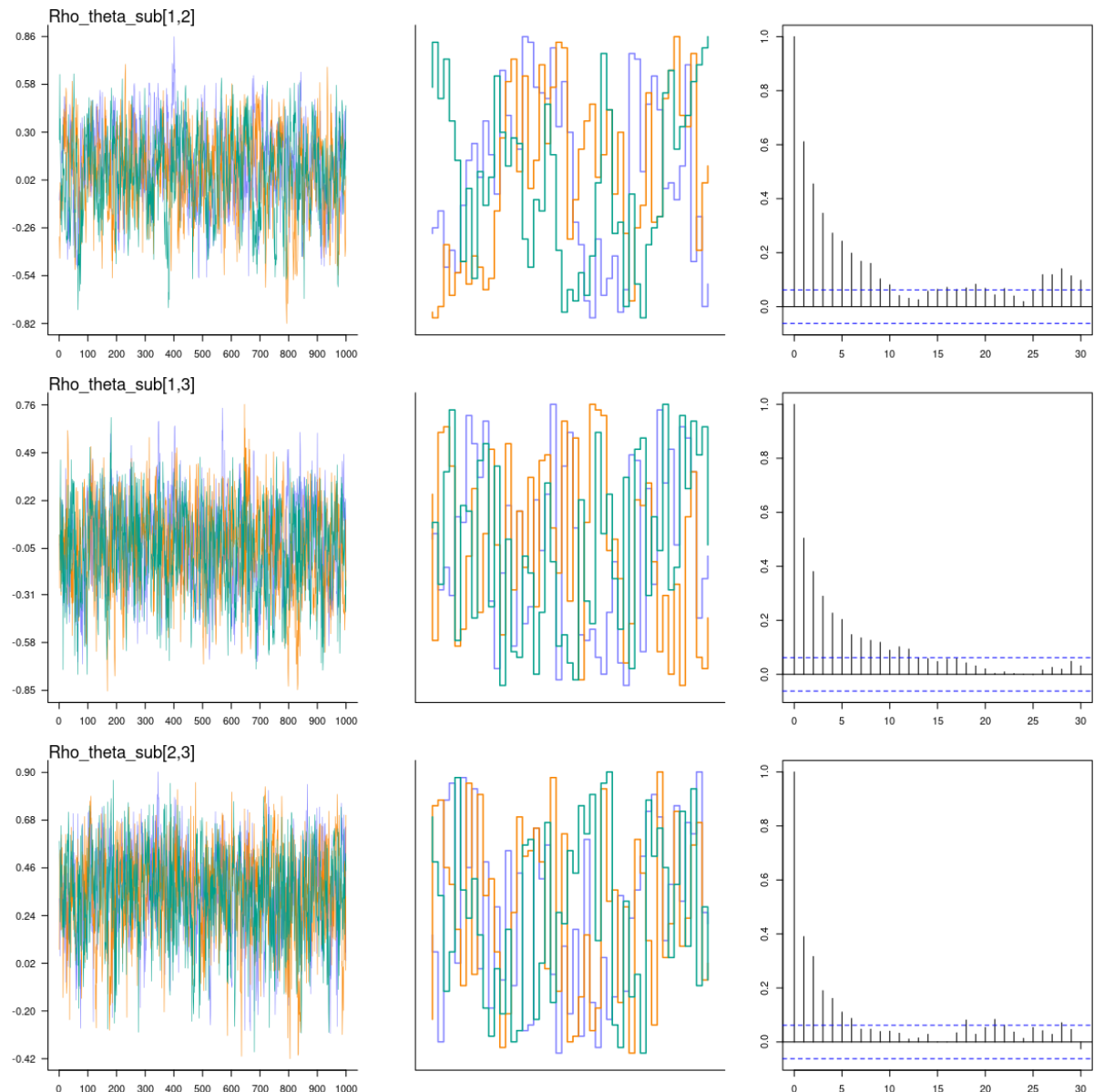


Figure A.24: Second-Order latent variable model (SOLV). Sample size 100, replica number 1. Non-centered parametrization. Correlation of sub-dimensions: (Left) trace plot, (Middle) trunk plot, (Right) auto-correlation plot.

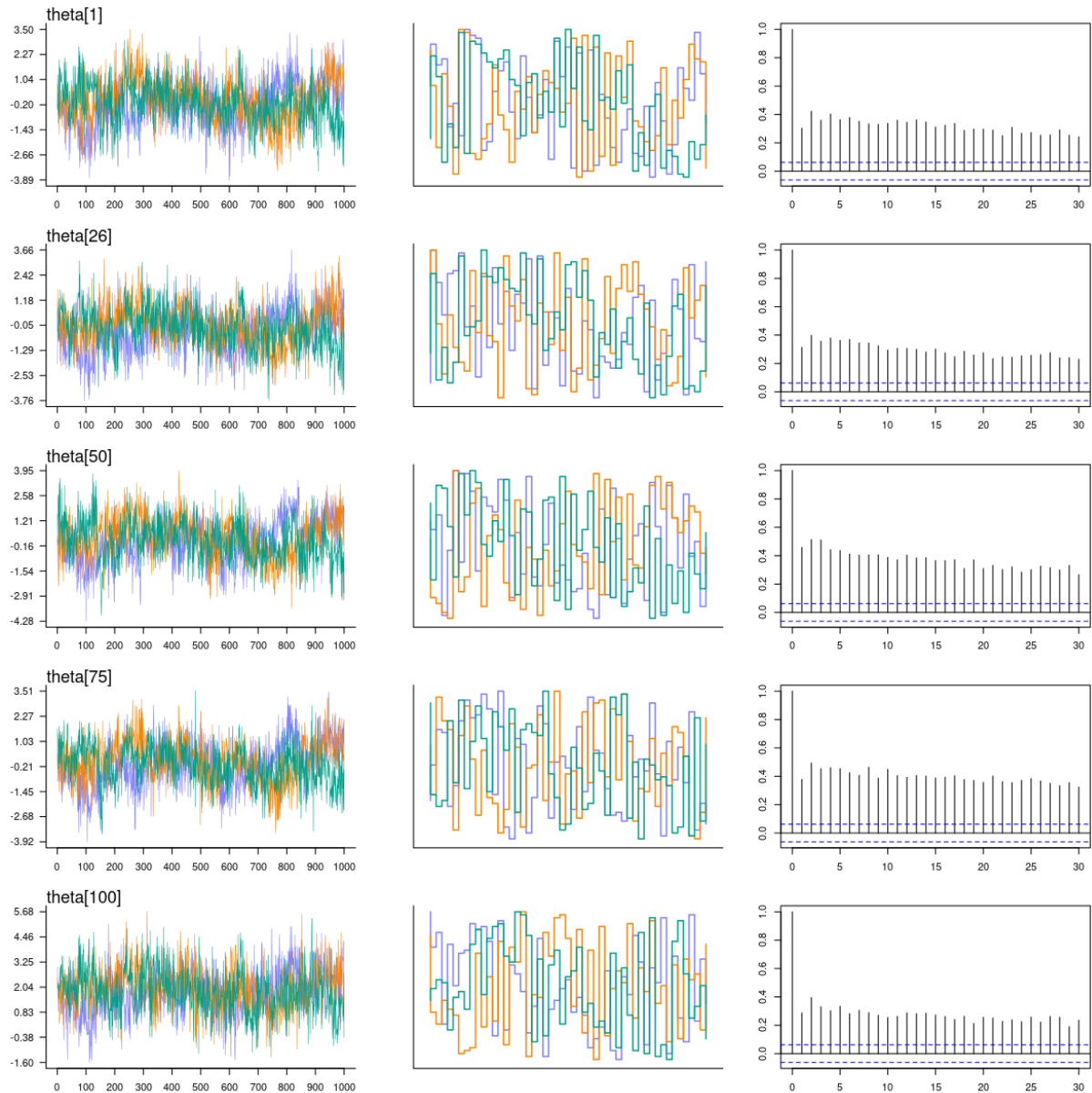


Figure A.25: Second-Order latent variable model (SOLV). Sample size 100, replica number 10. Centered parametrization. Highest-order dimension: (Left) trace plot, (Middle) trunk plot, (Right) auto-correlation plot.

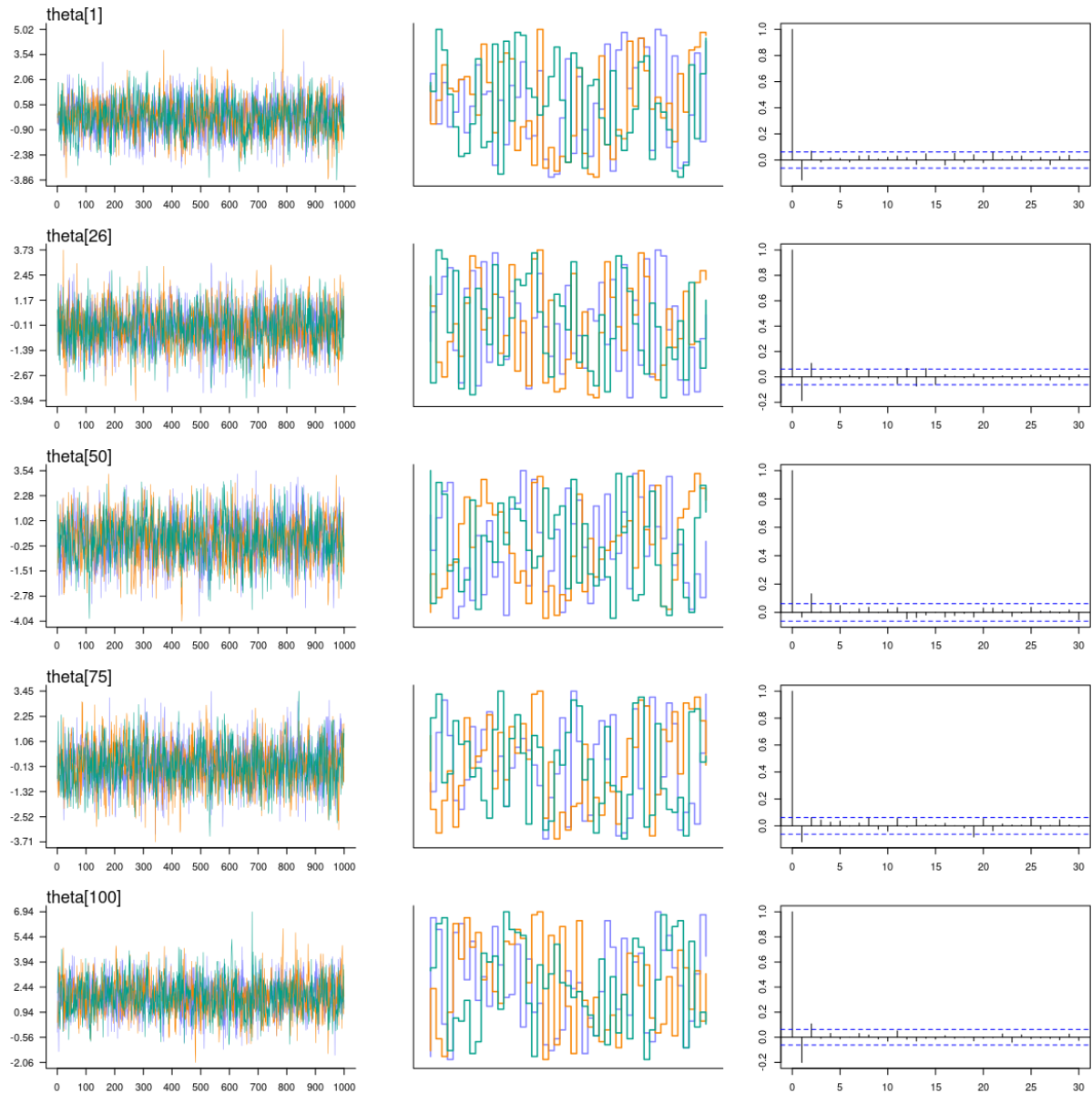


Figure A.26: Second-Order latent variable model (SOLV). Sample size 100, replica number 10. Non-centered parametrization. Highest-order dimension: (Left) trace plot, (Middle) trunk plot, (Right) auto-correlation plot.

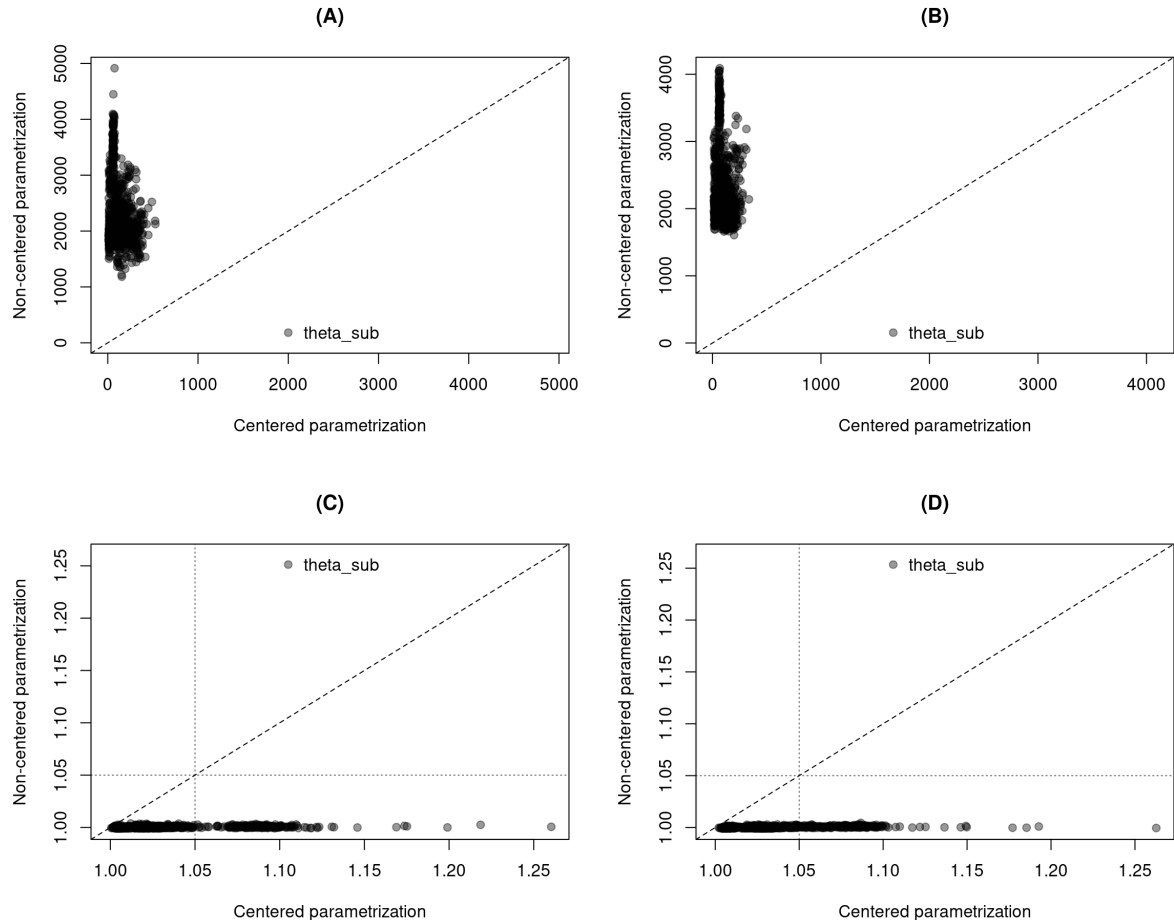


Figure A.27: First-order latent variable model (FOLV). Sample size 100, all replicas. CP and NCP comparison plot. (A) n_{eff} for the first sub-dimension. (B) n_{eff} for the second sub-dimensions. (C) Rhat for the first sub-dimension. (D) Rhat for the second sub-dimensions. Diagonal discontinuous line describes equality between CP and NCP. Vertical and horizontal discontinuous lines is set at $\text{Rhat} = 1.05$.

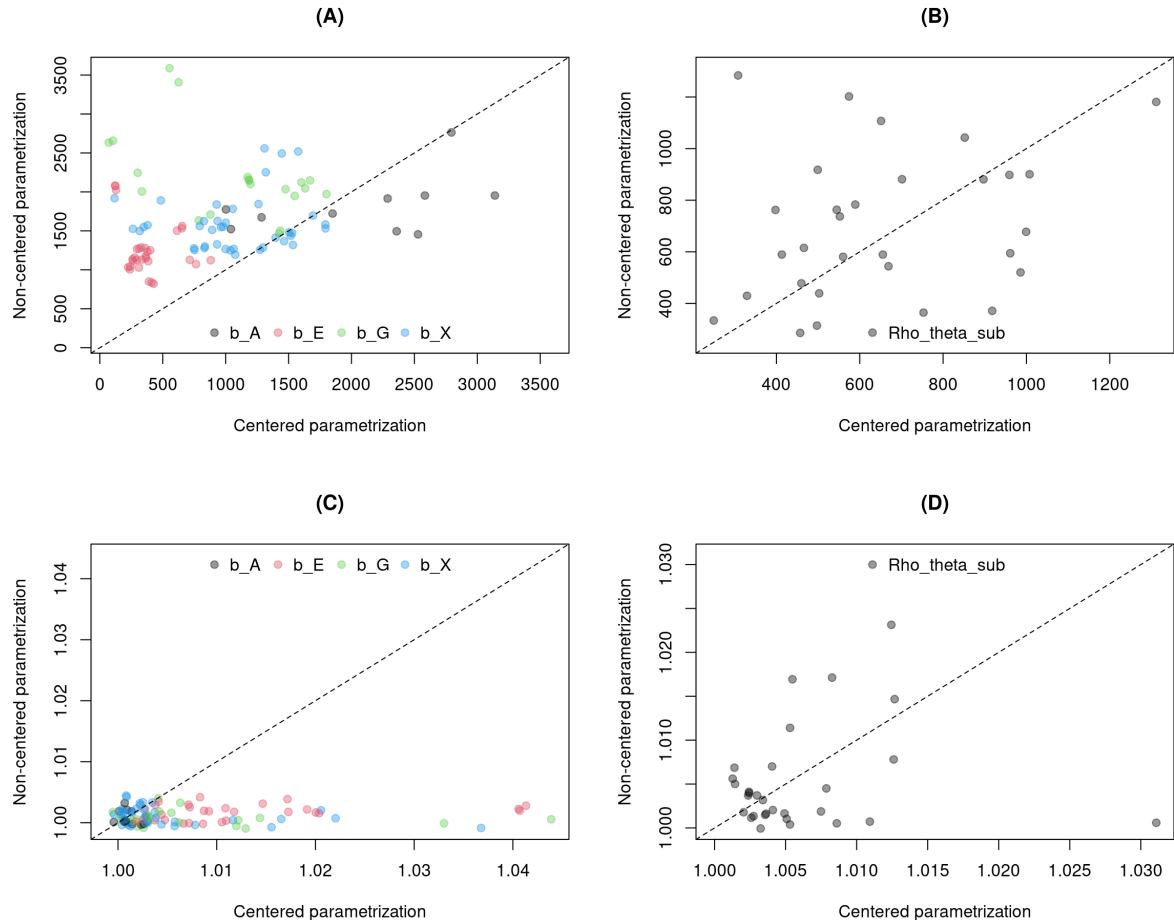


Figure A.28: First-order latent variable model (FOLV). Sample size 100, all replicas. CP and NCP comparison plot. (A) n_{eff} for regression parameters. (B) n_{eff} for correlations among sub-dimensions. (C) $Rhat$ for regression parameters. (D) $Rhat$ for correlations among sub-dimensions. Diagonal discontinuous line describes equality between CP and NCP. Vertical and horizontal discontinuous lines are set at $Rhat = 1.05$.

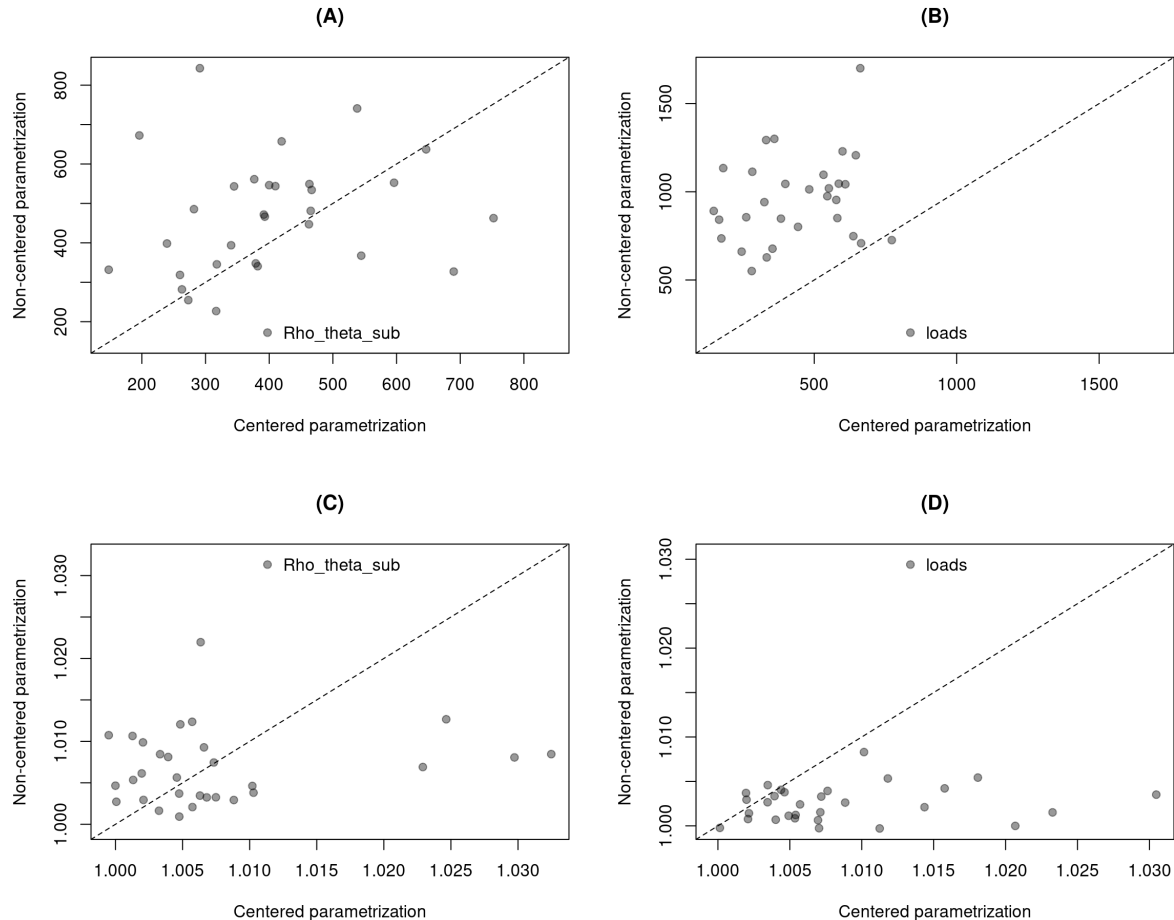


Figure A.29: Second-order latent variable model (SOLV). Sample size 100, all replicas. CP and NCP comparison plot. (A) n_{eff} for the correlations among sub-dimension. (B) n_{eff} for the loadings. (C) $Rhat$ for the correlation among sub-dimensions. (D) $Rhat$ for the loadings. Diagonal discontinuous line describes equality between CP and NCP. Vertical and horizontal discontinuous lines is set at $Rhat = 1.05$.

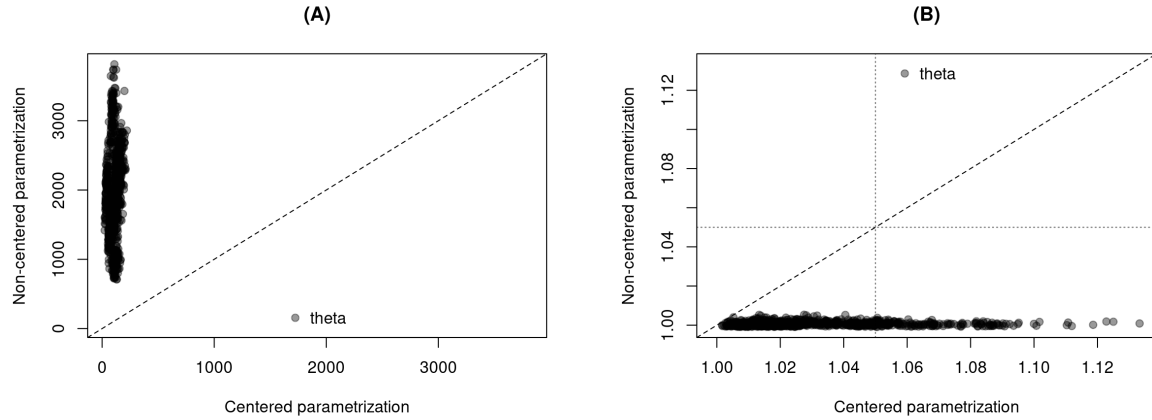


Figure A.30: Second-order latent variable model (SOLV). Sample size 100, all replicas. CP and NCP comparison plot. (A) n_{eff} for the higher-order latent variable. (B) Rhat for the higher-order latent variable. Diagonal discontinuous line describes equality between CP and NCP. Vertical and horizontal discontinuous lines is set at $\text{Rhat} = 1.05$.

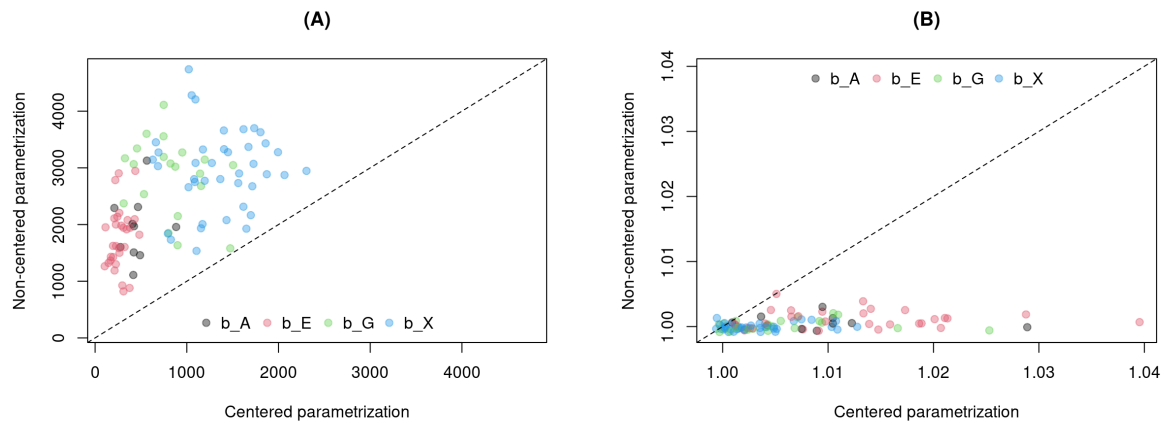


Figure A.31: Second-order latent variable model (SOLV). Sample size 100, all replicas. CP and NCP comparison plot. (A) n_{eff} for regression parameters. (B) Rhat for the first sub-dimension. (C) Rhat for regression parameters. (D) Rhat for the second sub-dimensions. Diagonal discontinuous line describes equality between CP and NCP. Vertical and horizontal discontinuous lines is set at $\text{Rhat} = 1.05$.

Appendix B

Code

B.1 Chapter 3: Bayesian estimation

B.1.1 To center or not to center

The devil's funnel, centered parametrization.

Stan

```
transformed data {
    int<lower=0> J;
    J = 1;
}
parameters {
    real theta[J];
    real v;
}
model {
    v ~ normal(0, 3);
    theta ~ normal(0, exp(v));
}
```

JAGS

```
model{
    v ~ dnorm(0,3)
    theta ~ dnorm(0, exp(v))
}
```

The devil's funnel, centered parametrization with priors.

Stan

```
transformed data {
    int<lower=0> J;
    J = 1;
}
parameters {
    real theta[J];
```

```

        real v;
}
model {
    v ~ normal(0, 1);
    theta ~ normal(0, exp(v));
}

```

JAGS

```

model{
    v ~ dnorm(0,1)
    theta ~ dnorm(0, exp(v))
}

```

The devil's funnel, non-centered parametrization.

Stan

```

transformed data {
    int<lower=0> J;
    J = 1;
}
parameters {
    real ztheta[J];
    real v;
}
transformed parameters{
    vector[J] theta;
    theta = exp(v) * to_vector(ztheta);
}
model {
    v ~ normal(0, 3);
    ztheta ~ normal(0, 1);
}

```

JAGS

```

model{
    v ~ dnorm(0,1)
    ztheta ~ dnorm(0,1)
    theta = v * ztheta
}

```

B.2 Chapter 4: Simulation study

B.2.1 Algorithm

Data generation

```

S = 10 # ten data sets
condition = expand_grid( J = c(100, 250, 500), load=0.95)
for(i in 1:nrow(condition)){

```

```

        for(s in 1:S){
            with(condition[i,],
                 data_generation( J=J, loads=rep(load, 3),
                                   Ndata=s, seed=4587+s+i, # different seeds
                                   file_dir=file.path(getwd(), 'data') ) )
        }
    }
}

```

Data generation function

```

# function:
#   data_generation
# description:
#   To generate data based on different parameter settings.
#   Only two parameters are effectively controlled in the experimentation:
#   sample size (J), and the loading from the SOLV to the FOLV (loads).
# characteristics of the sample design:
#   - one instrument
#   - hierarchical measurement scales with FOLV and SOLV
#   - one evaluation time
#   - one sample of individuals
#   - testlet items, multiple items come from one text
#   - with covariates
#   - NO missingness
# arguments:
#   J = individual sample sizes
#   loads = loadings from SOLV to FOLV (it control correlation)
#   Ndata = defines the number of data generated
#   file_dir = path to save generated data
#   s_theta = sd to simulate SOLV and FOLV
#   s_text = sd in generating items from a specific text
#   D = number of dimensions (default 3)
#   K = number of items (default 25)
#   L = number of texts (default 5), it has to be a multiple of K
#   seed = seed used to generate the simulation (default 1)
#   prec = rounding in abilities and item parameters (default 3)

data_generation =function( J=100, loads=rep(0.95, 3), Ndata=1, file_dir,
                           s_theta=0.5, s_text=0.5, D=3, K=25, L=5, seed=1, prec=3){

# -----
# 1. generation
# -----
set.seed(seed)

## 1.1. regression parameters
mom = expand_grid(a=loads[-3], b=loads[-1])
mom = mom[-3,]

betas = list( gender = c(0, 0.5),

```

```

age = -0.02,
edu = c(-0.5, 0.5, 0),
exp = c(-0.5, 0, 0.35, 0.5),
loads = loads, # loadings
exp_corr = with(mom, a*b) ) # expected correlation

## 1.2 covariates
abilities = data.frame( IDind=1:J,
    gender = sample(c(1,2), size=J, replace=T),
    age = sample(30:65, size=J, replace=T),
    edu = sample(c(1,2,3), size=J, replace=T),
    exp = sample(c(1,2,3,4), size=J, replace=T),
    theta=rep(NA,J), theta1=rep(NA,J),
    theta2=rep(NA,J), theta3=rep(NA,J) )

# variable indices
SOLV_loc = which(names(abilities)=='theta')
FOLV_loc = which(names(abilities)=='theta1'):
    which(names(abilities)==paste0('theta', D))

## 1.3. abilities
# SOLV
m_theta = rep(NA, J)
for(j in 1:J){
    ageC = with(abilities, age[j] - min(age) + 1 )

    m_theta[j] = with(abilities,
        betas$gender[ gender[j] ] +
        betas$age * ageC +
        betas$edu[ edu[j] ] +
        betas$exp[ exp[j] ] )
}
abilities[, SOLV_loc] = round( rnorm(J, m_theta, s_theta), prec)

# FOLV
# independent after considering SOLV
s_mult = diag( rep(s_theta, D) )
m_mult = data.frame( theta1=rep(NA, J),
    theta2=rep(NA, J),
    theta3=rep(NA, J) )
for(j in 1:J){
    m_mult[j,] = betas$loads * abilities$theta[j]
    abilities[j, FOLV_loc] = round(
        mvnrnorm(n=1, mu=unlist(m_mult[j,]), Sigma=s_mult), prec)
}

## 1.4 texts

```

```

texts = data.frame(IDtext=1:L, m_b=rep(NA, L), s_b=rep(NA, L))
texts$m_b = seq(-1.5, 1.5, length.out=L)
texts$s_b = rep(s_text, L)

## 1.5 items
items = data.frame(IDitem=1:K, IDtext=rep(NA,K),
IDdim=rep(NA,K), b=rep(NA, K))
kl = K/L # items per text
for(k in 1:nrow(texts)){
  items$b[(1:kl) + (k-1)*kl] = with(texts,
    round( rnorm(kl, m_b[k], s_b[k]), prec ) )
  items$IDtext[(1:kl) + (k-1)*kl] = k
}

## 1.6 dimensions
items$IDdim = sample(1:3, K, replace=T)

# -----
# 2. storage
# -----

## 2.1 parameters
data_true = list(
  seed=seed,
  # indices
  J = J,
  D = D,
  K = K,
  L = L,
  # abilities
  betas = betas,
  abilities = abilities,
  # texts and items
  texts = texts,
  items = items)

file_name = paste0('Parameters_J',J,'_l',loads[1],
'_Ndata',Ndata,'.RData')
save(data_true, file=file.path(file_dir, file_name) )

## 2.2 long format
data_eval = data.frame(

```

```

# individual data
IDind = rep(abilities$IDind, K),
gender = rep(abilities$gender, K),
age = rep(abilities$age, K),
edu = rep(abilities$edu, K),
exp = rep(abilities$exp, K),
theta = rep(abilities$theta, K),
theta1 = rep(abilities$theta1, K),
theta2 = rep(abilities$theta2, K),
theta3 = rep(abilities$theta3, K),

# items
IDitem = rep(items$IDitem, each=J),
IDtext = rep(items$IDtext, each=J),
IDdim = rep(items$IDdim, each=J),
b = rep(items$b, each=J) )

# appropriate ability
data_eval$theta_jkld = NA
for(i in 1:nrow(data_eval) ){
    data_eval$theta_jkld[i] = data_eval[i, FOLV_loc[ data_eval$IDdim[i]
}]

# linear predictor, probability, and outcome
data_eval$v_jkld = with(data_eval, theta_jkld - b)
data_eval$p_jkld = inv_logit( data_eval$v )
data_eval$y_jkld = rbinom( nrow(data_eval), 1, prob=data_eval$p)

file_name = paste0('LongFormat_J', J, '_l', loads[1],
                  '_Ndata', Ndata, '.RData')
save(data_eval, file=file.path(file_dir, file_name) )

## 2.3 estimation data
data_post = list(
    # evaluation data
    N = nrow(data_eval),
    J = J,
    K = K,
    L = L,
    D = D,
    IDj = data_eval$IDind,
    IDk = data_eval$IDitem,
    IDl = data_eval$IDtext,
    IDd = data_eval$IDdim,
    GE = data_eval$gender,
    AG = data_eval$age,
    ED = data_eval$edu,
    )

```

```

XP = data_eval$exp ,
y = data_eval$y_jkld ,

# individual data
IDind = abilities$IDind ,
G = abilities$gender ,
A = abilities$age ,
E = abilities$edu ,
X = abilities$exp ,

# items
IDitem = items$IDitem ,
IDtext = items$IDtext ,
IDdim = items$IDdim )

file_name = paste0('ListFormat_J',J,'_l',loads[1],
' _Ndata',Ndata,'.RData')
save(data_post, file=file.path(file_dir, file_name) )

}

```

B.2.2 Results

Models

it has the stan model used to analize the data

FOLV CP

```

data{
    // evaluation
    int N;
    int J;
    int K;
    int L;
    int D;
    int IDj[N];
    int IDk[N];
    int IDl[N];
    int IDd[N];
    int GE[N];
    real AG[N];
    int ED[N];
    int XP[N];
    int y[N];

    // individuals
    int IDind[J];
    int G[J];
    real A[J];
}

```

```

    int E[J];
    int X[J];

    // items
    int IDitem[K];
    int IDtext[K];
    int IDdim[K];
}
parameters{
    // items
    real m_b[L];
    real<lower=0> s_b[L];
    real b_k[K];

    // betas
    real a;
    real b_G[2];
    real b_A;
    real b_E[3];
    real b_X[4];

    // abilities
    // sub-dimensions: lit, inf, ref
    corr_matrix[D] Rho_theta_sub;
    vector[D] theta_sub[J];
}
model{
    // declare
    vector[D] m_mult[J];
    real v;
    real p;

    // items
    m_b ~ normal(0, 1);
    s_b ~ exponential(2);
    for(k in 1:K){           // priors
        b_k[k] ~ normal( m_b[ IDtext[k] ], s_b[ IDtext[k] ] );
    }

    // abilities
    a ~ normal(0, 0.5);
    b_G ~ normal(0, 0.5);
    b_A ~ normal(0, 0.5);
    b_E ~ normal(0, 1);
    b_X ~ normal(0, 0.5);
    Rho_theta_sub ~ lkj_corr(2);
    for(j in 1:J){
        m_mult[j,] = rep_vector( a + b_G[ G[j] ] +
            b_A * ( A[j] - min(A) ) +
            b_E[ E[j] ] +

```

```

        b_X[ X[j] ], D);
    // using the same predictor for the three latents
}
theta_sub ~ multi_normal( m_mult, Rho_theta_sub );

// model
for( i in 1:N ) {
    v = theta_sub[ IDj[i], IDd[i] ] - b_k[ IDk[i] ];
    p = inv_logit(v);
    y[i] ~ bernoulli(p);
}
}/*
## generated quantities{
##     vector[N] log_lik;
##     real v;
##     real p;
##
##     // likelihood
##     for( i in 1:N ) {
##         v = theta_sub[ IDj[i], IDd[i] ] - b_k[ IDk[i] ];
##         p = inv_logit(v);
##         log_lik[i] = bernoulli_lpmf( y[i] | p);
##     }
## }
```

FOLV NCP

```

data{
    // evaluation
    int N;
    int J;
    int K;
    int L;
    int D;
    int IDj[N];
    int IDk[N];
    int IDl[N];
    int IDd[N];
    int GE[N];
    real AG[N];
    int ED[N];
    int XP[N];
    int y[N];

    // individuals
    int IDind[J];
    int G[J];
    real A[J];
    int E[J];
    int X[J];
```

```

// items
int IDitem[K];
int IDtext[K];
int IDdim[K];
}

parameters{
    // items
    real m_b[L];
    real<lower=0> s_b[L];
    real zb_k[K];

    // betas
    real a;
    real b_G[2];
    real b_A;
    real b_E[3];
    real b_X[4];

    // abilities
    // sub-dimensions: lit, inf, ref
    cholesky_factor_corr[D] L_Rho_theta_sub;
    matrix[D, J] ztheta_sub;
}

transformed parameters{
    real b_k[K];
    matrix[D, D] Rho_theta_sub;
    matrix[J, D] m_mult;
    matrix[J, D] theta_sub;

    // items
    for(k in 1:K){
        b_k[k] = m_b[ IDtext[k] ] + s_b[ IDtext[k] ] * zb_k[k];
    }

    // abilities
    Rho_theta_sub = multiply_lower_tri_self_transpose(L_Rho_theta_sub);
    for(j in 1:J){
        m_mult[j,] = rep_row_vector( a + b_G[ G[j] ] +
            b_A * (A[j] - min(A) ) +
            b_E[ E[j] ] +
            b_X[ X[j] ], D);
    }
    theta_sub = (L_Rho_theta_sub * ztheta_sub)';
    theta_sub = theta_sub + m_mult;
}

model{
    // declare
    real v;
    real p;
}

```

```

// items
m_b ~ normal(0, 1);
s_b ~ exponential(2);
zb_k ~ normal(0, 1);

// abilities
a ~ normal(0, 0.5);
b_G ~ normal(0, 0.5);
b_A ~ normal(0, 0.5);
b_E ~ normal(0, 1);
b_X ~ normal(0, 0.5);
L_Rho_theta_sub ~ lkj_corr_cholesky(2);
to_vector(ztheta_sub) ~ normal(0,1);

// model
for( i in 1:N ) {
    v = theta_sub[ IDj[i], IDd[i] ] - b_k[ IDk[i] ];
    p = inv_logit(v);
    y[i] ~ bernoulli(p);
}
}

//# generated quantities{
//#     vector[N] log_li;
//#     real v;
//#     real p;
//#
//#     // likelihood
//#     for( i in 1:N ) {
//#         v = theta_sub[ IDj[i], IDd[i] ] - b_k[ IDk[i] ];
//#         p = inv_logit(v);
//#         log_li[i] = bernoulli_lpmf( y[i] | p);
//#     }
//# }
```

SOLV CP

```

data{
    // evaluation
    int N;
    int J;
    int K;
    int L;
    int D;
    int IDj[N];
    int IDk[N];
    int IDl[N];
    int IDd[N];
    int GE[N];
    real AG[N];
    int ED[N];
    int XP[N];
```

```

int y[N];

// individuals
int IDind[J];
int G[J];
real A[J];
int E[J];
int X[J];

// items
int IDitem[K];
int IDtext[K];
int IDdim[K];
}

parameters{
    // items
    real m_b[L];
    real<lower=0> s_b[L];
    real b_k[K];

    // betas
    real a;
    real b_G[2];
    real b_A;
    real b_E[3];
    real b_X[4];

    // abilities
    vector[J] theta;                      // reading comprehension
    real<lower=0> loads[D];              // loadings
    corr_matrix[D] Rho_theta_sub; // sub-dimensions: lit, inf, ref
    vector[D] theta_sub[J];
}

model{
    // declare
    vector[J] m_theta;
    vector[D] m_mult[J];
    real v;
    real p;

    // items
    m_b ~ normal(0, 1);
    s_b ~ exponential(2);
    for(k in 1:K){                      // priors
        b_k[k] ~ normal( m_b[ IDtext[k] ], s_b[ IDtext[k] ] );
    }

    // SOLV
    a ~ normal(0, 0.5);
    b_G ~ normal(0, 0.5);
}

```

```

b_A ~ normal(0, 0.5);
b_E ~ normal(0, 1);
b_X ~ normal(0, 0.5);
for(j in 1:J){
    m_theta[j] = a + b_G[ G[j] ] +
        b_A * ( A[j] - min(A) ) +
        b_E[ E[j] ] +
        b_X[ X[j] ];
}
theta ~ normal(m_theta, 1);
// setting the scale at this level

// FOLV
loads ~ lognormal(0, 0.5);
for(j in 1:J){
    m_mult[j,] = [ loads[1]*theta[j],
                    loads[2]*theta[j],
                    loads[3]*theta[j] ];
}
Rho_theta_sub ~ lkj_corr(2);
theta_sub ~ multi_normal( m_mult, Rho_theta_sub );
// also setting scale here

// model
for( i in 1:N ) {
    v = theta_sub[ IDj[i], IDd[i] ] - b_k[ IDk[i] ];
    p = inv_logit(v);
    y[i] ~ bernoulli(p);
}
}

## generated quantities{
##     vector[N] log_lik;
##     real v;
##     real p;
##
##     // likelihood
##     for( i in 1:N ) {
##         v = theta_sub[ IDj[i], IDd[i] ] - b_k[ IDk[i] ];
##         p = inv_logit(v);
##         log_lik[i] = bernoulli_lpmf( y[i] | p);
##     }
## }


```

SOLV NCP

```

data{
    // evaluation
    int N;
    int J;
    int K;
    int L;

```

```

int D;
int IDj[N];
int IDk[N];
int IDl[N];
int IDd[N];
int GE[N];
real AG[N];
int ED[N];
int XP[N];
int y[N];

// individuals
int IDind[J];
int G[J];
real A[J];
int E[J];
int X[J];

// items
int IDitem[K];
int IDtext[K];
int IDdim[K];
}

parameters{
    // items
    real m_b[L];
    real<lower=0> s_b[L];
    real zb_k[K];

    // betas
    real a;
    real b_G[2];
    real b_A;
    real b_E[3];
    real b_X[4];

    // abilities
    vector[J] ztheta;           // reading comprehension
    real<lower=0> loads[D];     // loadings
    cholesky_factor_corr[D] L_Rho_theta_sub; // sub-dimensions
    matrix[D, J] ztheta_sub;
}

transformed parameters{
    real b_k[K];
    vector[J] m_theta;
    vector[J] theta;           // reading comprehension
    matrix[D, D] Rho_theta_sub;
    matrix[J, D] m_mult;
    matrix[J, D] theta_sub;
}

```

```

// items
for(k in 1:K){
    b_k[k] = m_b[ IDtext[k] ] + s_b[ IDtext[k] ] * zb_k[k];
}

// SOLV
for(j in 1:J){
    m_theta[j] = a + b_G[ G[j] ] +
    b_A * ( A[j] - min(A) ) +
    b_E[ E[j] ] +
    b_X[ X[j] ];
}
theta = m_theta + 1 * ztheta;
// setting the scale at this level

// FOLV
Rho_theta_sub = multiply_lower_tri_self_transpose(L_Rho_theta_sub);
for(j in 1:J){
    m_mult[j,] = to_row_vector( [ loads[1]*theta[j] ,
    loads[2]*theta[j] ,
    loads[3]*theta[j] ] );
}
theta_sub = m_mult + (L_Rho_theta_sub * ztheta_sub)';
// also setting scale here
}

model{
    // declare
    real v;
    real p;

    // items
    m_b ~ normal(0, 1);
    s_b ~ exponential(2);
    zb_k ~ normal(0, 1);

    // abilities
    a ~ normal(0, 0.5);
    b_G ~ normal(0, 0.5);
    b_A ~ normal(0, 0.5);
    b_E ~ normal(0, 1);
    b_X ~ normal(0, 0.5);
    ztheta ~ normal(0,1);
    L_Rho_theta_sub ~ lkj_corr_cholesky(2);
    loads ~ lognormal(0, 0.5);
    to_vector(ztheta_sub) ~ normal(0,1);

    // model
    for( i in 1:N ) {
        v = theta_sub[ IDj[i], IDd[i] ] - b_k[ IDk[i] ];
        p = inv_logit(v);
    }
}

```

```

        y[i] ~ bernoulli(p);
    }
}

//# generated quantities{
//#     vector[N] log_li;
//#     real v;
//#     real p;
//#
//#     // likelihood
//#     for( i in 1:N ) {
//#         v = theta_sub[ IDj[i], IDd[i] ] - b_k[ IDk[i] ];
//#         p = inv_logit(v);
//#         log_li[i] = bernoulli_lpmf( y[i] | p );
//#     }
//# }
```

Prior predictive investigation

Prior predictive

```

model_path = file.path(getwd(), 'models_prior')
model_list = list.files( model_path )
model_list = model_list[ str_detect(model_list, '.stan') ]

run_prior( models = model_list,
model_path = model_path,
model_out = file.path(getwd(), 'chains_prior'),
data_path = file.path(getwd(), 'data') )
```

Prior predictive function

```

# function:
#   run_prior
# description:
#   To run each prior simulation for each model
# arguments:
#   models = list of model to run located in model_path
#   model_path = path where all models are located
#   model_out = path where chains have to be saved
#   data_path = path where data per condition is located

run_prior = function(models, model_path, model_out, data_path){

# data list
data_list = list.files( data_path )
data_list = data_list[str_detect(data_list, 'ListFormat')]

for(j in 1:length(models) ){

    # compile model
    set_cmdstan_path('~/cmdstan')
```

```

mod = cmdstan_model( file.path(model_path, models[j] ) )

# generate base name
base_nam = str_replace( data_list[1], 'ListFormat_',
str_replace( models[j], '.stan', '_') )
base_nam = str_replace( base_nam, '.RData', '' )

# load data
load( file.path(data_path, data_list[1] ) )

# run model
mod$sample(data = data_post,
            output_dir = model_out,
            output_basename = base_nam,
            chains=1, parallel_chains=1, adapt_delta=0.99)
}

}

```

Posterior predictive**Posterior predictive**

```

model_path = file.path(getwd(), 'models_post')
model_list = list.files( model_path )
model_list = model_list[ str_detect(model_list, '.stan') ]
model_list = model_list[c(1:2,5:6,3:4)]

run_post( models = model_list,
model_path = model_path,
model_out = file.path(getwd(), 'chains_post'),
data_path = file.path(getwd(), 'data') )

```

Posterior predictive function

```

# function:
#   run_post
# description:
#   To run each model for each data in all conditions
# arguments:
#   models = list of model to run located in model_path
#   model_path = path where all models are located
#   model_out = path where chains have to be saved
#   data_path = path where data per condition is located

run_post = function(models, model_path, model_out, data_path){

# data list
data_list = list.files( data_path )
data_list = data_list[str_detect(data_list, 'ListFormat')]

for(j in 1:length(models) ){

```

```

# compile model
set_cmdstan_path('~/cmdstan')
mod = cmdstan_model( file.path(model_path, models[j] ) )

for(i in 1:length(data_list) ){

  # generate base name
  base_nam = str_replace( data_list[i], 'ListFormat_',
  str_replace(models[j], '.stan', '_') )
  base_nam = str_replace( base_nam, '.RData', '' )

  # load data
  load( file.path(data_path, data_list[i] ) )

  # run model
  t0 = proc.time()
  mod$sample(data = data_post,
              output_dir = model_out,
              output_basename = base_nam,
              chains=3, parallel_chains=3, adapt_delta=0.99)
  t1 = proc.time()

  # saving time
  start = str_locate(base_nam, 'J')[2]
  m = str_sub( base_nam, start=1, end=(start-2) )
  J = str_sub( base_nam, start=start+1, end=(start+3) )

  start = str_locate(base_nam, 'l')[2]
  l = str_sub( base_nam, start=start+1, end=(start+3) )

  start = str_locate(base_nam, 'Ndata')[2]
  S = str_sub( base_nam, start=start+1, end=(start+2) )

  elapsed = (t1-t0)

  if(j==1 & i==1){
    time_elap = data.frame(
      Model=m,
      J=J,
      load=l,
      data=S,
      time=unlist(elapsed['elapsed']) )
  } else{
    time_elap = rbind(time_elap,
      c(m, J, l, S,
        unlist(elapsed['elapsed'])) )
  }

  # save time elapsed (saved at each iteration)
}

```

```
    write.csv( time_elap, row.names=F,  
              file=file.path(model_out, 'time_elapsed.csv' ) )  
  
  }  
}  
  
}
```

Bibliography

- [1] Azevedo, C. [2003]. *Métodos de estimação na teoria de resposta ao item*, Master's thesis, Universidade de São Paulo (USP).
url: <https://teses.usp.br/teses/disponiveis/45/45133/tde-05102004-163906/pt-br.php>.
- [2] Baker, F. [1998]. An investigation of the item parameter recovery characteristics of a gibbs sampling procedure, *Applied Psychological Measurement* **22**(22): 153–169.
doi: <https://doi.org/10.1177/01466216980222005>.
- [3] Baker, F. [2001]. The basic of item response theory, *Technical report*, ERIC Clearinghouse on Assessment and Evaluation.
- [4] Baker, F. and Kim, S. [1992]. *Item Response Theory: Parameter Estimation Techniques*, Statistics for the Social and Behavioral Sciences, CRC Press, Taylor and Francis Group.
doi: <https://www.doi.org/10.1201/9781482276725>.
- [5] Beaujean, A. [2014]. *Latent Variable Modeling Using R. A Step-by-Step Guide.*, Routledge.
- [6] Betancourt, M. and Girolami, M. [2012]. Hamiltonian monte carlo for hierarchical models.
url: arxiv.org/abs/1312.0906v1.
- [7] Bock, R. [1972]. Estimating item parameters and latent ability when responses are scored in two or more nominal categories, *Psychometrika* **37**(1).
doi: <https://doi.org/10.1007/BF02291411>.
- [8] Bradlow, E., Wainer, H. and Wang, X. [1999]. A bayesian random effects model for testlets, *Psychometrika* **64**(2): 153–168.
doi: <https://doi.org/10.1007/BF02294533>.
- [9] Chapaan, R. and Staelin, R. [1982]. Exploiting rank ordered choice set data within the stochastic utility model, *Journal of Marketing Research* **19**(3): 288–301.
doi: <https://www.doi.org/10.1177/002224378201900302>.
- [10] Chen, W. and Thissen, D. [1997]. Local dependence indexes for item pairs using item response theory, *Journal of Educational and Behavioral Statistics* **22**(3): 265–289.
doi: <https://doi.org/10.3102/10769986022003265>.

- [11] Duane, S., Kennedy, A., Pendleton, B. and Roweth, D. [1987]. Hybrid monte carlo, *Physics Letters B* **195**(2): 216–222.
doi: [https://doi.org/10.1016/0370-2693\(87\)91197-X](https://doi.org/10.1016/0370-2693(87)91197-X).
url: <https://www.sciencedirect.com/science/article/pii/037026938791197X>.
- [12] Edwards, J. and Bagozzi, R. [2000]. On the nature and direction of relationships between constructs and measures, *Psychological Methods* **5**(2): 155–174.
doi: <https://www.doi.org/10.1037/1082-989X.5.2.155>.
- [13] Flores, S. [2012]. *Modelos testlet logísticos y logísticos de exponente positivo para pruebas de compresión de textos*, Master's thesis, Pontificia Universidad Católica del Perú.
- [14] Fox, J. [2010]. *Bayesian Item Response Modeling, Theory and Applications*, Statistics for Social and Behavioral Sciences, fienberg, s. and van der linden, w. edn, Springer Science+Business Media, LLC.
- [15] Fujimoto, K. [2018a]. The bayesian multilevel trifactor item response theory model, *Educational and Psychological Measurement* **79**(3): 462–494.
doi: <https://doi.org/10.1177/0013164418806694>.
- [16] Fujimoto, K. [2018b]. A general bayesian multilevel multidimensional irt model for locally dependent data, *Br J Math Stat Psychol* **71**(3): 536–560.
doi: <https://doi.org/10.1111/bmsp.12133>.
- [17] Fujimoto, K. [2020]. A more flexible bayesian multilevel bifactor item response theory model, *Journal of Educational Measurement* **57**(2): 255–285.
doi: <https://doi.org/10.1111/jedm.12249>.
- [18] Gelfand, A., Sahu, S. and Carlin, B. [1995]. Efficient parametrisations for normal linear mixed models, *Biometrika* **82**(3): 479–488.
doi: <https://doi.org/10.1093/biomet/82.3.479>.
- [19] Gelfand, A., Sahu, S. and Carlin, B. [1996]. Efficient parameterizations for generalised linear models (with discussion), in J. Bernardo, J. Berger, A. Dawid and a. Smith (eds), *Bayesian Statistics*, Vol. 5, pp. 165–180.
- [20] Gelman, A. [1996]. Bayesian model building by pure thought: some principles and examples, *Statistica Sinica* **6**(1): 215–232.
url: <https://www.jstor.org/stable/24306008>.
- [21] Gelman, A., Bois, F. and Jiang, J. [1996]. Physiological pharmacokinetic analysis using population modeling and informative prior distributions, *Journal of the American Statistical Association* **91**(436): 1400–1412.
doi: <https://doi.org/10.2307/2291566>.
url: <https://www.jstor.org/stable/2291566>.
- [22] Gelman, A., Carlin, J., Stern, H., Dunson, D., Vehtari, A. and Rubin, D. [2014]. *Bayesian Data Analysis*, Texts in Statistical Science, third edn, Chapman and Hall/CRC.

- [23] Gelman, A. and Rubin, D. [1996]. Markov chain monte carlo methods in biostatistics, *Statistical Methods in Medical Research* **5**(4): 339–355.
doi: <https://doi.org/10.1177/096228029600500402>.
- [24] Geman, S. and Geman, D. [1984]. Stochastic relaxation, gibbs distributions, and the bayesian restoration of images, *IEEE Transactions on Pattern Analysis and Machine Intelligence PAMI* **6**(6): 721–741.
doi: <https://doi.org/10.1109/TPAMI.1984.4767596>.
- [25] Gorinova, M., Moore, D. and Hoffman, M. [2019]. Automatic reparameterisation of probabilistic programs.
url: <https://arxiv.org/abs/1906.03028>.
- [26] Hambleton, R. and Swaminathan, H. [1991]. *Item Response Theory*, Evaluation in Education and Human Services series, Springer Science+Business Media, LLC.
- [27] Hambleton, R., Swaminathan, H. and Rogers, H. [1991]. *Fundamentals of Item Response Theory*, SAGE Publications Inc.
- [28] Hastings, W. K. [1970]. Monte Carlo sampling methods using Markov chains and their applications, *Biometrika* **57**(1): 97–109.
doi: <https://doi.org/10.1093/biomet/57.1.97>.
url: <https://academic.oup.com/biomet/article-pdf/57/1/97/23940249/57-1-97.pdf>.
- [29] Heckman, J. [1979]. Sample selection bias as a specification error, **47**(1): 153–161.
doi: <https://www.doi.org/10.2307/1912352>.
url: <https://www.jstor.org/stable/1912352>.
- [30] Hsieh, M., Proctor, T., Hou, J. and Teo, K. [2010]. A comparison of bayesian mcmc and marginal maximum likelihood methods in estimating the item parameters for the 2pl irt model, *International Journal of Innovative Management, Information and Production* **1**(1): 81–89.
url: <http://ismeip.org/IJIMIP/contents/imip1011/10IN15T.pdf>.
- [31] Jaynes, E. [1985]. Highly informative priors, *Bayesian Statistics* **2**: 329–360.
- [32] Jiao, H., Kamata, A., Wang, S. and Jin, Y. [2012]. A multilevel testlet model for dual local dependence, *Journal of Educational Measurement* **49**(1): 82–100.
doi: <https://doi.org/10.1111/j.1745-3984.2011.00161.x>.
- [33] Keane, M. [1992]. A note on identification in the multinomial probit model, *Journal of Business and Economic Statistics* **10**(2): 193–200.
doi: <https://doi.org/10.2307/1391677>.
url: <https://www.jstor.org/stable/1391677>.
- [34] Kieftenbeld, V. and Natesan, P. [2012]. Recovery of graded response model parameters: A comparison of marginal maximum likelihood and markov chain monte carlo estimation, *Applied Psychological Measurement* **36**(5): 399–419.
doi: <https://www.doi.org/10.1177/0146621612446170>.

- [35] Kim, S. and Cohen, A. [1999]. Accuracy of parameter estimation in gibbs sampling under the two-parameter logistic model, *Annual Meeting of the American Educational Research Association*, American Educational Research Association.
- url:** <https://eric.ed.gov/?id=ED430012>.
- [36] Kline, R. [2012]. Assumptions in structural equation modeling, in R. Hoyle (ed.), *Handbook of Structural Equation Modeling*, The Guilford Press, chapter 7, pp. 111–125.
- [37] Lewandowski, D., Kurowicka, D. and Joe, H. [2009]. Generating random correlation matrices based on vines and extended onion method, *Journal of Multivariate Analysis* **100**(9): 1989–2001.
- doi:** <https://doi.org/10.1016/j.jmva.2009.04.008>.
- [38] Linacre, J. [2021]. *Winsteps® (Version 5.1.0) [Computer Software]*, Portland, Oregon.
- url:** <https://www.winsteps.com/>.
- [39] Lord, F. and Novik, M. [2008]. *Statistical Theories of Mental Test Scores*, Information Age Publishing.
- [40] Lunn, D., Spiegelhalter, D., Thomas, A. and Best, N. [2009]. The bugs project: Evolution, critique and future directions, *Statistics in Medicine* **28**(25): 3049–3067.
- [41] Lunn, D., Thomas, A., Best, N. and Spiegelhalter, D. [2000]. Winbugs - a bayesian modelling framework: Concepts, structure, and extensibility, *Statistics and Computing* (10): 325–337.
- doi:** <https://www.doi.org/10.1023/A:1008929526011>.
- [42] Martin, J. and McDonald, R. [1975]. Bayesian estimation in unrestricted factor analysis: A treatment for heywood cases, *Psychometrika* (40): 505–517.
- doi:** <https://doi.org/10.1007/BF02291552>.
- [43] McCullagh, P. and Nelder, J. [1989]. *Generalized Linear Models*, Monographs on Statistics Applied Probability, Chapman Hall/CRC Press.
- [44] McElreath, R. [2020]. *Statistical Rethinking: A Bayesian Course with Examples in R and Stan*, Texts in Statistical Science, 2 edn, Chapman and Hall/CRC.
- doi:** <https://doi.org/10.1201/9780429029608>.
- [45] Metropolis, N., Rosenbluth, A., Rosenbluth, M. and Teller, A. [1953]. Equation of state calculations by fast computing machines, *The Journal of Chemical Physics* **21**: 1087–1092.
- doi:** <https://doi.org/10.1063/1.1699114>.
- [46] Muller, P. [1991]. A generic approach to posterior integration and gibbs sampling, *Technical Report 91-09*, Department of Statistics, Purdue University.
- url:** <https://www.stat.purdue.edu/docs/research/tech-reports/1991/tr91-09.pdf>.
- [47] Muthén, L. and Muthén, B. [1998-2011]. *Mplus User's Guide*, CA: Muthén Muthén.

- [48] Neal, R. [2011]. Mcmc using hamiltonian dynamics, *in* S. Brooks, A. Gelman, G. Jones and X. Meng (eds), *Handbook of Markov Chain Monte Carlo*, Chapman Hall/CRC Press, chapter 5, pp. 113–162.
- [49] Nelder, J. and Wedderburn, W. [1972]. Generalized linear models, *Royal Statistical Society* **135**(3): 370–384.
doi: <https://doi.org/10.2307/2344614>.
url: <https://www.jstor.org/stable/2344614>.
- [50] Papaspiliopoulos, O., Roberts, G. and Skold, M. [2003]. Non-centered parameterisations for hierarchical models and data augmentation, *Bayesian Statistics* **7**: 307–326.
url: <http://econ.upf.edu/~omiro/papers/val7.pdf>.
- [51] Papaspiliopoulos, O., Roberts, G. and Skold, M. [2007]. A general framework for the parametrization of hierarchical models, *Statistical Science* **22**(1): 59–73.
doi: <https://www.doi.org/10.1214/088342307000000014>.
- [52] Patz, R. J. and Junker, B. W. [1999]. A straightforward approach to markov chain monte carlo methods for item response models, *Journal of Educational and Behavioral Statistics* **24**(2): 146–178.
doi: [10.3102/10769986024002146](https://doi.org/10.3102/10769986024002146).
- [53] Plummer, M. [2003]. Jags: A program for analysis of bayesian graphical models using gibbs sampling.
- [54] R Core Team [2015]. *R: A Language and Environment for Statistical Computing*, R Foundation for Statistical Computing, Vienna, Austria.
url: <http://www.R-project.org/>.
- [55] Rabe-Hesketh, S., Pickles, A. and Skrondal, A. [2003]. Correcting for covariate measurement error in logistic regression using nonparametric maximum likelihood estimation, *Statistical Modelling* **3**(3): 215–232.
doi: <https://doi.org/10.1191/1471082X03st056oa>.
- [56] Rabe-Hesketh, S., Skrondal, A. and Pickles, A. [2003]. Maximum likelihood estimation of generalized linear models with covariate measurement error, *The Stata Journal* **3**(4): 386–411.
doi: <https://doi.org/10.1177/1536867X0400300408>.
url: <https://journals.sagepub.com/doi/pdf/10.1177/1536867X0400300408>.
- [57] Rabe-Hesketh, S., Skrondal, A. and Pickles, A. [2004a]. Generalized multilevel structural equation modeling, *Psychometrika* **69**(2): 167–190.
doi: <https://doi.org/10.1007/BF02295939>.
- [58] Rabe-Hesketh, S., Skrondal, A. and Pickles, A. [2004b]. *GLLAMM Manual*, UC Berkeley Division of Biostatistics.
url: <http://www.biostat.jhsph.edu/~fdominic/teaching/bio656/software-gllamm.manual.pdf>.

- [59] Rabe-Hesketh, S., Skrondal, A. and Pickles, A. [2004c]. Maximum likelihood estimation of limited and discrete dependent variable models with nested random effects, *Journal of Econometrics* **128**(2): 301–323.
doi: <https://www.doi.org/10.1016/j.jeconom.2004.08.017>.
url: <http://www.sciencedirect.com/science/article/pii/S0304407604001599>.
- [60] Rabe-Hesketh, S., Skrondal, A. and Zheng, X. [2012]. Multilevel structural equation modeling, in R. Hoyle (ed.), *Handbook of Structural Equation Modeling*, The Guilford Press, chapter 30, pp. 512–531.
- [61] Rabe-Hesketh, S., Yang, S. and Pickles, A. [2001]. Multilevel models for censored and latent responses, *Statistical Methods in Medical Research* **10**(6): 409–427.
doi: <https://www.doi.org/10.1177/096228020101000604>.
- [62] Rasch, G. [1980]. *Probabilistic Models for Some Intelligence and Attainment Tests*, University of Chicago Press.
- [63] Raudenbush, S. and Bryk, A. [2002]. *Hierarchical linear models: Applications and data analysis methods* (Vol. 1), Advanced Quantitative Techniques in the Social Sciences, SAGE Publications Inc.
- [64] Reckase, M. [2009]. *Multidimensional Item Response Theory*, Statistics for Social and Behavioral Sciences, Springer Science+Business Media, LLC.
- [65] Rivera, J. [2019]. *El modelo de respuesta nominal: Aplicación a datos educacionales*, Master's thesis, Pontificia Universidad Católica del Perú.
url: <http://hdl.handle.net/20.500.12404/14600>.
- [66] Seaman, J., Seaman jr., J. and Stamey, J. [2011]. Hidden dangers of specifying noninformative priors, *The American Statistician* **66**(2): 77–84.
doi: <https://www.doi.org/10.1080/00031305.2012.695938>.
- [67] Skrondal, A. and Rabe-Hesketh, S. [2003a]. Multilevel logistic regression for polytomous data and rankings, *Psychometrika* **68**: 267–287.
doi: <https://www.doi.org/10.1007/BF02294801>.
- [68] Skrondal, A. and Rabe-Hesketh, S. [2003b]. Some applications of generalized linear latent and mixed models in epidemiology: Repeated measures, measurement error and multilevel modeling, *Norsk Epidemiologi* **13**(2): 265–278.
- [69] Skrondal, A. and Rabe-Hesketh, S. [2004a]. *Generalized Latent Variable Modeling: Multilevel, Longitudinal, and Structural Equation Models*, Interdisciplinary Statistics, Chapman Hall/CRC Press.
- [70] Skrondal, A. and Rabe-Hesketh, S. [2004b]. Generalized linear latent and mixed models with composite links and exploded likelihoods, in BiggeriA., E. Dreassi, C. Lagazio and M. Marchi (eds), *Proceedings of the 19th International Workshop on Statistical Modeling*, Firenze University Press, Florence, Italy, pp. 27–39.
url: <http://www.gllamm.org/compositeconf.pdf>.

- [71] Stan Development Team [2020a]. RStan: the R interface to Stan. R package version 2.21.2.
url: <http://mc-stan.org/>.
- [72] Stan Development Team. [2020b]. *Stan Modeling Language Users Guide and Reference Manual, version 2.26*, Vienna, Austria.
url: <https://mc-stan.org>.
- [73] Tarazona, E. [2013]. *Modelos alternativos de respuesta graduada con aplicaciones en la calidad de servicios*, Master's thesis, Pontificia Universidad Católica del Perú (PUCP).
url: <http://hdl.handle.net/20.500.12404/6175>.
- [74] Wainer, H., Bradlow, E. and Wang, X. [2007]. *Testlet response theory and its applications*, Cambridge University Press.
- [75] Wollack, J. A., Bolt, D. M., Cohen, A. S. and Lee, Y.-S. [2002]. Recovery of item parameters in the nominal response model: A comparison of marginal maximum likelihood estimation and markov chain monte carlo estimation, *Applied Psychological Measurement* **26**(3): 339–352.
doi: <https://www.doi.org/10.1177/0146621602026003007>.
- [76] Yen, W. [1984]. Effects of local item dependence on the fit and equating performance of the three-parameter logistic model, *Applied Psychological Measurement* **8**(2): 125–145.
doi: <https://doi.org/10.1177/014662168400800201>.

AFDELING
Straat nr bus 0000
3000 LEUVEN, BELGIË
tel. + 32 16 00 00 00
fax + 32 16 00 00 00
www.kuleuven.be

